

# A new hadrosauriform dinosaur from the Wessex Formation, Wealden Group (Early Cretaceous), of the Isle of Wight, southern England

Jeremy A. F. Lockwood<sup>a,b,\*</sup> , David M. Martill<sup>a</sup>  and Susannah C. R. Maidment<sup>b</sup> 

<sup>a</sup>School of Environment, Geography and Geosciences, University of Portsmouth PO1 2DT, UK; <sup>b</sup>Department of Earth Sciences, Natural History Museum, Cromwell Road, London SW7 5BD, UK

(Received 7 May 2021; accepted 4 September 2021)

A new genus and species of non-hadrosaurid hadrosauriform dinosaur, *Brighstoneus simmondsi* gen. et sp. nov., is described from the Lower Cretaceous Wessex Formation of the Isle of Wight. The new taxon has two autapomorphies, a nasal having a modest nasal bulla with convex sides, and primary and accessory ridges on the lingual aspect of the maxillary crown. The dentary has at least 28 alveolar positions, which is the highest number recorded in an ornithomimid with non-parallel sided alveoli, creating a character combination that is unique within Iguanodontia. The hadrosauriform fauna of the Barremian–Aptian Wealden Group on both the Isle of Wight and mainland England has been represented for almost a century by just two taxa, the robust *Iguanodon bernissartensis* and the more gracile *Mantellisaurus atherfieldensis*, with referred material often being fragmentary or based on unassociated elements. This discovery increases the known hadrosauriform diversity in England and, together with recent discoveries in Spain, suggests that their diversity in the upper Wealden of Europe was considerably wider than initially realized. This find also has important implications for the validity of the *Mantellisaurus atherfieldensis* hypodigm, and a reassessment of existing material is suggested.

<http://zoobank.org/urn:lsid:zoobank.org:pub:31F0D48F-C1DA-406E-A811-1F5937ED19F4>

**Keywords:** Iguanodontia; Hadrosauriformes; diversity; Wealden Group; Lower Cretaceous; Isle of Wight

## Introduction

Iguanodontia is a major clade of ornithischian dinosaurs that originated in the Middle Jurassic (Ruiz-Omeñaca *et al.* 2007) and became increasingly widespread and diverse during the Cretaceous (McDonald *et al.* 2010a). It includes *Camptosaurus*, the iconic *Iguanodon* and the hadrosaurids and is defined by Sereno (2005) as the most inclusive clade containing *Parasaurolophus walkeri* Parks, 1922 but not *Hypsilophodon foxii* Huxley, 1869 or *Thescelosaurus neglectus* Gilmore, 1913.

The Wealden Group exposed on the Isle of Wight, southern England, represents deposition in an Early Cretaceous near coastal floodplain, spanning the Barremian and earliest Aptian (Kerth & Hailwood 1988; Hughes & McDougall 1990). Although these strata yield fossils from a diverse range of dinosaurs, the palaeoecosystem was dominated by large basal iguanodontians, whose remains heavily outnumber those of other tetrapods (Martill & Naish 2001). This iguanodontian material is usually referred to either *Mantellisaurus atherfieldensis* (Hooley, 1925), or the larger and more robust *Iguanodon bernissartensis* Boulenger in Van Beneden, 1881 (Martill & Naish 2001; McDonald 2012a; Norman 2012). Historically other names have

been proposed for this material, such as *Iguanodon see-lyi* Hulke, 1882 and *Vectisaurus valdensis* Hulke, 1879, although these are generally regarded as synonyms of *Iguanodon bernissartensis* (Naish & Martill 2008) and *Mantellisaurus atherfieldensis* (Norman 1990), respectively. Other iguanodontian material from the dryosaurid *Valdosaurus canaliculatus* (Galton, 1975) is less common (Barrett *et al.* 2011; Barrett 2016). The Isle of Wight's Wealden Group has been closely linked with iguanodontians since the early nineteenth century, when, in 1829, William Buckland (1835) identified a large phalanx (OUMNH K859) from Sandown Bay as showing similarities to Gideon Mantell's then recently described '*Iguanodon*' (Mantell 1825). An iguanodontian sacrum from Brook Bay (NHMUK PV OR37685), then held in William Devonshire Saull's private London museum, was also to provide the crucial datum spurring Richard Owen to invent the clade Dinosauria (Owen 1842; Torrens 2014). Gideon Mantell also knew the Isle of Wight well and produced a comprehensive guidebook, *Geological excursions round the Isle of Wight*, which included a section on '*Iguanodon*' (Mantell 1847). Here, he alluded to some of the problems in dealing with material from the Isle of Wight. "The quantity of bones collected from the seashore ... is

\*Corresponding author. Email: [jeremy.lockwood@port.ac.uk](mailto:jeremy.lockwood@port.ac.uk)

very considerable ... and must have belonged to between 150 and 200 individuals ... though from their abraded and mutilated condition, but few of the specimens were instructive” (Mantell 1847, p. 310). That particular problem remains to this day. The gradual exposure of the bone-bearing horizons and the destructive nature of marine erosion frequently leads to episodic finds of isolated and fragmentary material, which are then often collected by different individuals, a process that obscures the fact that in many cases *in situ* material might have been articulated or at least associated. The perception that the bones of large iguanodontians are plentiful on the Isle of Wight is certainly true, but associated material in public collections, especially from the cranium, is rare. In addition, the informal attribution of larger material to either *Mantellisaurus atherfieldensis* or *Iguanodon bernissartensis* is commonly based on little more than the relative size and robustness of the bones rather than on autapomorphies or viewing the bone in the context of associated material, while smaller examples, especially from character-poor regions of the skeleton such as the axial column and distal limbs, are currently difficult to distinguish from dryosaurids. These factors, when combined with poorly refined stratigraphy, may well be obscuring a wider diversity in populations with low disparity or evolving through phyletic gradualism. Here, we describe an associated partial skeleton from the Wessex Formation, which, although incomplete, has several character-rich cranial and postcranial elements that allow its interpretation as a new, large hadrosauriform. This represents the first discovery of a well-characterized, novel hadrosauriform taxon from the Isle of Wight in the one hundred years since Hooley obtained the skeleton of *Mantellisaurus atherfieldensis* in 1914 (Hooley 1917). This has important implications for the interpretation of material currently referred to *Mantellisaurus atherfieldensis* and for our understanding of hadrosauriform diversity in the Barremian–Aptian non-marine sequences in Britain and other European countries.

### Institutional abbreviations

**AMNH**, American Museum of Natural History, New York City, NY, USA; **CEUM**, College of Eastern Utah Prehistoric Museum, Price, UT, USA; **GDF**, Fossils from the Gadoufaoua locality stored at the Musée National du Niger, Niamey, Niger; **IWCMS**, Isle of Wight County Museum Service (**MIWG**, Museum of Isle of Wight Geology, was also used for accessions prior to 1994), Dinosaur Isle Museum, Isle of Wight, UK; **MAP**, Museo Aragonés de Paleontología (Fundación Conjunto Paleontológico de Teruel-

Dinopolis), Teruel, Spain; **NHMUK**, Natural History Museum, London, UK; **OUNNH**, Oxford University Museum of Natural History, Oxford, UK; **PIN**, Palaeontological Institute Nauk, Moscow, Russia; **SBDE**, The Sino-Belgian Dinosaur Expedition, stored at the Inner Mongolian Museum, Hohhot, China; **SMU**, Southern Methodist University, Shuler Museum of Paleontology, Dallas, TX, USA; **USNM**, National Museum of Natural History, Washington, DC, USA; **XMDFEC**, Xixia Museum of Dinosaur Fossil Eggs of China, Xixia, China; **YHZ**, Yizhou Fossil Museum, Yixian City, China; **YPM**, Yale Peabody Museum, New Haven, CT, USA; **ZMNH**, Zhejiang Museum of Natural History, Zhejiang, China.

### Geological setting

The Wealden Group on the Isle of Wight (Fig. 1) comprises two distinct formations. The older Wessex Formation is composed primarily of varicoloured over-bank mudstones and siltstones with interbedded fluvial sandstones, and represents deposition in a meander-belt, fluvio-lacustrine setting (Stewart 1978). The overlying Vectis Formation, represented by argillaceous deposits and occasional interbedded sandstone and shelly limestones, was deposited predominantly in a shallow

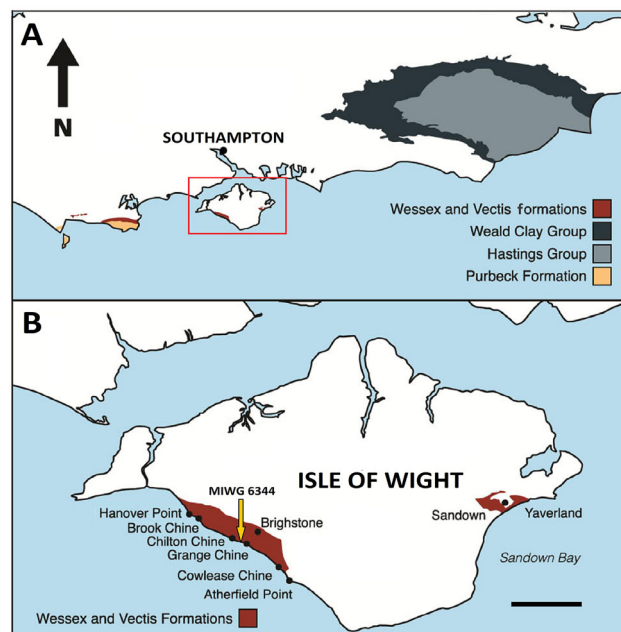


**Figure 1.** **A**, the south coast of England; **B**, an enlarged view of the Isle of Wight (scale bar = 5 km). Arrow labelled MIWG 6344 marks the locality of the *Brighthoneus simmondsi* gen. et sp. nov. excavation site.

coastal lagoon of fluctuating salinity (Radley & Barker 1998, 2000; Radley *et al.* 1998; Fig. 2). The Wessex Formation also contains plant debris beds (*sensu* Oldham 1976; see Sweetman & Insole 2010) that, although a tiny fraction of the overall succession (Fig. 2), are the main sources of dinosaur and other vertebrate fossils on the Isle of Wight. Sweetman & Insole (2010, p. 409) interpreted these beds as representing a “locally generated sheet flood, which was then transformed on the floodplain into a debris flow by the acquisition of localised surface material”.

The Wealden Group is well-exposed on the south-west coast of the Isle of Wight with a smaller exposure on the east coast at Yaverland (Fig. 1). These exposures form the cores of two anticlines, one centred on Brighstone Bay and the other on Sandown Bay. Estimates vary but the Wessex Formation on the Isle of Wight is approximately 180 m thick (Stewart 1978) and the Vectis Formation is 40 m or more (Radley & Barker 1998).

The central core of the Brighstone anticline lies to the west of Sudmoor Point and has been placed close to Hanover Point at the so called ‘Pine raft’, a collection of fossilized logs of the conifer *Pseudofrenelopsis* (Robinson & Hesselbo 2004), although much of this has now been destroyed by storms. The exposed core of the Brighstone anticline is composed of variegated mudstones, which are poorly correlated across the Isle of Wight. The strata at Hanover Point represent the oldest units of the exposed Wealden Group, although using borehole data Falcon & Kent (1960) showed that the Wealden Group on the Isle of Wight reaches a total thickness of 592 m. The lack of volcanics and biostratigraphically useful fossils has hampered accurate dating; however, studies including palynological evidence suggest that the exposed Wessex Formation on the Isle of Wight is entirely Barremian in age (Hughes & McDougall 1990; Allen & Wimbledon 1991), while carbon-isotope stratigraphy places the ‘Pine Raft’ within Chronozone CM3 (Robinson & Hesselbo 2004) and just above the Hauterivian–Barremian boundary. Studies on the overlying Vectis Formation show that the Barremian–Aptian boundary lies within the Shepherds Chine Member, which forms the youngest unit of the formation (Kerth & Hailwood 1988; Robinson & Hesselbo 2004).

The palaeoenvironment has been interpreted as a sequence of alluvial meander plains, that overran the Wessex Sub-basin (Allen 1998), together with seasonally ephemeral lakes and ponds (Martill & Naish 2001). The climate was variable ‘Mediterranean’ and the differentiated palaeosols that dominate the succession show swelling and shrinkage features typical of modern,

warm, semi-arid areas (Allen 1998). The uneven growth rings in the locally abundant conifer *Pseudofrenelopsis paraceramosa* also indicate a probable annual change from hot-drier to cool-wetter weather of a Mediterranean type rather than monsoonal (Francis 1987), but still with times of considerable precipitation. Higher ground to the north had forested areas of pino-phytes and ginkgophytes, with pteridophytes, cycadophytes and angiosperms also present (Sweetman & Insole 2010, and references therein). Forest fires and floods were common, depositing plant debris into the basin (Sweetman & Insole 2010). High-sinuosity rivers in the basin would have provided for a rich riparian ecosystem (Sweetman 2011), while the locality more generally provided a diversity of habitats, which appeared stable until the late Barremian, when marine influences became more pronounced.

## Systematic palaeontology

**Dinosauria** Owen, 1842

**Ornithischia** Seeley, 1887

**Ornithopoda** Marsh, 1881

**Iguanodontia** Dollo, 1888

**Ankylopollexia** Sereno, 1986

**Styracosterna** Sereno, 1986

**Hadrosauriformes** Sereno, 1997

***Brighstoneus*** gen. nov.

**Etymology.** *Brighstoneus* is named after the village of Brighstone on the Isle of Wight, which is close to the excavation site and was home to the Reverend William Fox, a celebrated Victorian fossil collector whose discoveries had a major impact on early dinosaurian research.

**Type species.** *Brighstoneus simmondsi* gen. et sp. nov.

**Diagnosis.** As for type and only species (see below).

**Locality and horizon.** Wessex Formation, early Barremian, Lower Cretaceous. MIWG 6344 was excavated during 1978, from a plant debris bed (L9 of Stewart 1978) to the west of Grange Chine on the south coast of the Isle of Wight (Fig. 2).

**Comment on association.** The skeleton was found associated with one of the UK’s most complete theropods, *Neovenator salerii* Hutt *et al.*, 1996 (MIWG 6348; Brusatte *et al.* 2008). Both individuals were contained, with some overlap, in an area of  $\sim 3 \times 6$  m. There was no articulated material, but preservation was consistent across individual elements and there was no replication of material or other iguanodontian material found during

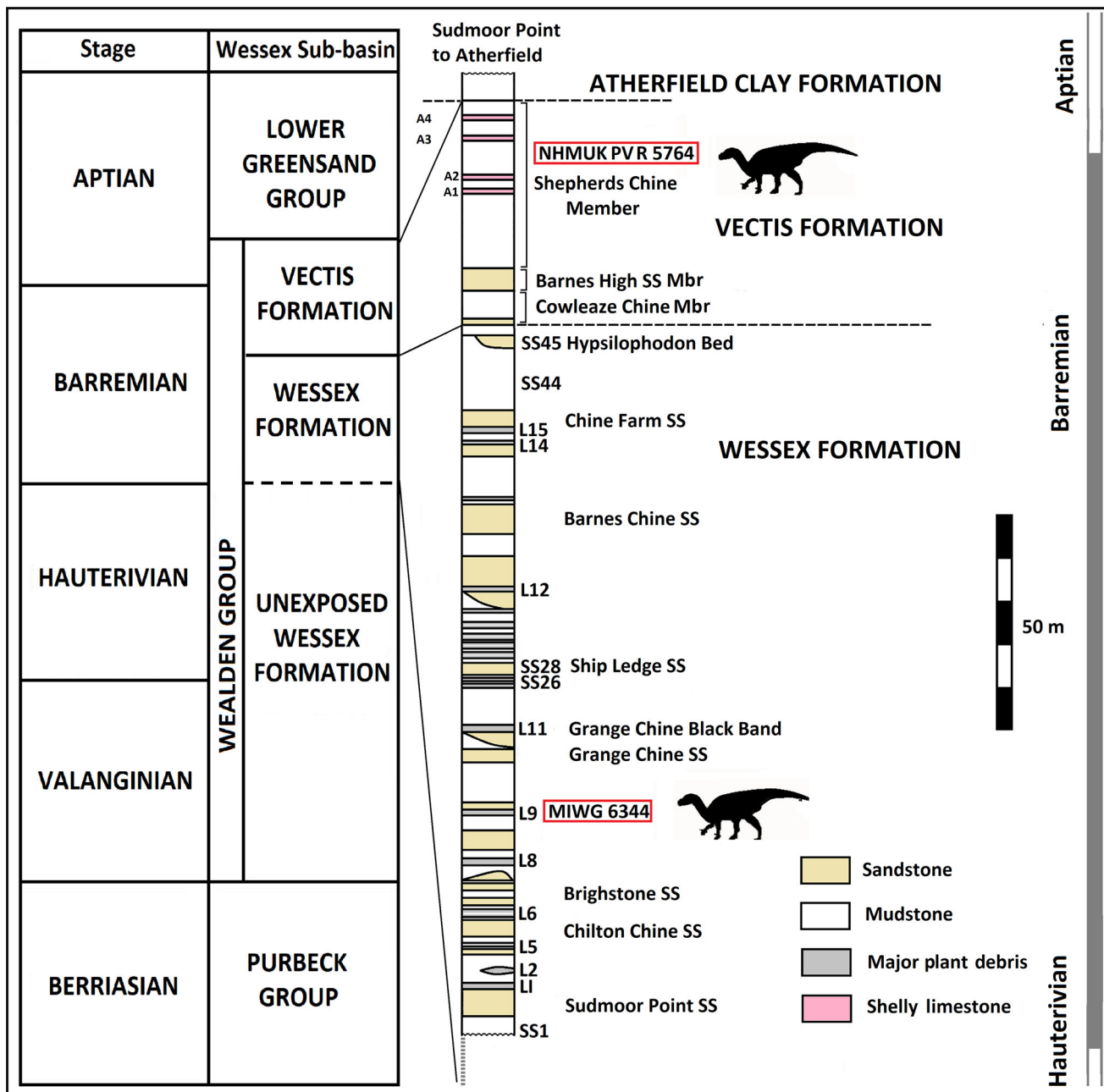


**Figure 2.** Generalized stratigraphical log modified from Allen & Wimbledon (1991). Schematic lithological logs of Wealden exposure between Sudmoor and Atherfield on the Isle of Wight showing sites of *Brighstoneus simmondsi* gen. et sp. nov. (MIWG 6344) and the *Mantellisaurus atherfieldensis* holotype (NHMUK PV R5764). Adapted from Sweetman (2007). **Abbreviations:** Mbr, member; SS, sandstone.

the excavation. The material was stored at the Museum of the Isle of Wight Geology, who were also involved in the excavation. The then curator is confident that the material was associated (S. Hutt, pers. comm. 2021). Some photographs and drawings of the site are included in [Supplementary material \(Figs S1–S5\)](#) and hard copies of other contemporaneous records have been accessioned under MIWG 6344.

**Comment on stratigraphy.** The base of the Barremian stage within the Wessex Formation lies west of Sudmoor Point and has been dated to 126.5 Ma (Gale *et al.* 2020), while the Barremian–Aptian boundary at the base of Chron M0, on the basis of dates from Svalbard (Zhang *et al.* 2019), is given as 121.4 Ma (Gale *et al.* 2020). This gives the Barremian a duration of approximately 5.1 Ma compared to earlier estimates

of 4.5 Ma based on phosphorus burial rates (Bodin *et al.* 2006). The *Mantellisaurus atherfieldensis* holotype was found following a cliff fall from the Shepherds Chine Member of the Vectis Formation in 1914 (Hooley 1925) and was probably from earliest Aptian strata, making it approximately 4.0 Ma younger than *Brighstoneus simmondsi*, assuming uniform depositional rates.

*Brighstoneus simmondsi* gen. et sp. nov.

(Figs 3–22, 24)

**Etymology.** The specific name honours Mr Keith Simmonds who made the discovery of the specimen.

**Holotype.** MIWG 6344, a partial skeleton composed of the following elements: dorsal process of right premaxilla; both maxillae; both jugals; left palpebral; left nasal; both dentaries; prementary; one transitional dorsal and seven dorsal vertebrae; sacrum; six caudal vertebrae; dorsal ribs, nine from the left side and five from the right side; both ilia; right ischium; possible prepubic process; and the right femur. Some parts of the same individual (including two dorsal vertebrae and other fragments) remain in private ownership and are not described herein.

**Diagnosis.** Differs from all other iguanodontians by possessing the following autapomorphies and unique combination of characters (autapomorphies indicated with an asterisk): maxillary crowns possessing both a primary ridge and mesially placed accessory ridges on the lingual surface\*; nasal expanded postnarily to produce a modest nasal bulla with convex lateral walls\*. A character combination of at least 28 dentary tooth positions in a dentary with one active crown and one replacement tooth for each position and non-parallel alveolar septa.

In addition, *Brighstoneus* can be distinguished from other Barremian–Aptian Wealden Group iguanodontians by possession of the following combination of features: ratio of precoronoid length of the dentary to minimum depth  $> 6.0$ ; coronoid process projects at approximately  $90^\circ$  with respect to the dorsal margin of dentary; bilobed ‘heart-shaped’ ventral prementary process with prominent anterior denticles with concave mesial and distal edges; posteriorly positioned maxillary ascending process in lateral view with length of the anterior section approximately twice the length of the posterior section; prominent anterodorsal process present on maxilla; anterior (maxillary) process of jugal relatively long (60% of overall length) and tapers distally to form a triangular ending; ventral section of the posterior margin of the jugal (heel) projects posteriorly to form a spur-like feature; in dorsal view the jugal is straight; ventral border overlapped by maxillary process of premaxilla;

anteroventral nasal process forms posteroventral margin of external narial opening; ventral surface of ischiadic peduncle of ilium parallel with the anteroventral margin of the postacetabular process; ischiadic peduncle of ilium has flat lateral wall with no pronounced posterolateral boss; ventral shelf at base of iliac preacetabular process weakly developed; dorsoventrally deep preacetabular process with little or no axial twist; deep and short iliac central plate with ratio of depth to length  $> 1.2$ .

## Description

Overall, MIWG 6344 is excellently preserved with little distortion or crushing (measurements are available in the [Supplementary material](#)). Many of the bones exhibit unusual eroded areas, which have left smooth, ‘scooped out’ regions extending down to and including the internal trabecular bone. Some of these areas are partially covered by the original sediment, suggesting these features formed prior to, or soon after, burial. It is unlikely that this damage resulted from prolonged sub-aerial exposure as the cortical surface is generally well preserved (Behrensmeyer 1978). As many of these eroded features are associated with highly cartilaginous regions, it is possible that they are examples of invertebrate bioerosion, potentially by isopterans (Britt *et al.* 2008, and references therein; Huchet *et al.* 2011), which are known from the Wealden Group (Jarzembowski 1981). The term ‘eroded’ is used in the descriptive text to indicate these areas. There is also evidence, particularly on the ribs, of shallow circular pits varying between 2–4 mm in diameter, which might represent dermestid beetle activity (Britt *et al.* 2008).

## Premaxilla

Only the dorsal (nasal) process of the right premaxilla is preserved, but without its posterior-most tip (Fig. 3). In lateral view, the fragment has a long mediolaterally thin process, which is gently curved, convex dorsally and gradually tapers as it extends posteriorly. The lateral surface is rounded and grooved in the posterior three-fifths of its length for contact with the anterodorsal process of the nasal (Fig. 3A: this area is described as ‘bevelled’ in *Mantellisaurus atherfieldensis* rather than grooved: Norman 1986). Anteriorly the ventral margin curves ventrally forming a thin blade of bone, which is incomplete but would have contributed to the internarial septum. The medial surface of the dorsal process is flat for articulation with its antimer.

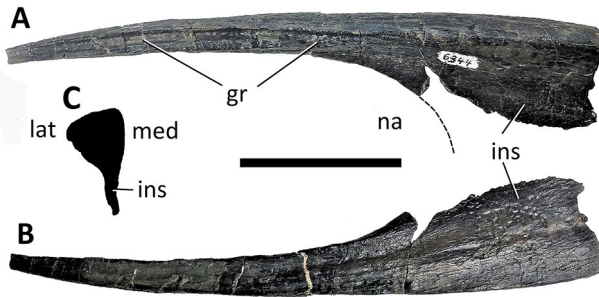


**Figure 3.** *Brighstoneus simmondsi* gen. et sp. nov. (MIWG 6344), right dorsal process of premaxilla in **A**, lateral and **B**, medial views. **C**, cross-section at anterior end. **Abbreviations:** **gr**, groove for anterodorsal process of nasal; **ins**, internarial septum; **lat**, lateral; **med**, medial; **na**, external naris. Scale bar = 50 mm.

### Maxilla

Both maxillae are present, with the left being the better preserved. The left maxilla (Fig. 4) is almost complete, although it has lost parts of the anterior ends of the anteroventral and anterodorsal processes. Between the anterior processes a fragment of bone has been glued into a position that is probably anatomically incorrect (Fig. 4A, C). The ascending process is almost complete, having a thin fractured margin, but preserving the groove for reception of the maxillary process of the premaxilla. The maxilla has been subjected to minor transverse lateral compression that has slightly relocated the incomplete jugal process medially.

The maxilla is a robust bone but is relatively thinner in dorsal and ventral views than that of *Mantellisaurus atherfieldensis* (NHMUK PV R5764). Its general shape in lateral view is of an anteroposteriorly expanded triangle. The apex is directed dorsally as the ascending process but is situated in a markedly posterior position, and if complete the section anterior to this process would have been approximately twice the length of the posterior section. A ratio of  $\sim 2.0$  or higher is also seen in *Altirhinus kurzanovi* (2.1: Norman 1998), *Zhanghenglong yangchengensis* (2.3: Xing *et al.* 2014), *Protohadros byrdi* (2.3: Head 1998), *Proa valdearinnoensis* (2.4: McDonald *et al.* 2012a) and *Ouranosaurus nigeriensis* (2.6: Taquet 1976). In contrast the ratio is 1.4 in *Mantellisaurus atherfieldensis* (NHMUK PV R5764). In lateral view the ventral edge of the maxilla is shallowly concave, the tooth row being almost straight for most of its length. There are 29 tooth positions: most of the alveoli are empty but two established and two emerging replacement crowns are present (see below). In ventral view the tooth row is straight for most of its length but posteriorly the last quarter curves laterally. The bone preservation of the lateral surface is better in the right maxilla, which has eight small

nutrient foramina (1–3 mm in diameter) that open anterolaterally and form an anteroposteriorly orientated row in the ventral half of the maxilla. Anteriorly, the ventral surface of the maxilla forms an anteroventral process that, although incomplete, follows the curve of the tooth row and tapers anteriorly in lateral view. The first alveolus is situated at the base of this process, anterior to which the process is edentulous. Although the area dorsal to the anteroventral process has suffered some damage, a prominent anterodorsal process is present. Posteriorly the transverse cross-section of this process is triangular with a gently dorsoventrally concave lateral surface, a flat ventromedial surface and a dorsomedial surface that is roughened and has a longitudinal groove in its posterior section. Extending anteriorly, the process becomes increasingly compressed transversely to form a thin blade, whose end is missing. Possession of an anterodorsal process is considered ancestral for Archosauria (Wagner & Lehman 2009) and has been employed as a character in iguanodontian phylogeny (e.g. Sues & Averianov 2009; Xing *et al.* 2014; McDonald *et al.* 2017). Its presence has been used to distinguish Saurolophinae from Lambeosaurinae (Wagner & Lehman 2009), but it is also present in non-hadrosaurids such as *Altirhinus kurzanovi* (Norman 1998), *Bactrosaurus johnsoni* (Godefroit *et al.* 1998), *Eolambia caroljonesa* (CEUM 35492: McDonald *et al.* 2012b) and *Gilmoresaurus mongoliensis* (Prieto-Márquez & Norell 2010), and is especially prominent in *Protohadros byrdi* (Head 1998).

The anterior and posterior dorsal edges of the lateral wall of the maxilla meet to form the apex of the transversely compressed ascending process. The jugal process arises from the base of the posterior edge of the ascending process (Fig. 4A, D). The trough between the jugal process and lateral body of the maxilla expands posteriorly to form a mediolaterally broad ectopterygoid shelf. When viewed dorsally the posterior maxilla is more ovoid (long axis anteroposterior) and the medial wall more convex than in *Mantellisaurus atherfieldensis* (NHMUK PV R5764). Below the apex of the ascending process and situated posteriorly is a depressed area, which would presumably have contributed to the antorbital fenestra and might have formed a small antorbital fossa (Fig. 4A). This depressed area is also present in *Iguanodon bernissartensis* (Norman 1980), *Mantellisaurus atherfieldensis* (NHMUK PV R5764), *Ouranosaurus nigeriensis* (Taquet 1976), *Camptosaurus dispar* (Gilmore 1909) and *Bolong yixianensis* (Wu & Godefroit 2012). There is no evidence of an antorbital fenestra in *Altirhinus kurzanovi* (Norman 1998) or *Jinzhousaurus yangi* (Wang & Xu 2001; Barrett *et al.* 2009) and this feature is not described in *Equijubus*

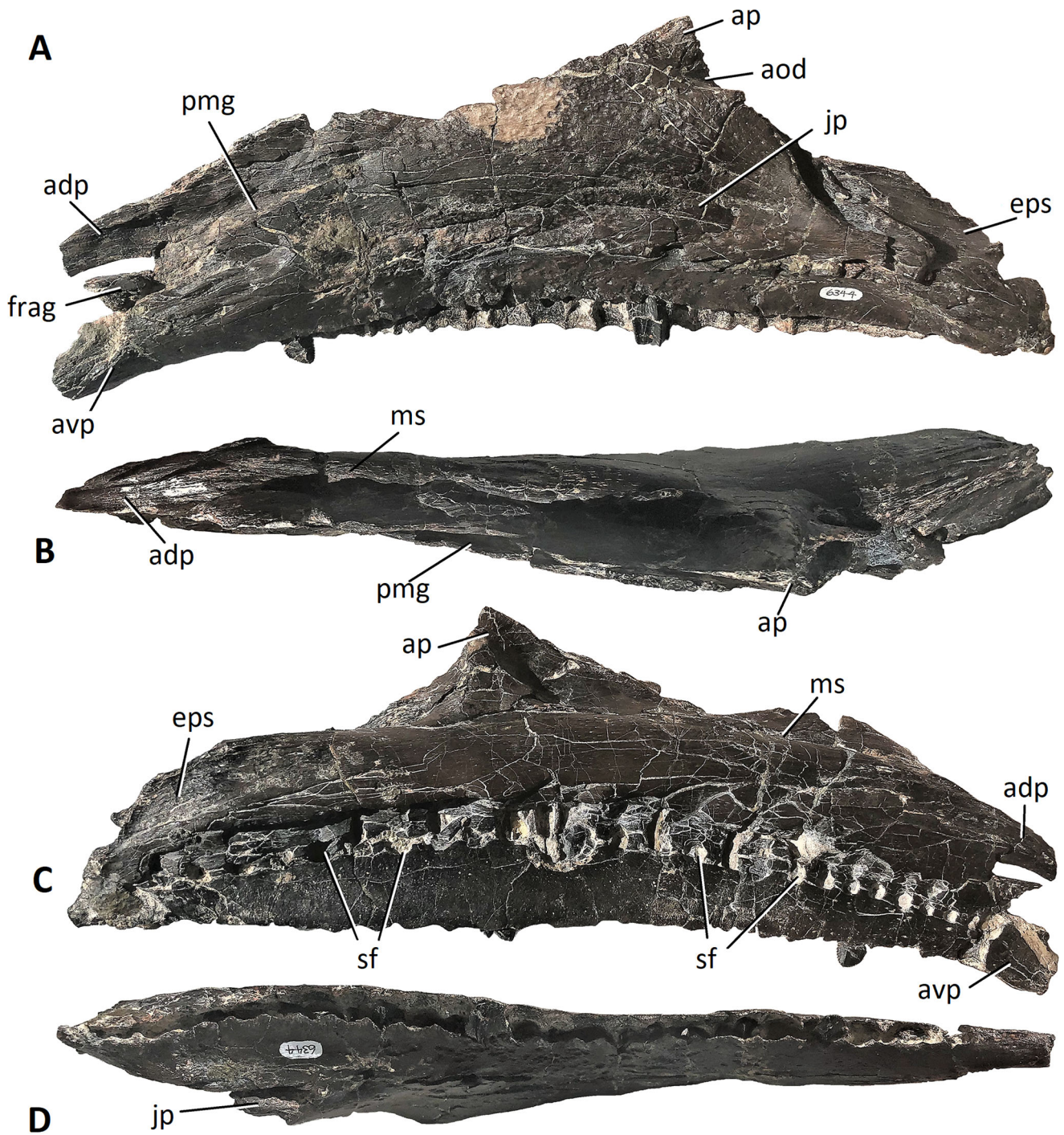


**Figure 4.** *Brighstoneus simmondsi* gen. et sp. nov. (MIWG 6344), left maxilla in **A**, lateral, **B**, dorsal, **C**, medial and **D**, ventral views. **Abbreviations:** **adp**, anterodorsal process; **aod**, antorbital depression; **ap**, ascending process; **avp**, anteroventral process; **eps**, ectopterygoid shelf; **frag**, fragment of bone, probably erroneously placed; **jp**, jugal process; **ms**, medial shelf; **pmg**, premaxillary groove; **sf**, special foramina. Scale bar = 100 mm.

*normani* (McDonald *et al.* 2014). Anteriorly, the lateral part of the dorsal surface is furrowed to form the premaxillary groove for contact with the premaxilla (Fig. 4A, B). Medially the maxilla has a vertical surface that

has an elongate rectangular outline with the ascending process rising above its dorsal edge. Above the tooth row is a concave arcade of circular special foramina (*sensu* Edmund 1957) or replacement foramina (*sensu*

Jin *et al.* 2010), the curve of which is considerably deeper than the ventral edge (Fig. 4C). Between the special foramina and the tooth row the bone is thin with a textured surface and forms the alveolar parapet. Dorsally there is a medial shelf that is damaged anteriorly but appears to have a rounded edge.

### Nasal

Only the left nasal is preserved (Fig. 5). It is undistorted but broken at both ends, so missing the posterior articulation for the frontal and prefrontal. The nasal is elongate anteroposteriorly, relatively broad and convexly curved mediolaterally so that with its antimere the external surface formed a vault over the nasal cavity.

Anteriorly the nasal is divided into two processes. The anterodorsal process is dorsoventrally deeper in lateral view than the anteroventral process. The anterodorsal section, which articulated with the dorsal process of the premaxilla, is incomplete but the area that contributed to the posterior margin of the external naris is intact. The base of the anteroventral process is present showing that the nasal also made a contribution to the posteroventral margin of the external naris. There is no anteroventral process in *Iguanodon bernissartensis* (Norman 1980), *Mantellisaurus atherfieldensis* (Norman 1986), *Protohadros byrdi* (Head 1998), *Bactrosaurus johnsoni* (Godefroit *et al.* 1998), *Equijubus normani* (McDonald *et al.* 2014) or *Gobihadros mongoliensis* (Tsogtbaatar *et al.* 2019). In hadrosaurids an anteroventral process is usually present, for example in *Maiasaura peeblesorum* and *Gryposaurus notabilis* (Prieto-Márquez & Norell 2010) and is particularly prominent in *Brachylophosaurus canadensis* (Prieto-Márquez 2001) and *Edmontosaurus annectens* (Campione & Evans 2011). Among non-hadrosaurid hadrosauriforms, an abbreviated anteroventral process is present in *Altirhinus kurzanovi* (Norman 1998), with longer processes in *Ouranosaurus nigeriensis* (Taquet 1976), *Jinzhousaurus yangi* (Wang & Xu 2001; Barrett *et al.* 2009) and *Bolong yixianensis* (Wu & Godefroit 2012). The posterior margin of the external naris is almost straight and posteroventrally orientated. The ventral border of the lateral surface of the nasal has a shallowly bevelled surface (Fig. 5C, E) and presumably underlapped the maxillary process of the premaxilla as a scarf joint, although anteriorly there is also a slight groove along the dorsal edge of this surface. The nasals of *Gobihadros mongoliensis* and *Choyrodon barsboldi* have a grooved ventrolateral surface (Tsogtbaatar *et al.* 2019) and both appear to underlap the posterolateral process of the premaxilla; *Bactrosaurus johnsoni* (Godefroit *et al.* 1998) and *Altirhinus kurzanovi* (Norman 1998) are grooved along their ventral borders.

The medial border of the dorsal surface is grooved anteriorly in *Brighstoneus simmondsi*, presumably where it articulated with the dorsal process of the premaxilla, but tapers to a thin blade posteriorly that most likely formed a simple butt joint with its antimere (see Weishampel 1984) as in *Altirhinus kurzanovi* (Norman 1998) and *Jinzhousaurus yangi* (Barrett *et al.* 2009), although in *Ouranosaurus nigeriensis* the nasals are asymmetrical with one having a blade and the other a groove along the dorsal edge (Taquet 1976).

When viewed laterally in life position the dorsal border of the nasal is sinusoidal and forms a distinct anterior convexity with the most dorsal part of the curve situated posterior to the posterior border of the external naris. The section of the lateral wall of the nasal, posterior to the naris, is slightly convex in ventral view. Collectively these features would have produced a rounded bulge and formed a distinct step between the anterior and posterior sections of the nasal (Fig. 5E). This is less prominent but similar in shape and position to the nasal bulla of the iguanodontian *Muttaborrasaurus langdoni* (Bartholomai & Molnar 1981), although in *Muttaborrasaurus* the lateral walls are slightly concave. A high arched region, dorsal to the posterior narial, is also seen in *Altirhinus kurzanovi* (Norman 1998), *Choyrodon barsboldi* (Gates *et al.* 2018) and in some hadrosaurids, for example *Gryposaurus notabilis* (Lambe 1914) and *Kritosaurus navajovius* (Brown 1910). *Ouranosaurus nigeriensis* also has a rounded protuberance, but this is situated more posteriorly on both nasals, just anterior to the suture for the frontals (Taquet 1976), while *Jinzhousaurus yangi* has mediolaterally convex nasals with a sagittal depression between them (Barrett *et al.* 2009), a feature also seen in *Altirhinus kurzanovi* (Norman 1998) and *Choyrodon barsboldi* (Gates *et al.* 2018). There is no evidence of a sagittal trough in *Brighstoneus simmondsi*. Temporal and geographical separation, together with the pattern of phylogenetic relationships and variety of morphologies in these examples, suggests that nasal ornamentation evolved independently on several occasions in iguanodontids. This feature also appears to be unique among the Wealden Group iguanodontids.

### Jugal

Both jugals are preserved and are almost complete (Fig. 6). The dorsal sections of the postorbital process and the process overlapping the quadratojugal are broken.

It is a triradiate bone with an anteriorly directed maxillary process, a central dorsally projecting postorbital process and a posterior dorsally projecting quadratojugal process. Both jugals are very straight and narrow in

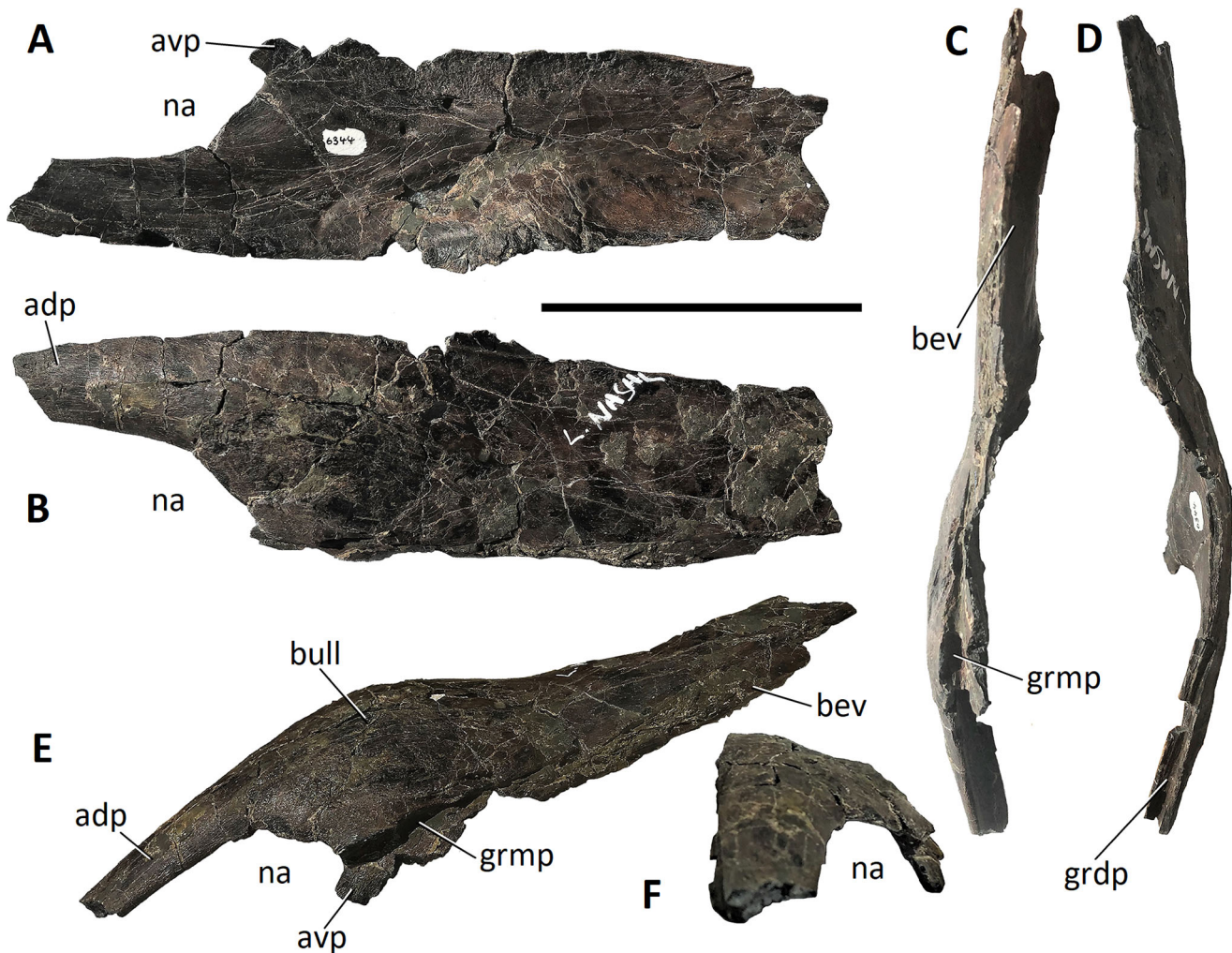


**Figure 5.** *Brighstoneus simmondsi* gen. et sp. nov. (MIWG 6344), left nasal in **A**, ventromedial (internal surface), **B**, dorsolateral (external surface), **C**, ventral, **D**, dorsal, **E**, lateral (in life position) and **F**, anterior views. **Abbreviations:** **adp**, anterodorsal process; **avp**, anterovernal process; **bev**, bevelled surface; **bull**, nasal bulla; **grdp**, groove for dorsal process of the premaxilla; **grmp**, groove for maxillary process of the premaxilla; **na**, external naris. Scale bar = 100 mm.

dorsal view (Fig. 6E, F) compared to *Mantellisaurus atherfieldensis* (NHMUK PV R5764), which is laterally convex with a relatively wider orbital shelf.

The maxillary process in lateral view occupies 60% of the total length of the jugal (ratio of length anterior to midpoint of postorbital process/maximum length = 0.60). This ratio varies considerably in iguanodontians, from 0.29 in *Xuwulong yueluni* (You *et al.* 2011) and 0.33 in *Iguanodon bernissartensis* (Norman 1980) to 0.56 in *Mantellisaurus atherfieldensis* (NHMUK PV R 5764) and 0.62 in *Ouranosaurus nigeriensis* (Taquet 1976). However, in most hadrosauriforms including hadrosaurids this ratio ranges between 0.40 and 0.54. For example, *Altirhinus kurzanovi* (0.46: Norman 1998), RBINS R57 (0.52: Norman 1986), *Equijubus normani* (0.49: You *et al.* 2003), *Eolambia caroljonesa* (0.48: McDonald *et al.* 2012b), *Brachylophosaurus*

*canadensis* (0.51: Prieto-Márquez 2001) and *Gryposaurus latidens* (0.48: Prieto-Márquez 2012). The maxillary process in lateral view is gently curved with a convex ventral margin and a concave dorsal margin. The process is quite gracile and lacks the dorsoventral expansion seen in many hadrosauriforms, such as those present in *Probactrosaurus gobiensis* (Norman 2002); *Eolambia caroljonesa* (McDonald *et al.* 2012b) and *Gobihadros mongoliensis* (Tsogtbaatar *et al.* 2019), instead the anterior dorsal margin slopes anteroventrally to join the ventral margin as a point. This slope forms a facet for articulation with the lacrimal. A maxillary process with a pointed end, lacking dorsoventral expansion, is also seen in *Altirhinus kurzanovi* (Norman 1998), *Batyrosaurus rozhdestvenskyi* (Godefroit *et al.* 2012), *Dakotadon lakotaensis* (Weishampel & Bjork 1989) and *Choyrodon barsboldi* (Gates *et al.* 2018). The maxillary

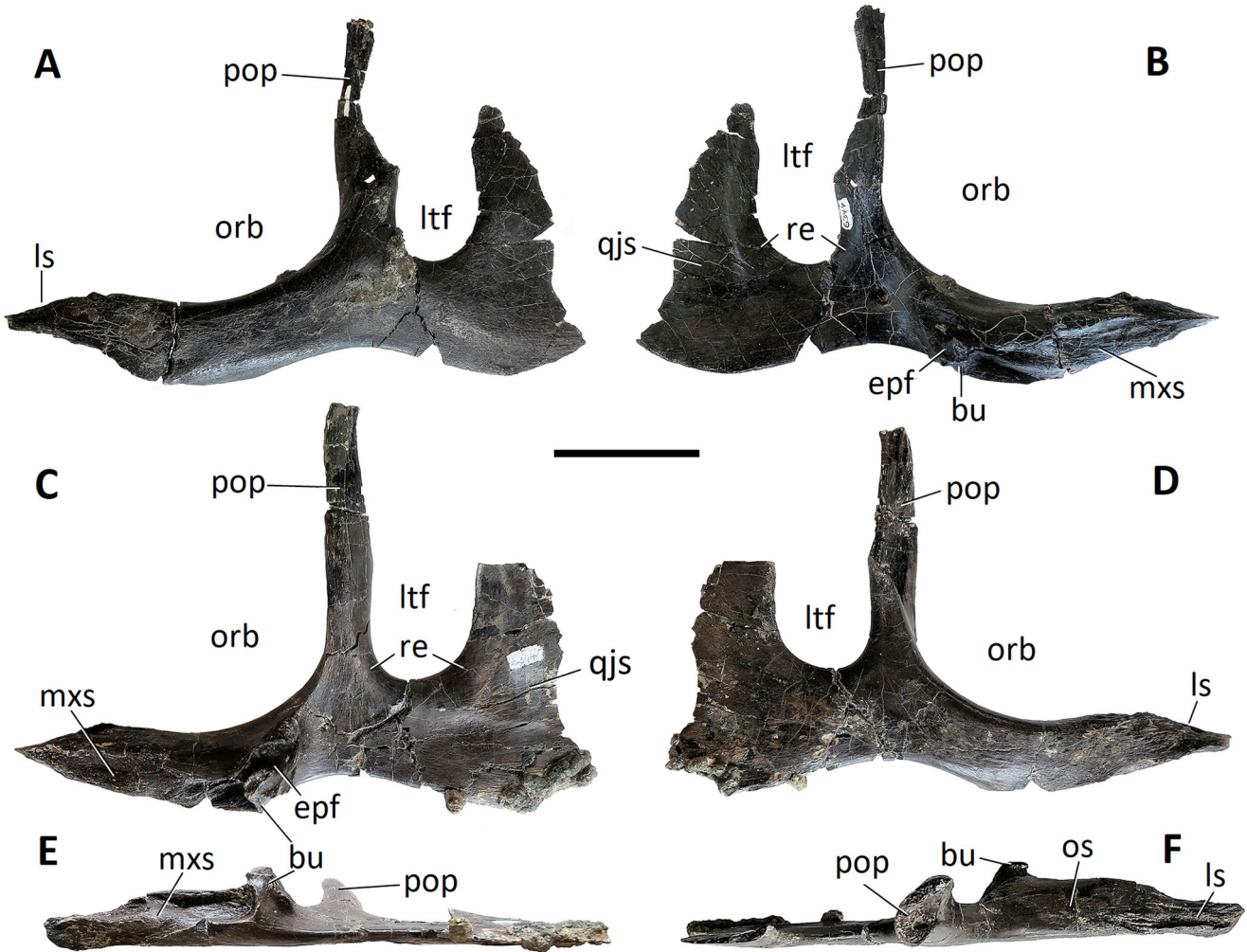


**Figure 6.** *Brighstoneus simmondsi* gen. et sp. nov. (MIWG 6344). Left (A, B) and right (C–F) jugals in A, lateral, B, medial, C, medial, D, lateral, E, ventral and F, dorsal views. **Abbreviations:** bu, buttress; epf, ectopterygoid facet; ls, lacrimal suture; ltf, lateral temporal fenestra; mxs, maxillary suture; orb, orbit; os, orbital shelf; pop, postorbital process; qjs, area of suture with the quadratojugal; re, rolled edge. Scale bar = 50 mm.

process of the jugal in *Mantellisaurus atherfieldensis* (NHMUK PV R 5764) is not dorsoventrally expanded but has a much blunter, less tapered anterior end, albeit with some damage ventrally. Medially the maxillary process is deeply excavated to form an anteroposteriorly elongate facet with a roughened surface for reception of the finger-like jugal process of the maxilla. The jugal is expanded medially at the posterior end of the maxillary facet to form a buttress (Fig. 6E, F) for the distal end of the jugal process of the maxilla. Posterior to the maxillary facet is a posterodorsally orientated ridge that separates the facet from a shallow oval fossa for the ectopterygoid. Between the maxillary and postorbital processes, the dorsal surface is concave in lateral view and provided a shelf, forming the ventral margin of the orbit. The orbit is bounded posteriorly by the postorbital process, which is long, straight and ascends

perpendicular to the main axis of the jugal body. Dorsally it develops an anterolaterally facing facet for suture with a reciprocal facet on the jugal process of the postorbital. Between the postorbital process and the quadratojugal process is a ‘U’-shaped embayment that forms the ventral border of the lateral temporal fenestra. On its medial surface, the posterior and ventral margins of the fenestra have a subtle, smooth and shallowly convex rolled edge (Fig. 6B, C), which is not readily apparent in other hadrosauriforms, including *Mantellisaurus atherfieldensis* (NHMUK PV R 5764), *Eolambia carolinjonesa* (McDonald *et al.* 2012b) and *Sirindhorna khora-tensis* (Shibata *et al.* 2015).

The right jugal has a nutrient foramen ~1 mm in diameter, located medially below the ventral border of the fenestra and postorbital process, while on the left jugal two foramina are present (with diameters of 4 mm

and 2 mm). The presence or absence of a relatively large foramen ventral to the postorbital process is a character used by McDonald *et al.* (2017: character 51), but the configuration in *Brighstoneus simmondsi* suggests that there may be considerable individual variation in this feature, perhaps calling into question its phylogenetic utility.

In lateral view, the ventral border of the jugal is sinuous, being concave ventral to the postorbital process and convex ventral to the maxillary and quadratojugal processes, the latter forming the ventral flange of the quadratojugal process (Fig. 6). The posterior border of the quadratojugal process is slightly concave in its ventral half, although the posteroventral corner of the ventral flange is developed posteriorly and forms an angular heel-like expansion, although damage makes the full extent of this unknown. Posterior expansion of the ventral flange is seen in *Camptosaurus dispar* (Gilmore 1909), *Equijubus normani* (McDonald *et al.* 2014: where it is spur-like), *Zalmoxes robustus* (Weishampel *et al.* 2003) and *Z. shqiperorum* (Godefroit *et al.* 2009), although in *Zalmoxes* spp. this is due to the presence of a posterior quadratojugal recess that is not present in other iguanodontians. On the medial surface of the posterior process a faint ridge extends anteroposteriorly, slightly ventral to the ventral margin of the lateral temporal fenestra. Above this is a roughened area that presumably denoted the area of overlap with the quadratojugal, although this is neither as deeply marked nor as well-defined as in *Mantellisaurus atherfieldensis* (NHMUK PV R 5764), *Altirhinus kurzanovi* (Norman 1998), *Probactrosaurus gobiensis* (Norman 2002) or *Zalmoxes robustus* (Weishampel *et al.* 2003). Faint muscle scars are present on the medial surface of the heel area.

### Palpebral

Only the left palpebral is preserved (Fig. 7). It is largely complete although the posterior tip is a recent fracture, so it is unknown whether an accessory palpebral was present. An accessory palpebral is known in *Iguanodon bernissartensis* (Norman 1980) and *Jinzhouosaurus yangi* (Barrett *et al.* 2009). Anteriorly the palpebral has an ovate and anteroposteriorly concave articular surface that faces anteromedially, presumably for articulation with the convex surface of the prefrontal. It extends posteriorly as a tapering process that is almost straight and dorsoventrally compressed in lateral view but broader and curved with concave internal and convex external surfaces in dorsal and ventral views. The ventral and medial surfaces are smooth, but the lateral and dorsal surfaces are rugose. The posterior rim of the articular surface is expanded medially, forming a process that

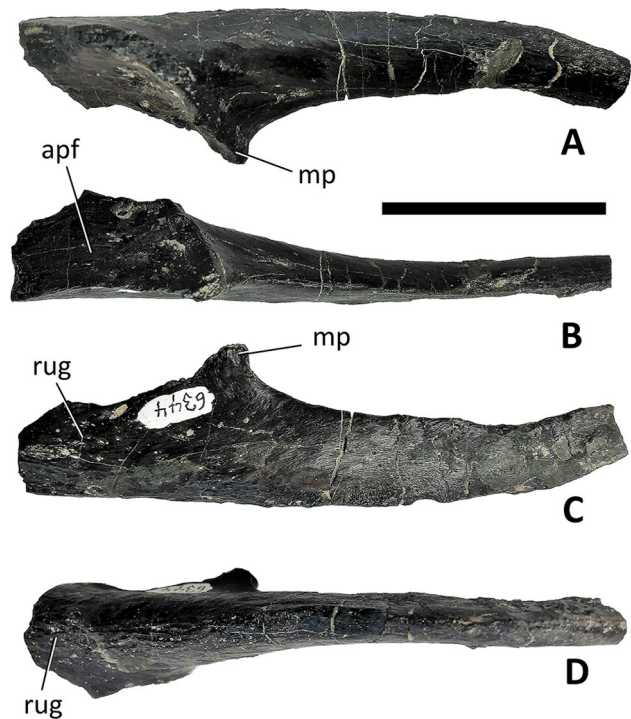


**Figure 7.** *Brighstoneus simmondsi* gen. et sp. nov. (MIWG 6344), left palpebral in **A**, ventral, **B**, medial, **C**, dorsal and **D**, lateral views. **Abbreviations:** **apf**, articular surface with prefrontal; **mp**, medial process; **rug**, rugosity. Scale bar = 50 mm.

stands proud of the main body of the palpebral (Fig. 7A, C), such that when articulated the body of the palpebral would have been raised clear of the prefrontal and postorbital. A similar palpebral is found in RBINS R57 (formerly known as IRSNB 1551: Norman 1986), *Ouranosaurus nigeriensis* (Taquet 1976), *Altirhinus kurzanovi* (Norman 1998), *Bactrosaurus johnsoni* (Godefroit *et al.* 1998), *Bolong yixianensis* (Wu & Godefroit 2012), *Gobihadros mongoliensis* (Tsogtbaatar *et al.* 2019) and *Xuwulong yueluni* (You *et al.* 2011). The body of the palpebral is more rod-like in *Tethyshadros insularis* (Dalla Vecchia 2009) and it has been suggested that it became fused with the prefrontals in hadrosaurids (Maryńska & Osmólska 1979).

### Predentary

The predentary is exceptionally well preserved but slightly compressed transversely (Fig. 8). In dorsal view it has a horseshoe-shaped outline, with the convex anterior section overlying the dentary symphysis, and almost parallel lateral processes extending posteriorly, which curve slightly medially in their distal portions. This is similar to the ‘U’-shape seen in all non-hadrosaurid hadrosauriforms except for *Proa valdearinnoensis* (McDonald *et al.* 2012a), in which the sides diverge

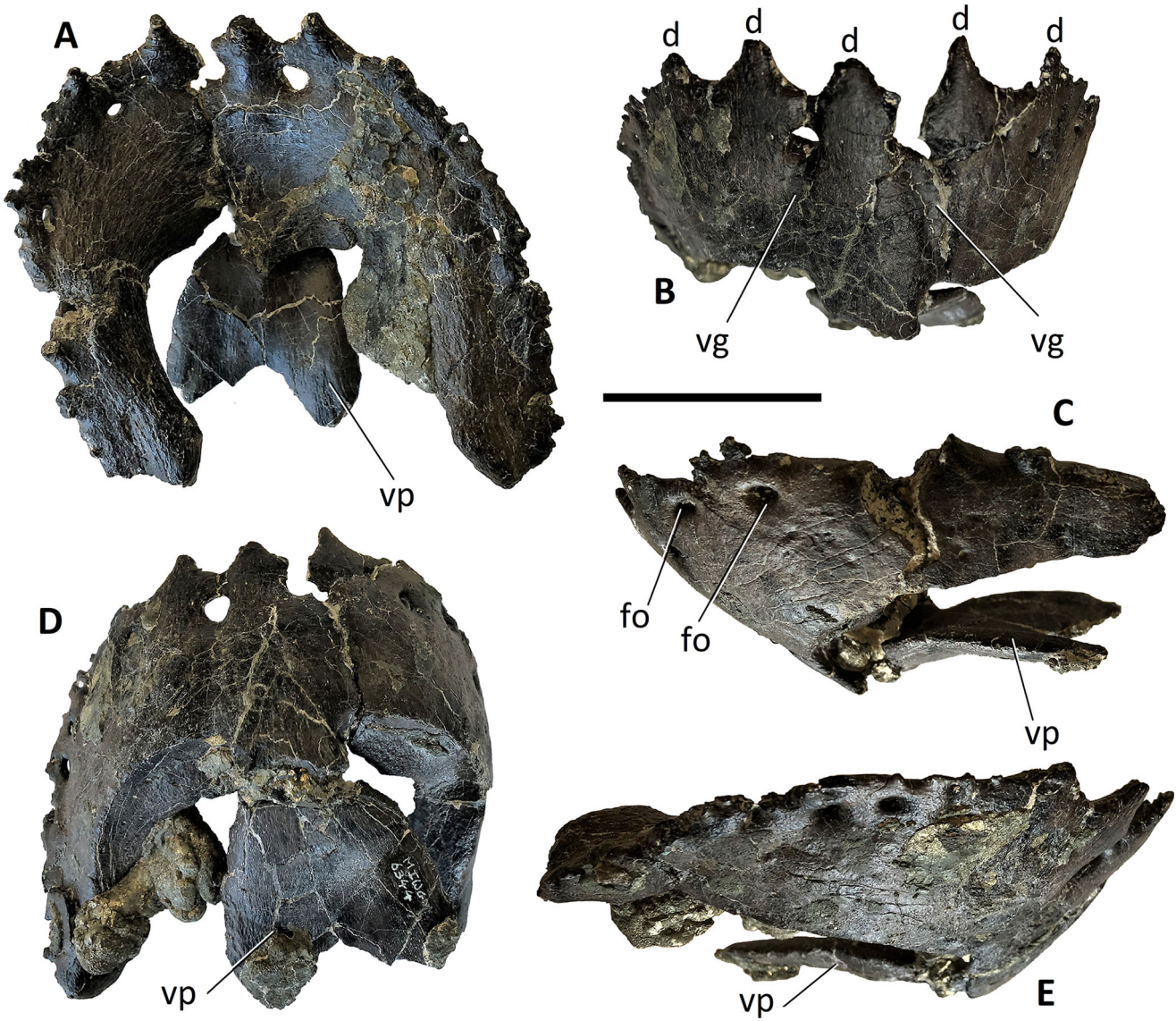


**Figure 8.** *Brighstoneus simmondsi* gen. et sp. nov. (MIWG 6344), predentary in **A**, dorsal, **B**, anterior, **C**, left lateral, **D**, ventral and **E**, right lateral views. **Abbreviations:** **d**, denticle; **fo**, foramina; **vg**, vascular groove; **vp**, ventral process. Scale bar = 50 mm.

posteriorly and form a ‘V’-shaped angle of  $\sim 50^\circ$  anteriorly. The ventral surface is bevelled and fits against a groove on the anterior dentaries. The lingual surface has a rough texture compared to the smooth ventral and lateral surfaces. There is no posteriorly projecting dorso-medial process extending in the sagittal plane from the posterodorsal surface of the ventral process, nor a dorso-medial process arising from the distal lateral processes. A dorsomedial process is known in *Eotrachodon orientalis* (Prieto-Márquez *et al.* 2016), *Plesiohadros djadokhtaensis* (Tsogtbaatar *et al.* 2014), *Proa valdearinnoensis* (McDonald *et al.* 2012a), *Iguanacolossus fortis* (McDonald *et al.* 2010a) and *Bayannurosaurus perfectus* (Xu *et al.* 2018), and on the distal lateral processes in *Gobihadros mongoliensis*

(Tsogtbaatar *et al.* 2019) and *Plesiohadros djadokhtaensis* (Tsogtbaatar *et al.* 2014). However, in *Brighstoneus simmondsi* a midline process arises from the ventral surface and projects posteriorly as a bilobed ‘heart-shaped’ structure, which has a similar morphology to the process in *Proa valdearinnoensis* (McDonald *et al.* 2012a) and *Bayannurosaurus perfectus* (Xu *et al.* 2018). It is likely that this would have enclosed the ventral surfaces of the dentaries, thereby bracing the symphysis. The lateral walls of the predentary curve convexly dorsoventrally, while anteriorly the surface is flatter and directed anterodorsally forming a slope of  $\sim 45^\circ$ . The entire occlusal margin is highly irregular, with five prominent denticles anteriorly, the central one situated sagittally. These denticles are pointed and prominent with distinct concave

mesial and distal edges, giving the interdenticle spaces a circular appearance. More posteriorly, some of the irregularity probably represents much smaller denticles. Prominent anterior denticles are reported widely across Iguanodontia from *Tenontosaurus dossi* (Winkler *et al.* 1997) to hadrosaurids, for example *Eotrachodon orientalis* (Prieto-Márquez *et al.* 2016). Below the occlusal margin is a series of foramina. The largest of these foramina are situated anteriorly on either side of the median denticle and, although the area has some damage, there appear to be ventrally directed vascular grooves associated with them.

### Dentary

Both dentaries are preserved with little distortion (Fig. 9). The left dentary has a damaged and incomplete symphysis. In lateral view, the dentary forms an elongate rectangle that is ventrally deflected anteriorly. The dorsal edge of the dentary is straight apart from anteriorly where it initially curves convexly. The ventral edge in lateral view forms a gentle concave arc so that the depth of the dentary is lowest in the central section and greatest in the anterior and posterior sections. The posterior-most part of the ventral margin is missing in both dentaries.

Anteriorly the ventral deflection of the dentary twists so that its medial wall faces dorsally, while also curving medially to meet its antimeres at the symphysis. When viewed laterally the anterior margin of the ventrally deflected section is slightly concave. In dorsal view, the medial margin of the symphysis and the lateral margin of the dentary diverge posteriorly. Ventral deflection of the dentary symphysis is common in iguanodontians. In early-diverging taxa such as *Zalmoxes robustus* (Weishampel *et al.* 2003), *Tenontosaurus tilletti* (Thomas 2015), *Mochlodon vorosi* (Ösi *et al.* 2012) and *Dysalotosaurus lettowvorbecki* (Hübner 2010) the dentary is almost straight, but the distal tip is deflected slightly. In *Brighstoneus simmondsi* there is a more pronounced ventral deflection of the anterior third of the body, the ventral border of which, in lateral view, forms an angle of 16° with the ventral border of the midsection. The range of deflection angles in hadrosauriforms varies, but *Brighstoneus simmondsi* has a similar angle to that found in *Proa valdearinnensis* (18°: McDonald *et al.* 2012a), *Mantellisaurus atherfieldensis* (20°: NHMUK PV R5764: Fig. 10), *Batyrosaurus rozhdzhevskiyi* (15°: Godefroit *et al.* 2012) and *Choyrodon barsboldi* (19°: Gates *et al.* 2018). Some hadrosaurids have much greater deflections and several non-hadrosaurid taxa are not deflected at all, including *Ouranosaurus nigeriensis* (Taquet 1976), *Hypselospinus*

*fittoni* (Norman 2015) and *Kukufeldia tilgatensis* (McDonald *et al.* 2010b).

The tooth row includes 28 alveolar positions although a small pit at the anterior end of the row of the right dentary may signify a further diminutive alveolus. This represents the highest number of dentary alveolar positions recorded in any hadrosauriform taxon that possesses one active and one replacement crown per alveolar position and alveolar septa shaped by the teeth (Supplementary material, Table S2), in contrast to more deeply nested taxa with higher numbers of replacement teeth. Other non-hadrosaurid hadrosauriforms with similar alveolar counts first appeared in the Cenomanian with 30 in *Eolambia caroljonesa* (Kirkland 1998; McDonald *et al.* 2012b) and 28 in *Protohadros byrdi* (Head 1998), although both of these taxa possess more hadrosaurid-like dentaries with parallel-sided alveolar septa as well as more teeth in each tooth position (two active and two replacement teeth for each alveolar position in the former [McDonald *et al.* 2012b] and at least three and possibly four teeth per tooth file in the latter [Head 1998]). In dorsal view the alveolar row forms a slight sigmoid curve but is essentially straight for most of its length, except posteriorly where it curves laterally to meet the base of the coronoid process. The alveolar septa are not parallel and reflect tooth crown shape. This is the usual morphology in early-diverging hadrosauriforms such as *Altirhinus kurzanovi* (Norman 1998), *Fukuisaurus tetoriensis* (Kobayashi & Azuma 2003), *Proa valdearinnensis* (McDonald *et al.* 2012a), *Lanzhousaurus magnidens* (You *et al.* 2005), *Mantellisaurus atherfieldensis* (NHMUK PV R5764) and *Iguanodon bernissartensis* (Norman 1980). In more derived hadrosauriforms such as *Probactrosaurus gobiensis* (Norman 2002), *Bactrosaurus johnsoni* (Godefroit *et al.* 1998) and all hadrosaurids the alveolar walls are parallel (Horner *et al.* 2004). In *Brighstoneus simmondsi* the tooth sizes (estimated from the mesiodistal diameters of alveoli) are maximal in the mid-section of the tooth row and become progressively smaller at both ends. In dorsal view the alveolar row is situated medially, as in all iguanodontians, while laterally there is a buccal shelf that is widest posteriorly (Fig. 9E, F). There appears to be a relative difference in the width of this shelf between the two dentaries, with the right side being bulkier, especially in its posterior half, although this has been exaggerated by an area of taphonomic crushing. The buccal shelf of *Brighstoneus simmondsi* tapers anteriorly but extends to the end of the tooth row and, as in *Ouranosaurus nigeriensis* (Taquet 1976), *Sirindhorna khoratensis* (Shibata *et al.* 2015) and *Zhanghenglong yangchengensis* (Xing *et al.* 2014), is a relatively narrow structure. In most non-hadrosaurid

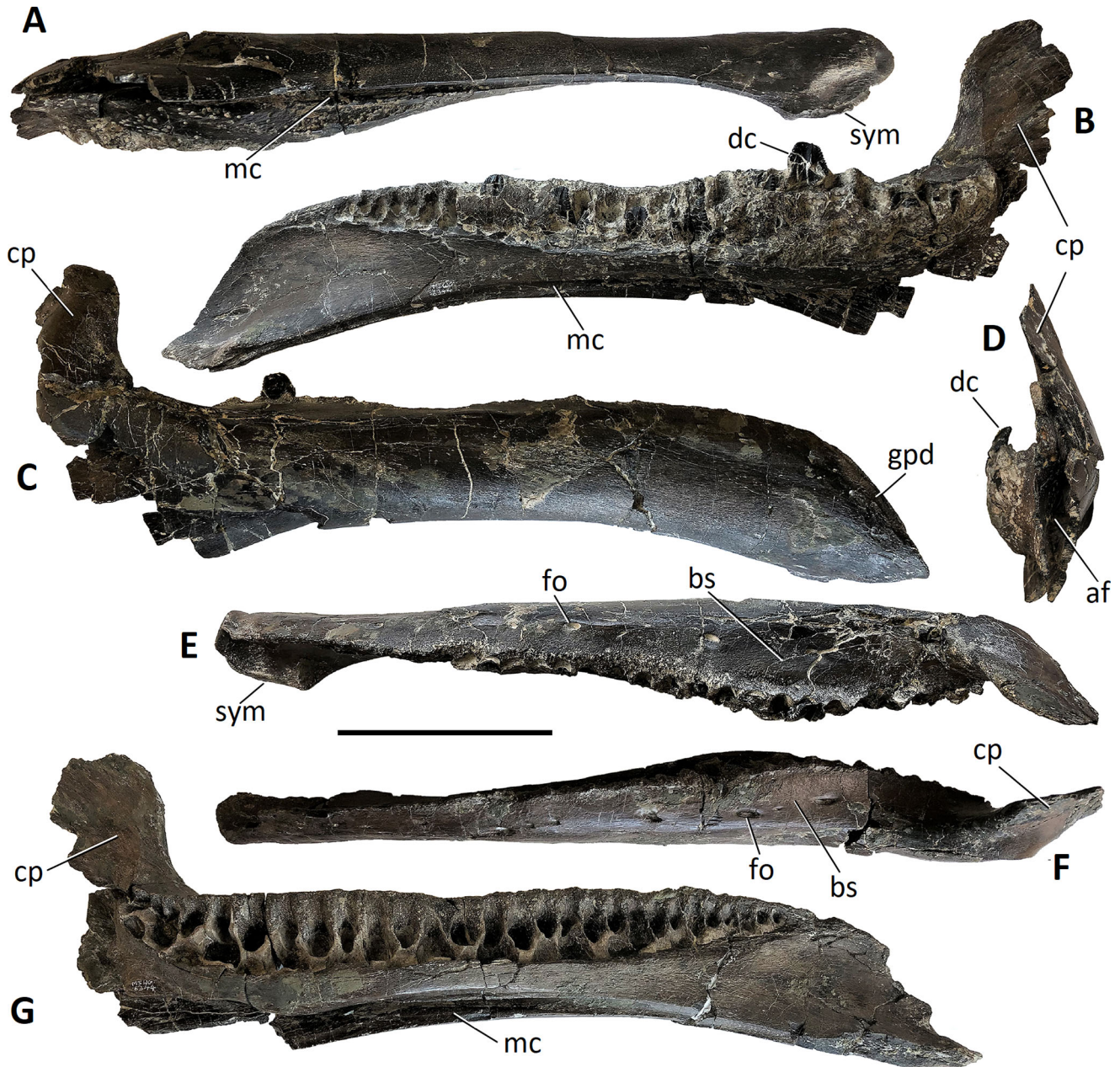


**Figure 9.** *Brighstoneus simmondsi* gen. et sp. nov. (MIWG 6344), right (A–E) and left (F, G) dentaries in A, ventral, B, medial, C, lateral, D, posterior, E, dorsal, F, dorsal and G, medial views. **Abbreviations:** af, adductor fossa; bs, buccal shelf; cp, coronoid process; dc, dentary crown; fo, foramen; gpd, groove for predentary; mc, Meckelian canal; sym, symphysis. Scale bar = 100 mm.

hadrosauriforms the shelf has a relatively greater transverse width, especially posteriorly, including in *Iguanodon bernissartensis* (Norman 1980), *Mantellisaurus atherfieldensis* (NHMUK PV R5764), *Proa valdearinoensis* (McDonald *et al.* 2012a), *Eolambia caroljonesa* (McDonald *et al.* 2012b) and *Shuangmiaosaurus gilmorei* (You *et al.* 2003), with a markedly wider shelf in *Bactrosaurus johnsoni* (Godefroit *et al.* 1998) and *Probactrosaurus gobiensis*

(Norman 2002). The shelf has a steep margin that forms the lateral wall of the dentary. This is predominantly dorsoventrally convex but becomes vertically flat anterior to the sixth tooth position. There are several large foramina along the dorsolateral surface. Anteriorly these are replaced by pairs of smaller, closely associated foramina that are orientated dorsoventrally, signifying bifurcation of the arteries prior to exiting the dentary. In both dentaries there are four nutrient foramina arranged

along the inflected section of the dentary as it descends to the symphysis. In dorsal view, the middle section of the lateral wall is slightly convex.

Anteriorly the tooth row is preceded by a diastema of approximately three tooth positions in length, as also seen in *Choyrodon barsboldi* (Gates *et al.* 2018), *Mantellisaurus atherfieldensis* (NHMUK PV R5764) and *Bolong yixianensis* (Wu & Godefroit 2012). There is no diastema in *Dakotadon lakatoensis* (Weishampel & Bjork 1989) or *Fukuisaurus tetoriensis* (Kobayashi & Azuma 2003) and only a short diastema in *Iguanodon bernissartensis* (Norman 1998). The edentulous rim almost immediately begins to descend ventrally leaving only a small horizontal element, before forming a moderately long convex arc that broadens transversely to form an articular surface for the predentary.

On the medial wall of the dentary below the tooth row, an anteroposteriorly orientated line of special (replacement) foramina is present, forming a ventrally convex arcade, although the dorsal margins of the foramina and the alveolar parapet are largely incomplete in both dentaries. Those foramina that remain intact are elliptical in outline with their long axes extending anteroposteriorly. The Meckelian canal is exposed ventrally and becomes broader posteriorly, eventually merging with the adductor fossa. The adductor fossa is undistorted and narrower than in *Mantellisaurus atherfieldensis* (NHMUK PV R5764). The Meckelian canal is visible on the right dentary as little more than a groove in the anterior third, which ends just anterior to the first alveolar position. Anterior to this is a flat surface that extends for a few millimetres separating the Meckelian canal from the groove for the predentary. The alveolar parapet and all the teeth are missing from the left dentary, although the alveolar sockets are perfectly preserved. The first four alveolar sockets are round and small. There is a replacement tooth socket placed medial to the alveolus for the functional dentary crown.

The medial surface of the coronoid process is divided into anterodorsal and posteroventral areas by a low ridge, which extends diagonally across the surface in an anteroventral direction to meet the most posterior alveolar socket at the midpoint of the base of the coronoid process. The posteroventral area is heavily striated with the striae lying parallel to the ridge. This contrasts with *Mantellisaurus atherfieldensis* (NHMUK PV R5764), where there is a much more pronounced ridge but weaker striae. There is no buccal platform in *Brighstoneus simmondsi* separating the base of the coronoid process from the tooth row and the posterior alveoli excavate the base of the coronoid process. The absence of a buccal platform is plesiomorphic in iguanodontians and is common in hadrosauriforms prior to the

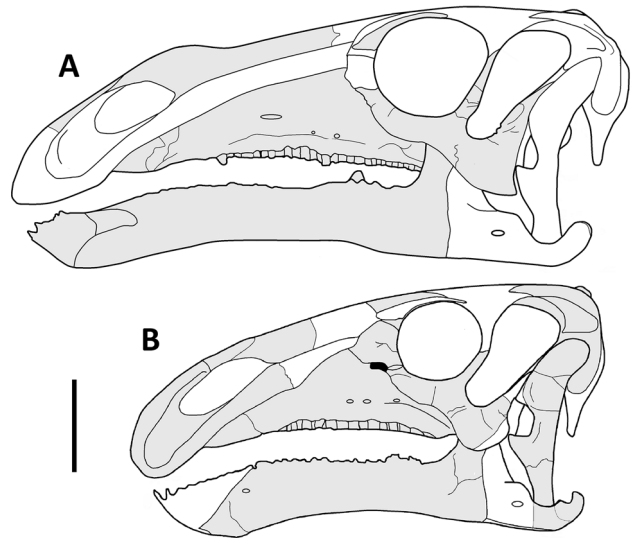


**Figure 10.** Preliminary reconstructions of the skulls of **A**, *Brighstoneus simmondsi* gen. et sp. nov. (MIWG 6344) and **B**, *Mantellisaurus atherfieldensis* (NHMUK PV R5764) in lateral view. Shaded areas represent material present in the holotypes. Scale bar = 100 mm.

Aptian, for example *Mantellisaurus atherfieldensis* (NHMUK PV R5764), *Iguanodon bernissartensis* (Norman 1980), *Hypselospinus fittoni* (Norman 2015), *Hippodraco scutodens* (McDonald *et al.* 2010a) and *Lanzhousaurus magnidens* (You *et al.* 2005), with the possible exception of *Tenontosaurus tilletti* (Thomas 2015). By the Albian its presence in iguanodontians becomes almost universal.

## Dentition

**Maxillary dentition.** The left maxilla preserves three crowns, one broken, one emergent and one in position six that is nearly complete and leaf-shaped with no wear facet (Fig. 11B, H). The lingual side of this crown is not as heavily coated with enamel as the labial surface. The labial surface of the crown has a strong and straight primary ridge, which extends from the base of the crown to its apex and is set distally, dividing the crown at its widest point into a distal third and a mesial two-thirds. A primary ridge, set distally to this degree, is also seen in *Bayannurosaurus perfectus* (Xu *et al.* 2018) and *Altirhinus kurzanovi* (Norman 1998). As the apex is set so far distally the crown is asymmetrical with a more gently convex curve mesially, which bears more marginal denticles (14 mesially, although the base is damaged, and the total count was probably nearer 20, *vs* nine on the distal margin). The marginal denticles are wedge-shaped and distally larger, more robust and obliquely positioned, whereas mesially they are set more vertically. The apical margins are mammillated, with up

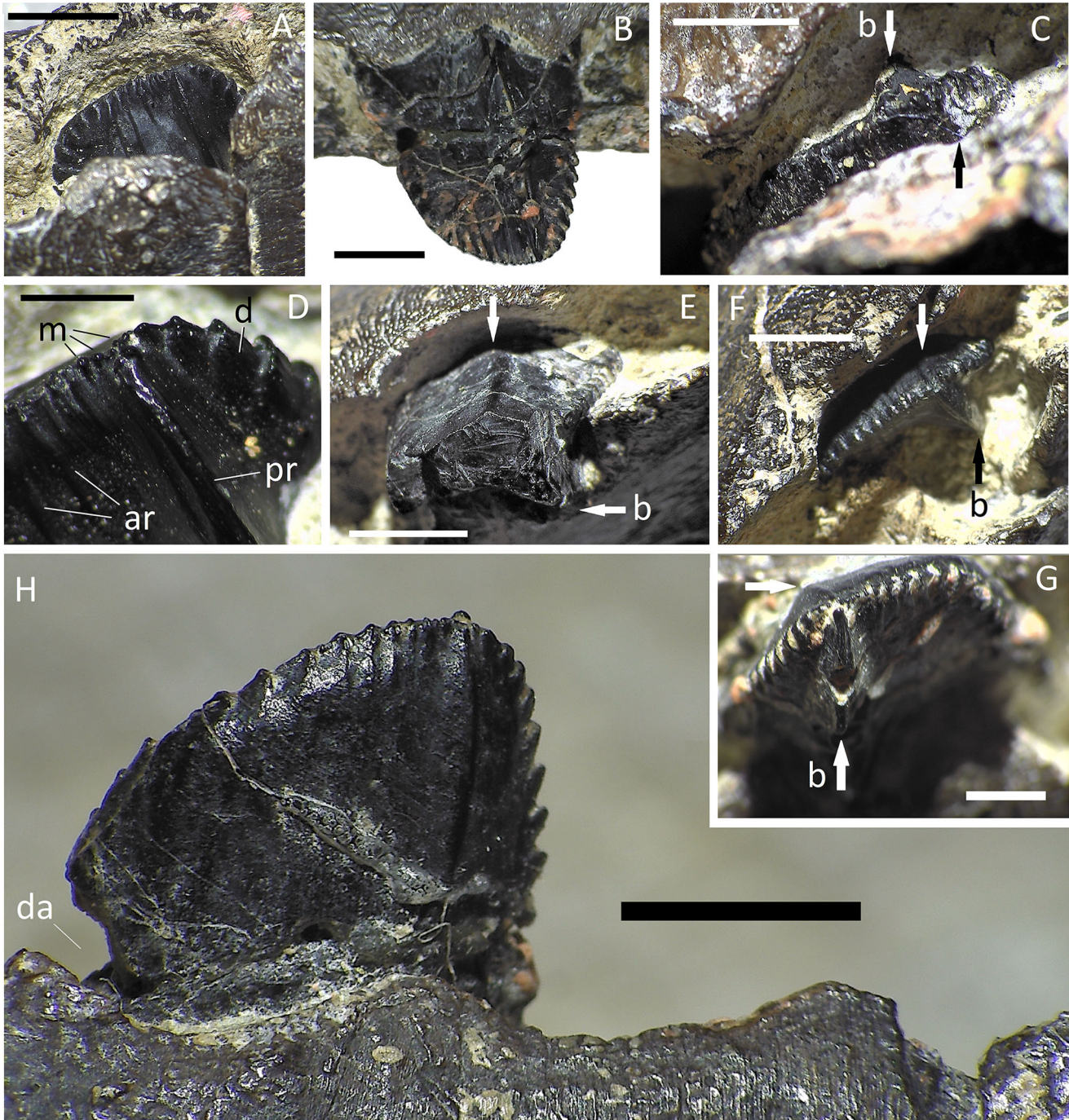


**Figure 11.** *Brighstoneus simmondsi* gen. et sp. nov. (MIWG 6344), maxillary crowns. **A**, right crown in buccal view; **B**, left crown in buccal view; **C**, left broken crown dorsal view; **D**, close-up of **A** showing mammillae on denticles; **E**, left broken crown in ventral view; **F**, ventral view of **A**; **G**, left crown in ventral view; **H**, lingual view of **B** showing primary and accessory ridges. Arrow labelled **b** = buccal primary ridge, unlabelled = lingual ridge. **Abbreviations:** **ar**, accessory ridge; **d**, denticle; **da**, damaged area; **m**, mammilla; **pr**, primary ridge. Scale bars = 5 mm (**A**, **B**, **C**, **E**, **F**, **H**) and 2 mm (**D**, **G**).

to three small, spherical mammillae arranged labiolingually on the marginal denticles approaching the apical region of the crown, reducing to one or two at the apex. An emergent crown on the left maxilla has three or four

mammillae, reducing to two at the apex, implying that the numbers are variable within the dentition. The mammillae are not as pronounced as on the dentary crowns (see below).

Accessory ridges are present on the labial surface, situated mesial to the primary ridge. In the complete crown there are six accessory ridges: the distal four extend basally but the mesial two terminate very rapidly. Five accessory ridges are visible on the emergent crown in the left maxilla. Other crowns are more damaged but appear consistent with this morphology.

The complete crown on the left maxilla is also visible lingually. There is a primary ridge on this surface, which is straight, extends up to the alveolar margin and is distally offset, mirroring the position of the primary ridge on the labial surface. This lingual ridge is much less prominent but appears to be a distinct feature rather than a change in slope between the lingual surface and the facet for the adjacent replacement crown. Under low power magnification some faint accessory ridges are visible, all located mesial to the primary ridge (Fig. 11H). A primary ridge on the lingual side of a maxillary crown has only been described in *Koshisaurus katsuyama* (Shibata & Azuma 2015), a contemporaneous basal hadrosauriform from the Kitidani Formation in Japan (Barremian–early Aptian), where the character was considered autapomorphic. No accessory ridges were observed on the lingual surface of the maxillary crowns of *Koshisaurus katsuyama* and to our knowledge are not reported in other iguanodontians. Among non-iguanodontians, in the basal ornithopod *Hypsilophodon foxii*, numerous faint longitudinal ridges are seen on the lingual surfaces of the maxillary teeth (Galton 1974). However, an isolated tooth referred to *Hypsilophodon foxii* shows stronger ridges on the lingual and labial maxillary tooth surfaces, although this feature is not described in the text (Galton 2009, fig. 3N, O). Within Iguanodontia, we regard the presence of primary and accessory ridges on the lingual surface of the maxillary crown as an autapomorphy of *Brighstoneus simmondsi*. This character is only properly observable on the one maxillary crown of *Brighstoneus simmondsi*, although a lingually placed primary ridge also appears to be present in some of the cross-sections of broken crowns (Fig. 11C, E, F, G), being perhaps more prominent anteriorly. A primary ridge is also seen on the lingual surface of a maxillary crown from another partial skeleton from the Wessex Formation of the Isle of Wight (IWCMS 2001.445), which is possibly referable to *Brighstoneus simmondsi*, but that is currently unprepared.

**Dentary dentition.** Several functional and emerging dentary crowns are present in the right dentary, of which three are sufficiently intact to allow a description. They are heavily enamelled and ornamented on their lingual surfaces. All are virtually complete, lack an occlusal wear facet and possess a marked primary ridge that is placed slightly distal to the midline, marking the apex

of the tooth, thus making the crown slightly asymmetrical (Fig. 12). A distally placed primary apical ridge occurs in non-hadrosaurid hadrosauriforms such as *Iguanodon bernissartensis* (Norman 1980), *Equijubus normani* (You *et al.* 2003) and *Telmatosaurus transsylvanicus* (Weishampel *et al.* 1993) but it is centrally positioned in most hadrosaurids such as *Edmontosaurus annectens* (Prieto-Márquez & Norell 2010) and *Lambeosaurus lambei* (Prieto-Márquez & Norell 2010) and may be either central or mesially positioned in earlier diverging ornithopods such as in *Hypsilophodon foxii* (Galton 1974), *Dryosaurus altus* (Galton 1983) and *Tenontosaurus tilletti* (Thomas 2015). In one crown with a slightly worn surface a distinct secondary ridge is present, which extends to the occlusal surface and lies mesial to the primary ridge, separated from it by a shallowly mesiodistally concave groove (Fig. 12C). A short accessory ridge is also present mesially. In the other two crowns, secondary and accessory ridges are not clearly defined. The crowns are mesiodistally expanded with denticulate margins, the denticles being wedge-shaped and largest in the mid-height region. The marginal denticles are approximately the same size on both surfaces but mesially they become more vertically orientated towards the apex. The occlusal surfaces of the denticles generally support three or more small spherical mammillae arranged labiolingually.

### Axial skeleton

**Dorsal vertebrae.** Eight dorsal vertebrae are preserved (Fig. 13) that have been labelled A–H based on their estimated sequence in the axial skeleton, which has been established largely on centrum shape, the orientation of transverse processes and the positions of the parapophyses. Vertebrae A and B represent anterior dorsals; C, D and E probably represent middle dorsals, possibly dorsals 8, 9 and 10; F is an early posterior dorsal; and G and H are placed posteriorly due to the relative height of the centra, although both are distorted by compaction. The neurocentral sutures of the dorsal series are fused but remain clearly visible, at least where the surface is better preserved in vertebrae C–E.

**Dorsal vertebra A.** This vertebra is opisthocoelous, the centrum having a shallowly concave posterior articular surface and a moderately convex anterior articular surface (Fig. 14A–C). Although these features are often found in iguanodontian cervicals, other characteristics of dorsal A are more consistent with a transitional dorsal vertebra than a posterior cervical. The relatively large parapophysis is shallowly concave and slightly ovoid with its long axis orientated posterodorsally, which suggests a relatively substantial rib attachment. The

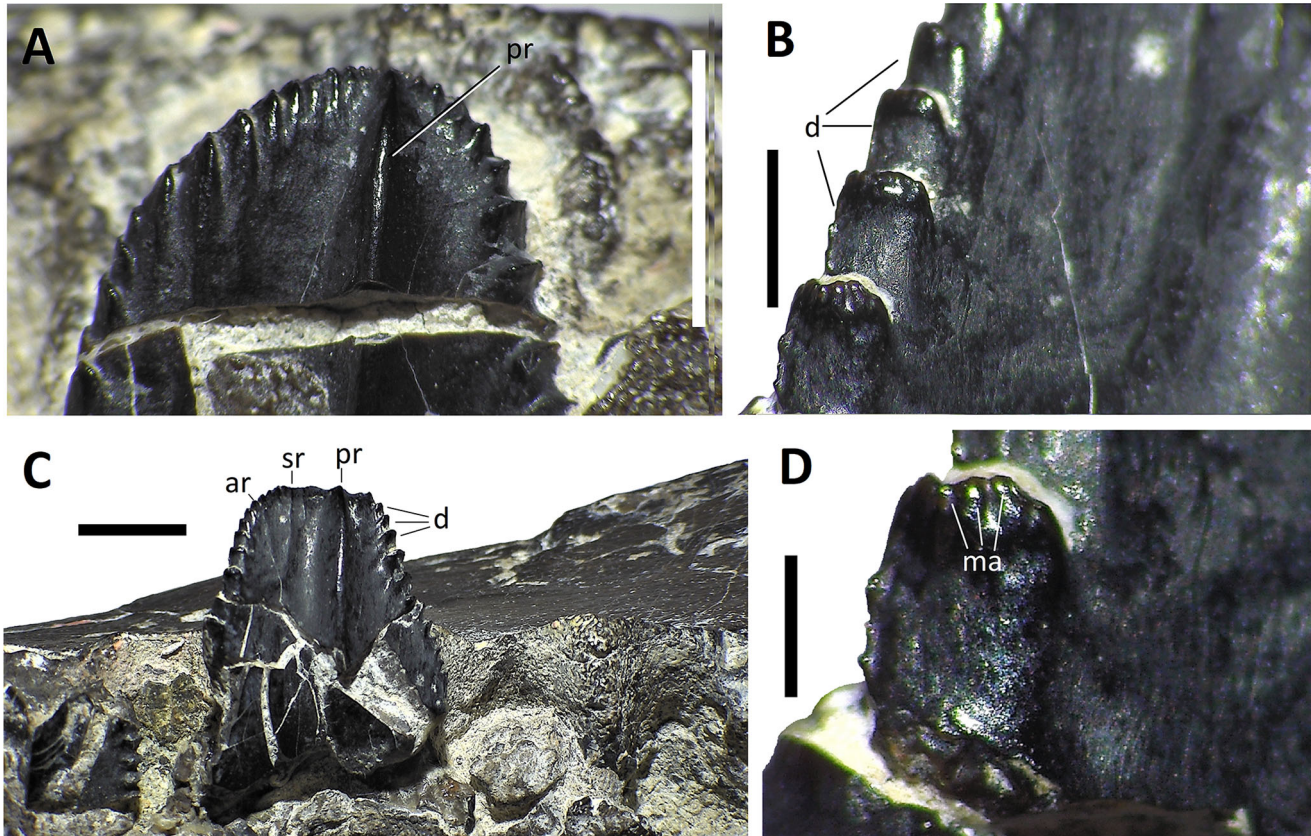


**Figure 12.** *Brighstoneus simmondsi* gen. et sp. nov. (MIWG 6344), crowns from right dentary (posterior is to the right). **A**, dentary crown in lingual view; **B**, close-up of A showing denticles; **C**, dentary crown in lingual view; **D**, close-up of denticle from A showing mammillae. **Abbreviations:** ar, accessory ridge; d, marginal denticle; ma, mammilla; pr, primary ridge; sr, secondary ridge. Scale bars = 10 mm (A), 5 mm (B, C) and 1 mm (D).

neurocentral suture is not visible but the parapophysis appears to be situated entirely on the neural arch. The centrum articular surfaces are broader than high (ratio of maximum width/height of anterior articular surface = 1.32) whereas in those iguanodontians where this feature is preserved and visible in the first dorsal vertebra, the centra are usually more laterally compressed as, for example, in *Equijubus normani* (0.82: McDonald *et al.* 2014), *Magnapaulia laticaudus* (0.98: Prieto-Márquez *et al.* 2012), *Ouranosaurus nigeriensis* (1.04: Bertozzo *et al.* 2017), *Zhanghenglong yangchengensis* (1.16: Xing *et al.* 2014), *Uteodon aphanocetes* (1.19: Carpenter & Wilson 2008) and *Eolambia caroljonesa* (1.24: McDonald *et al.* 2012b). In lateral view, the centrum of vertebra A is only slightly anteroposteriorly longer than dorsoventrally high (length/height ratio = 1.04), although this may have been exaggerated by crushing. A similar ratio is seen in the first dorsal vertebra of *Eolambia caroljonesa* (1.06: McDonald *et al.* 2012b), while *Iguanodon bernissartensis* is taller than long (0.96: Norman 1980) and others are considerably longer than high, for example *Probractrosaurus gobiensis* (1.24:

Norman 2002), *Ouranosaurus nigeriensis* (1.29: Bertozzo *et al.* 2017), *Mantellisaurus atherfieldensis* (1.32: Norman 1986), *Equijubus normani* (1.46: McDonald *et al.* 2014) and *Uteodon aphanocetes* (1.48: Carpenter & Wilson 2008). In ventral view, the lateral walls of the centrum are concave and despite some damage a definite keel is present on the ventral surface. Dorsal to the parapophyses the transverse processes extend slightly posterodorsolaterally although distally the diapophyses are missing. Seated on the dorsal surfaces of the transverse processes, close to their origin, the prezygapophyses have large, flat dorsomedially facing facets that are ovoid in shape, with their long axes extending anteroposteriorly. The postzygapophyses are missing. The neural spine curves slightly posterodorsally into a hook-like shape, but has lost its apex. This morphology is commonly seen in the first transitional dorsal vertebrae of hadrosauriforms, although the spine of *Brighstoneus simmondsi* is considerably taller than most of this clade and exceeds the height of its centrum. The ratio of neural spine height above the postzygapophyseal facet to height of centrum for *Brighstoneus*

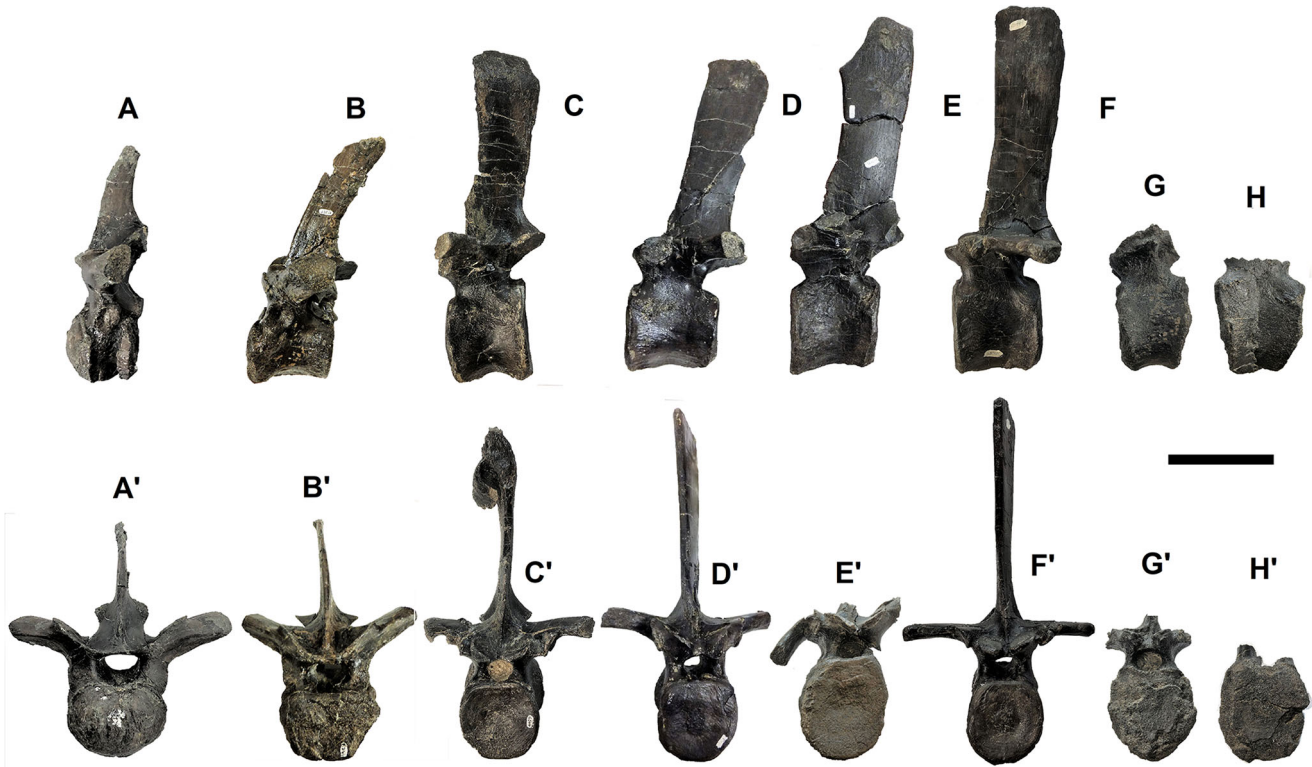


**Figure 13.** *Brighstoneus simmondsi* gen. et sp. nov. (MIWG 6344), dorsal vertebrae series arranged in probable anterior to posterior order. A–H, left lateral views of dorsals A–H; A', dorsal A anterior view; B', dorsal B anterior view; C', dorsal C anterior view; D', dorsal D posterior view; E', dorsal E anterior, view; F', dorsal F anterior view; G', dorsal G anterior view; H', dorsal H posterior view. Scale bar = 100 mm.

*simmondsi* is 1.14, compared to *Iguanodon bernissartensis* (0.76: Norman 1980), *Mantellisaurus atherfieldensis* (0.55: Norman 1986), *Probactrosaurus gobiensis* (0.79: Norman 2002) and *Zhanghenglong yangchengensis* (0.66: Xing *et al.* 2014). An exception is *Ouranosaurus nigeriensis* (Bertozzo *et al.* 2017), which is known for its exceptionally tall dorsal neural spines and has a ratio of 1.57.

**Dorsal vertebra B.** The anterior articular surface of the centrum is essentially flat but has a very slight convexity in lateral view although this is probably due to distortion (Fig. 14D–F). The posterior articular surface is slightly concave. The centrum has been crushed anteroposteriorly on the left side and its ventral surface has been distorted although it appears that a keel was present. The lateral surfaces of the centrum are concave anteroposteriorly, convex dorsoventrally and continuous dorsally with the neural arch. The parapophysis is more circular, more dorsally placed on the neural arch and larger than in dorsal A. The transverse processes have eroded lateral ends and are angled dorsolaterally. They are broadly triangular in cross-section with an angular ventral surface and a slightly anteroposteriorly convex

dorsal surface. The neural spine curves posterodorsally and is relatively short although still taller and more expanded anteroposteriorly than in dorsal A. These characters indicate that this vertebra was close to the transition between the cervical and dorsal vertebrae, possibly the second or third dorsal. The neural canal is narrow and dorsoventrally compressed. The articular facets of the prezygapophyses face dorsomedially. The neural spine appears to be intact, but its dorsal end is obscured by matrix. It is inclined slightly posterodorsally with a gently convex anterior margin in lateral view. Just posterior to the anterior margin a faint groove lies parallel to it. The neural spine to centrum height ratio is 1.7. The postzygapophyseal facets face ventrolaterally and extend considerably beyond the posterior articular surface of the centrum. A fragment of extraneous bone has become attached to the posterior neural arch, obscuring detail. Dorsals A and B appear to represent transitional dorsals. Dorsal A has a relatively tall neural arch and both have relatively tall neural spines, making them closer in appearance to transitional dorsals of *Iguanodon bernissartensis* (Norman 1980) and *Ouranosaurus nigeriensis* (Bertozzo *et al.* 2017) than to those of *Mantellisaurus atherfieldensis* (Norman 1986).

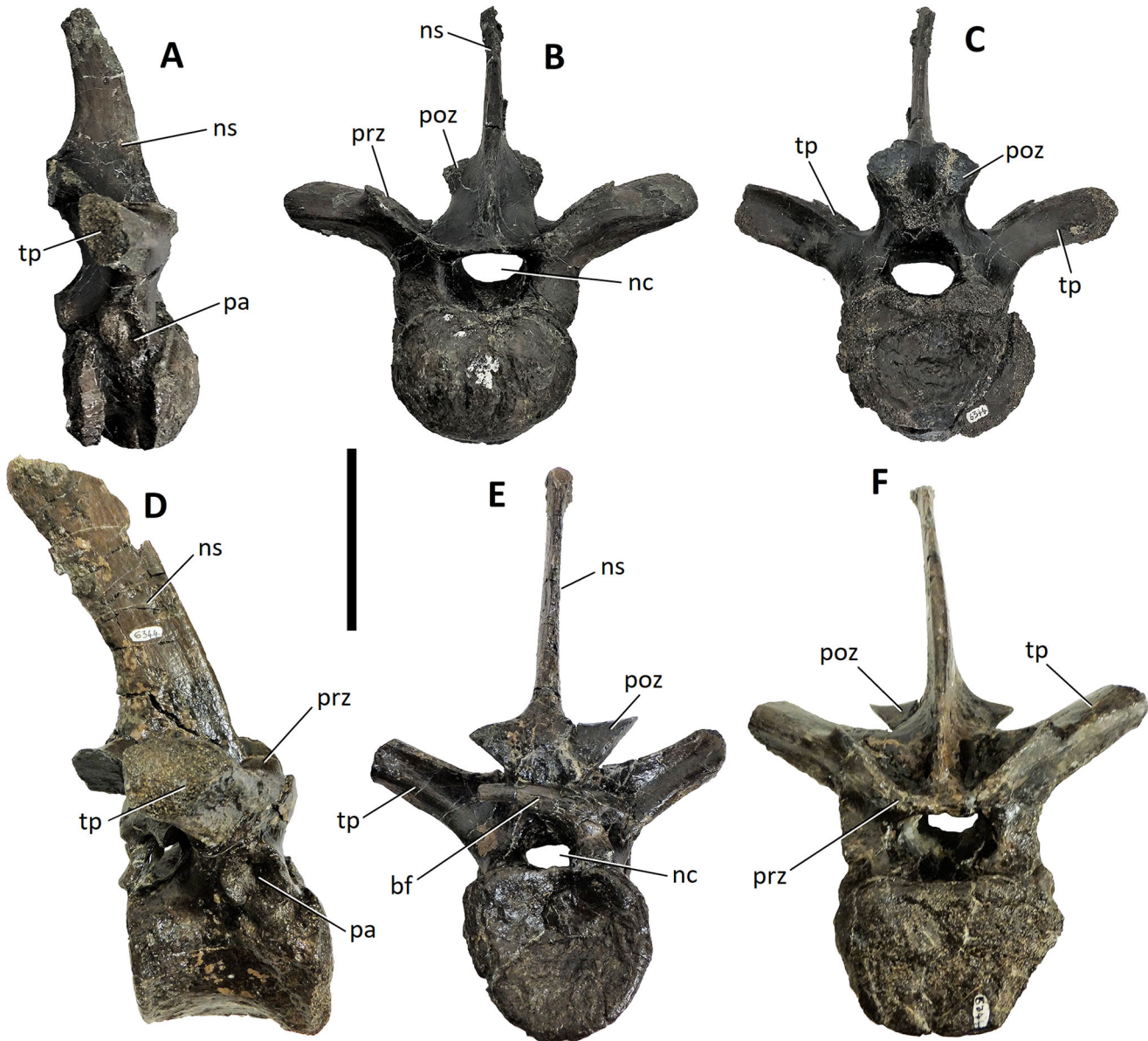


**Figure 14.** *Brighstoneus simmondsi* gen. et sp. nov. (MIWG 6344), anterior dorsal vertebrae. **A–C**, ‘dorsal A’, probably D1 in **A**, right lateral, **B**, anterior and **C**, posterior views. **D–F**, ‘dorsal B’, probably D2 in **D**, right lateral, **E**, posterior and **F**, anterior views. **Abbreviations:** **bf**, extraneous bone fragment; **nc**, neural canal; **ns**, neural spine; **pa**, parapophysis; **poz**, postzygapophysis; **prz**, prezygapophysis; **tp**, transverse process. Scale bar = 50 mm.

**Dorsal vertebrae C–F.** Vertebrae C–F (Figs 13, 15) appear to be middle dorsals. The centra are amphiplatyan although the anterior and posterior articular surfaces exhibit minimal concavity, which is slightly more pronounced posteriorly. The articular surfaces of the centra are all a little taller than wide and the posterior surfaces are all slightly larger than the anterior surfaces. Dorsal F has evidence of a notochordal boss in the centre of each articular surface, which is more pronounced anteriorly. Among ornithopods this has also

been seen in some posterior dorsal vertebrae of *Iguanodon bernissartensis* (Norman 1980) and *Zalmoxes robustus* (Weishampel *et al.* 2003). The centra in lateral view are mostly taller than long (length/height ratios: C = 0.8; D = 1.1; E = 0.9; F = 0.9). Dorsal C has a mid-line ventral prominence anteriorly, but taphonomic damage makes it unclear if this extended posteriorly as a keel. Dorsals D, E and F have faint ventral keels. The parapophyses migrate up the neural arch onto the transverse processes along the series. The neural spines of

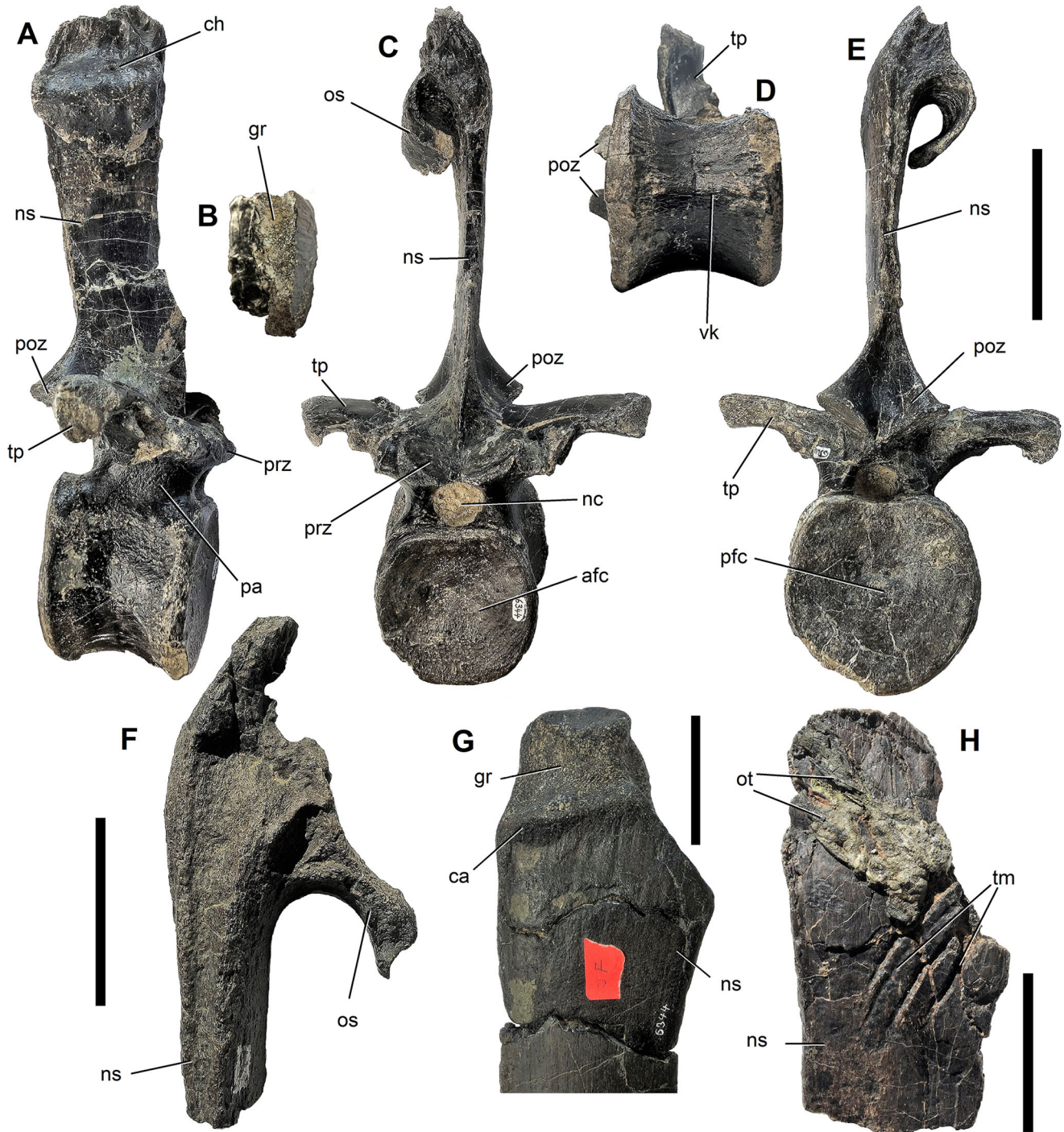


**Figure 15.** *Brighstoneus simmondsi* gen. et sp. nov. (MIWG 6344), dorsal vertebrae. **A–E**, 'dorsal C' in **A**, right lateral, **B**, dorsal (of neural spine), **C**, anterior, **D**, ventral and **E**, posterior views. **F**, close-up of fracture site on neural spine of 'dorsal E'. **G**, fragment of pathological dorsal neural spine. **H**, section of neural spine with bite marks. **Abbreviations:** **afc**, anterior surface of centrum; **ca**, callus; **ch**, channel; **gr**, groove; **nc**, neural canal; **ns**, neural spine; **os**, ostosis; **ot**, ossified tendons; **pa**, parapophysis; **pfc**, posterior surface of centrum; **poz**, postzygapophysis; **prz**, prezygapophysis; **tm**, tooth marks; **tp**, transverse process; **vk**, ventral keel. Scale bars = 100 mm (A–E) and 50 mm (F–H).

dorsals C–H have all been affected by possible bioerosion at the apex of the spine. Dorsals C and E have suffered pre-mortem fracture damage, with C showing a

displaced fracture, presumably splinted in place by a partially intact ossified tendon meshwork (Fig. 15A, B, C, E), and vertebra E showing callus formation

undergoing remodelling (Fig. 15F); therefore, the true height of the spines is unknown. However, measurements on the available material show that the neural spines were at least three times as long as the centrum height and possibly much longer (neural spine to centrum height ratios: C = 2.8; D = 3.4; E = 3.0; F = 3.3). In most iguanodontians the ratio of neural spine to centrum height is <3.0 and in earlier diverging taxa, <2.0. Taxa where the ratio exceeds three include *Hypselospinus fittoni* (3.7: Norman 2010), RBINS R57 (3.1: Norman 1986), *Ouranosaurus nigeriensis* (5.1: Bertozzo *et al.* 2017), *Bactrosaurus johnsoni* (3.7: Gilmore 1933) and *Morelladon beltrani* (4.0: Gasulla *et al.* 2015).

**Dorsal vertebrae G and H.** The articular surfaces of the centrum are damaged in dorsal G, but it appears to be amphiplatyan (Fig. 13). Ventrally the centrum is smoothly convex and does not have a keel. Dorsal H is badly crushed ventrally with the suggestion of a ventral keel. Unplaceable neural spine fragments are also preserved, two showing notable features. One dorsal fragment appears to show callus formation and a displaced fracture (Fig. 15G), which is similar to that on dorsal C, while a second appears to have theropod (or possibly crocodylian) bite marks on its surface (Fig. 15H).

**Dorsal ribs.** Fourteen partial and complete dorsal ribs are preserved, nine from the left side and five from the right. As far as can be ascertained, there appears to be little difference between those of *Brighstoneus simmondsi* and those of *Iguanodon bernissartensis* (Norman 1980) and *Mantellisaurus atherfieldensis* (Norman 1986). It is not possible to accurately place the ribs in specific positions but there are examples from the anterior, middle and posterior members of the dorsal series (Fig. 16) and general descriptions are given of these.

The capitulum or head of the rib bears a medially facing articular facet, which is supported by a medially directed process. The dorsal surface of this process is either flat or forms a gentle ridge and is quite rugose. Laterally, the tuberculum is circular or ovoid, with a posteromedially facing articulation on a slightly raised pedestal. From here the shaft of the rib extends ventrally, and in the anterior and middle part of the dorsal series forms an angle of  $\sim 90^\circ$  with the capitulum. Immediately below the tuberculum the cross-section of the rib shaft is sub-triangular with anteromedially, posteromedially and laterally facing surfaces. In anterior view a rounded ridge extends ventrally from the base of the tuberculum and crosses the shaft diagonally to the anterior leading margin of the blade of the rib, below which the cross-section is ovoid with the long axis

directed anteroposteriorly. Posteriorly, below the tuberculum a shallow costal groove develops laterally that extends ventrally and is bounded at the lateral margin by a relatively thin ridge. The ridge and groove disappear in the middle third of the rib shaft, although the groove reappears in the ventral third in one of the complete specimens. This groove was presumably for a neurovascular bundle, with the ridge perhaps providing attachment for intercostal musculature and additional protection in the proximal region. The anterior dorsal ribs appear to terminate in a point, but the middle dorsal series increase in length and have a blunt spatulate end, which suggests that they might have articulated with the sternal cartilaginous ribs (Norman 1980).

The posterior dorsal ribs become gradually shorter and the angle between the shaft and the capitulum-bearing process becomes more oblique. The tuberculum, which is ovoid or circular in the anterior and middle series, is smaller and becomes more elongate posteriorly. The tuberculum and capitulum also move closer to each other although a small gap remains between them (Fig. 16D) for the passage of a vertebral artery (Romer 1956). In one posterior specimen (Fig. 16D) it appears that the transverse process and tuberculum have started to fuse.

**Sacral vertebrae.** The sacrum of *Brighstoneus simmondsi* (Fig. 17) consists of six co-ossified vertebrae although the anterior part of the first vertebra is missing. It is likely that it originally had a sacral count of seven co-ossified vertebrae, as the possession of a sacrodorsal (SD) vertebra is present in all non-hadrosaurid hadrosauriform taxa with intact sacra. A sacral count of 6+SD is seen in *Barilium dawsoni* (Norman 2011), *Mantellisaurus atherfieldensis* (Norman 1986), *Gobihadros mongoliensis* (Tsogtbaatar *et al.* 2019), *Bactrosaurus johnsoni* (Godefroit *et al.* 1998) and *Ouranosaurus nigeriensis* (Bertozzo *et al.* 2017). A count of 5+SD is present in *Morelladon beltrani* (Gasulla *et al.* 2015), *Equijubus normani* (You *et al.* 2003) and probably *Cedroestes crichtoni* (Gilpin *et al.* 2007), although it is difficult to determine in disarticulated material, such as that of *Morelladon beltrani* and *Equijubus normani*, if a sixth true sacral vertebra failed to fuse until late in ontogeny and did not preserve. S1 is distorted, eroded on its right lateral surface and is obscured by a sacral rib on the left. The posterior half flares out to meet a similar anterior expansion on S2. Due to distortion, it is difficult to interpret the incomplete ventral surface of S1 but a keel was probably present. When viewed ventrally S2 expands anteriorly to meet S1 and is firmly fused to S3 posteriorly, which in turn is fused to S4, so that S2–4 form a rod of broadly uniform width. The ventral surfaces of S2–4 are flat

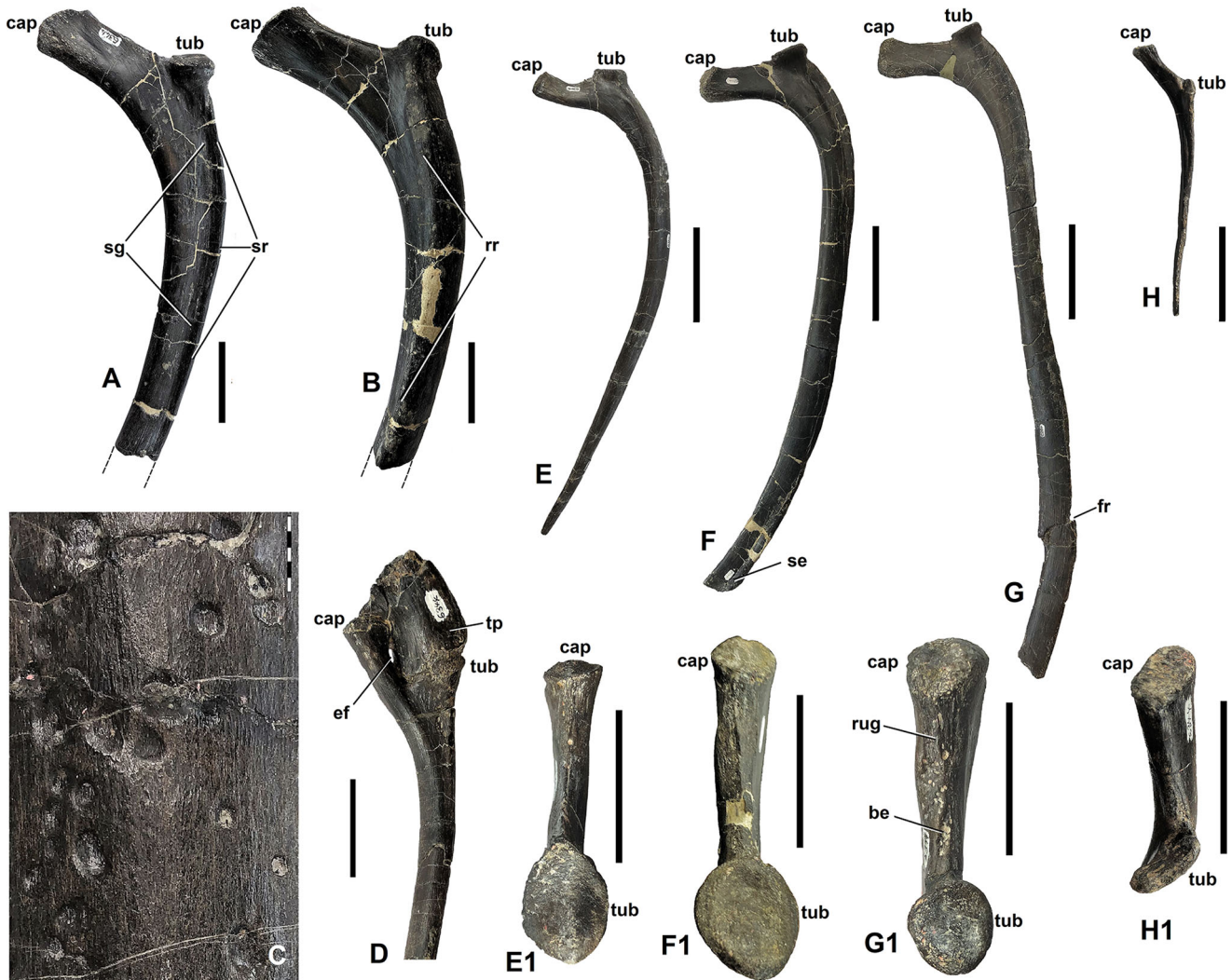


**Figure 16.** *Brighstoneus simmondsi* gen. et sp. nov. (MIWG 6344), dorsal ribs. **A**, proximal section of right rib in posterior view; **B**, specimen 'A' in anterior view (image reversed); **C**, close-up of F showing possible bioerosion; **D**, posterior series rib head with distal transverse process; **E**, anterior series, left rib, anterior view and **E'**, dorsal view; **F**, middle series (image reversed), left rib, posterior view and **F'**, dorsal view; **G**, middle series (image reversed), left rib, posterior view and **G'**, dorsal view; **H**, posterior series, right rib, posterior view and **H'** dorsal view. **Abbreviations:** **be**, bioerosion; **cap**, capitulum; **ef**, elliptical foramen; **fr**, fracture; **rr**, rounded ridge; **rug**, rugosity; **se**, spatulate end; **sg**, shallow groove; **sr**, sharp ridge; **tp**, transverse process; **tub**, tuberculum. Scale bars = 50 mm (A, B, D, E', F', G', H'), 100 mm (E–H) and 5 mm (C).

with no central keel and are bounded laterally on each side by a shallow rounded ridge, although this does not form a true sulcus. S5 is expanded a little posteriorly. Its ventral surface has been transversely crushed but probably lacked a keel. S6 is much more robust and flares out considerably posteriorly, where the margin of the centrum is heavily striated. Its posterior articular surface is ovoid with the long axis orientated dorsoventrally (Fig. 17B). The vertebra has been anteroposteriorly crushed, which has affected the posterior articular surface. The ventral surface is smooth and transversely convex without a keel. *Morelladon beltrani* (Gasulla *et al.* 2015) has keeled ventral surfaces on S1–4

(anterior half only in S2–4) and a flat S5; *Mantellisaurus atherfieldensis*, based on referred material, is described by Norman (1986) as having keeled surfaces on S1–3 and a flat ventral surface or sulcus on S4–5. Hooley's (1925) description of the holotype differs, however, giving the ventral surface of S1 as being transversely flat. S2 is not described, presumably due to damage, S3 and S4 have a wide sulcus ending at S5, and there is a slight keel on S6. *Iguanodon bernissartensis* (RBINS R55) has a ventral keel on S1–3, a sulcus on S4–6 and flat surface on S7 (Norman 1980). The siting of ventral keels and sulci shows intraspecific variation in some taxa, for example in *Bactrosaurus*

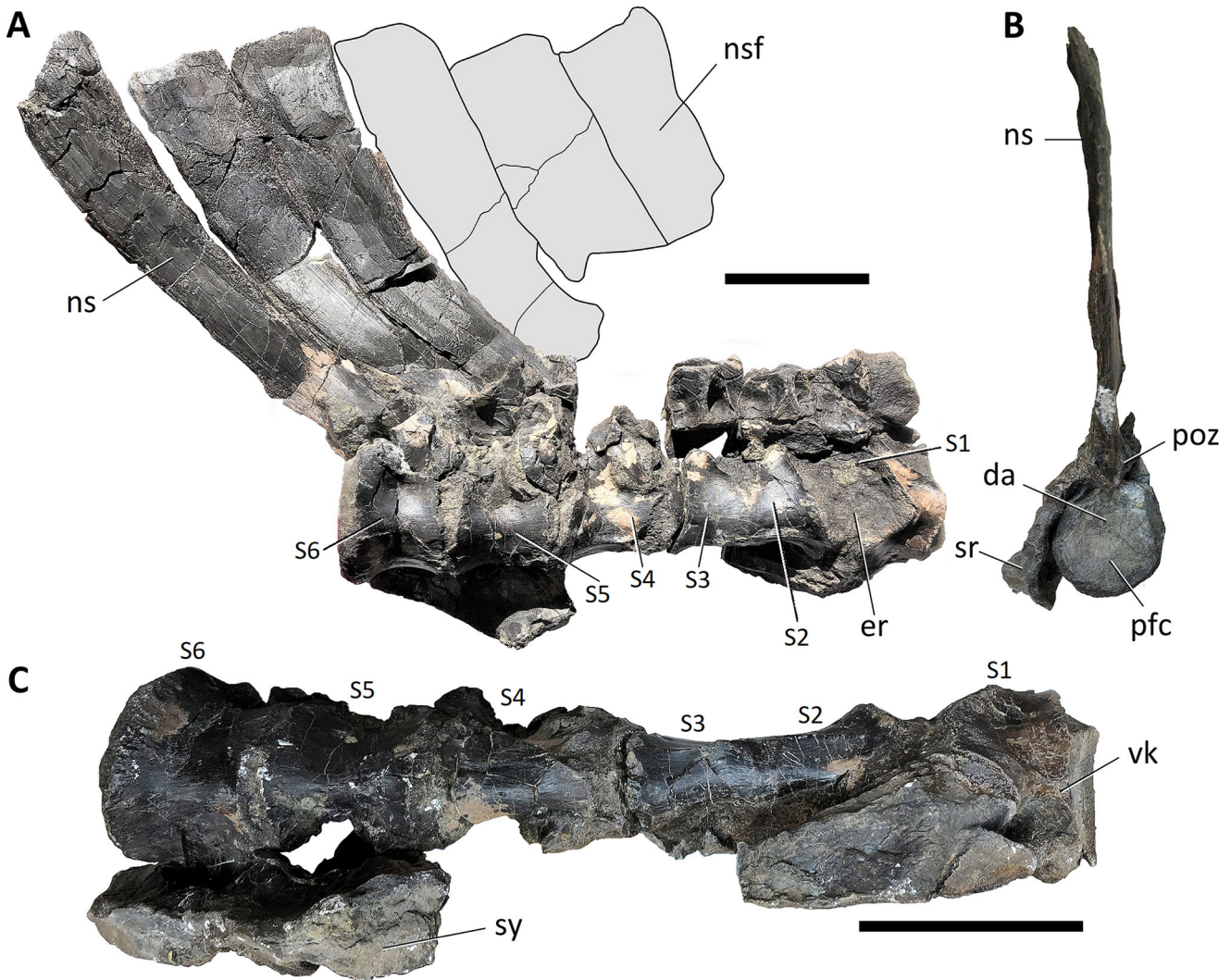


**Figure 17.** *Brighstoneus simmondsi* gen. et sp. nov. (MIWG 6344), sacrum in **A**, right lateral, **B**, posterior and **C**, ventral views. **Abbreviations:** da, depressed area; er, eroded area; ns, neural spine; nsf, neural spine fragments in presumed position; pfc, posterior surface of centrum; poz, postzygapophysis; s, sacral vertebra; sr, sacral rib; sy, sacral yoke; vk, ventral keel. Scale bars = 100 mm.

*johnsoni* (Godefroit *et al.* 1998), and caution is required interpreting their phylogenetic significance. The sacral neural spines are robust and tall, being approximately 360 mm long and directed posterodorsally at an angle of approximately 45° in lateral view, presumably due to taphonomic distortion. The neural spines have been eroded dorsally where an anteroposterior groove has formed, therefore the heights are a minimum value. The anterior surface is wider than the posterior surface and grooved so that the sacral neural spines would have locked against each other. In lateral view, as the neural spines extend dorsally, they also expand slightly anteroposteriorly and become gently curved, concave anteriorly. Fragments of the dorsal section of three neural spines were recovered, which also have grooves anteriorly and probably represent the missing three anterior

sacral neural spines. In the reconstruction (Fig. 17A) it appears that the anteroposterior width of the spines in lateral view diminishes posteriorly. Sacral ribs are present but damaged and distorted. They appear to be firmly fused and form a sacricostal yoke for attachment to the ilium.

**Caudal vertebrae.** Six caudal vertebrae are preserved (Fig. 18), four from the proximal series (possessing caudal ribs) and two from the middle series (possessing chevron facets but no caudal ribs). They have been labelled A–F in presumed anterior to posterior order although this does not imply an articulation sequence.

**Proximal caudal series.** Caudal A (Fig. 18A, B) has a centrum with a very rounded anterior articular surface with a slight bulge on the dorsal half (also noted

by Norman [1986] in the first caudal of RBINS R57). The anterior articular surface is slightly wider than tall and is essentially flat but minimally concave with an everted margin. The posterior articular surface also has an everted margin but is more heart-shaped and a little more concave than the anterior articular surface. There is a boss situated dorsal to the centre of the posterior surface that might represent a notochordal remnant. The lateral walls of the centrum are deeply striated close to its anterior and posterior margins, especially anteriorly. There is no keel or chevron facet ventrally, the latter indicating that caudal A is probably the first caudal. The bases of the caudal ribs are present but badly damaged and the zygapophyses are angled steeply dorsally, with the facets of the prezygapophyses diverging approximately 20° from the sagittal plane. The neural spine is tall and angled slightly posterodorsally. A shallow groove extends dorsoventrally just posterior to the anterior margin in the ventral half of the spine. Near the dorsal extremity the spine expands transversely, while the dorsal surface itself has been eroded to expose a cavity, which is interpreted as pathological. The loss of the dorsal surface means the true length of the spine is unknown, but it is consistent with the sacral neural spine height and probably almost complete. The ratio of the incomplete neural spine height to centrum height is 3.9, which is greater than the ratio seen in the first caudal of *Ouranosaurus nigeriensis* (3.4: Bertozzo *et al.* 2017) and an anterior caudal in *Hypselospinus fittoni* (3.2: Norman 2015), both of which have long dorsal neural spines. No caudals are preserved in the ‘sail-backed’ iguanodontian *Morelladon beltrani* (Gasulla *et al.* 2015). By contrast, the first caudal in *Iguanodon bernissartensis* is 1.8 (Norman 1980). The *Mantellisaurus atherfieldensis* holotype (NHMUK PV R5764) has no surviving caudal neural spines and RBINS R57 has been heavily restored, although the ratio in the latter, based on Norman (1986, fig. 39), is approximately 2.6. The lack of keel in the first caudal is shared with *Barilium dawsoni* (Norman 2011), *Iguanodon bernissartensis* (Norman 1980) and *Mantellisaurus atherfieldensis* (Norman 1986), but differs from *Ouranosaurus nigeriensis*, which has a keel on the first and second caudals, and a faint keel on the third (Bertozzo *et al.* 2017). Caudal B (Fig. 18C, D) is slightly more platycoelous than caudal A. It is otherwise similar except that it has a posterior chevron facet but lacks an anterior facet, suggesting a second caudal position. As with caudal A there is no ventral keel. The articular surfaces of the centrum are of almost equal height and maximum width, and both are heart-shaped. The neural spine is also eroded dorsally and expanded transversely, with the latter again interpreted as

pathological. The incomplete neural spine to centrum height ratio is 3.6. The caudal ribs, which are incomplete, extend laterally and are almost horizontal. In anterior view they describe a gentle curve that is concave ventrally. The posterior centrum and caudal ribs of caudal C (Fig. 18E, F) are crushed. It is essentially amphiplatyan but both articular surfaces are minimally concave. The articular surfaces are both heart-shaped but are slightly taller than wide. Ventrally it has anterior and posterior chevron facets, but no definite ventral keel, although crushing damage makes this uncertain. The neural spine is shorter than in caudals A and B (neural spine to centrum height ratio 3.4) and also angled more posterodorsally. As with caudals A and B the apex of the neural spine has been eroded into a shallow anteroposterior groove, therefore the true length is unknown, but the presumed pathological transverse expansion in caudals A and B is not apparent. The rate at which the height of the neural spines decreases in more posterior anterior caudal vertebrae varies between taxa. In *Ouranosaurus nigeriensis* the height of the neural spines decreases rapidly after the third caudal (Bertozzo *et al.* 2017), but they reduce more gradually in RBINS R57 (Norman 1986) and *Iguanodon bernissartensis* (Norman 1980). Caudal D (Fig. 18G–K) has similar morphology to caudal C but lacks its neural spine. The size of the centrum is a little smaller than in caudals A–C so it was presumably more posteriorly positioned. Ventrally the posterior chevron facet forms a ‘B’-shaped outline, the straight margin being posterior, while the anterior facet is ‘D’-shaped, the straight margin being anterior. Broad ridges connect the two facets laterally leaving a shallow anteroposteriorly directed sulcus in between (Fig. 18K).

**Middle caudal series.** Two vertebrae in good condition are preserved from the middle part of the caudal series. Both are of similar size, with amphiplatyan centra, although caudal E (Fig. 18L, M) has a slight concavity posteriorly. The articular surfaces of the centrum are sub-circular, being a little taller than wide. There is a very weakly developed longitudinal ridge extending anteroposteriorly along the midline of the centrum in lateral view and some irregularity at the base of the neural arch that could indicate a vestigial caudal rib. This would mark caudal E as transitional between the anterior and middle caudal series. Anterior and posterior chevron facets are present, the anterior facet being semi-circular and the posterior having a double-headed ‘B’-shaped outline. A broad ridge extends anteroposteriorly between each of the two posterior facet heads and the anterior facet, producing a shallow midline sulcus. The neural spine is angled posteriorly at approximately 45° and gradually expands anteroposteriorly as it extends



**Figure 18.** *Brighstoneus simmondsi* gen. et sp. nov. (MIWG 6344), caudal vertebrae. **A**, 'caudal A' in left lateral view; **B**, 'caudal A' in posterior view; **C**, 'caudal B' in right lateral view; **D**, 'caudal B' in posterior view; **E**, 'caudal C' in left lateral view; **F**, 'caudal C' in anterior view; **G**, 'caudal D' in anterior view; **H**, 'caudal D' in left lateral view; **I**, 'caudal D' in posterior view; **J**, 'caudal D' in dorsal view; **K**, 'caudal D' in ventral view; **L**, 'caudal E' in left lateral view; **M**, 'caudal E' in anterior view; **N**, 'caudal E' in ventral view; **O**, 'caudal F' in right lateral view; **P**, 'caudal F' in posterior view. **Abbreviations:** ahf, anterior haemapophyseal facet; lr, lateral ridge; ns, neural spine; phf, posterior haemapophyseal facet; plp, pleurapophysis (caudal rib); poz, postzygapophysis; prz, prezygapophysis; sb, small boss. Scale bars = 100 mm.

dorsally (in contrast to the anterior series, which have almost parallel margins). The incomplete neural spine has a spine to centrum height ratio of 1.3, which is much lower than in the anterior series. Caudal F (Fig. 18O, P) is of similar size and shape to caudal E but has no trace of a caudal rib and a stronger lateral ridge on the centrum, which gives the articular surfaces a distinctive hexagonal shape, which can be observed in many iguanodontians (Barrett & Bonsor 2021).

## Ilium

Both ilia are preserved (Fig. 19). The right has suffered considerable erosive damage with most of the ventral border including both peduncles missing. Furthermore, some of the medial surface and the posterior postacetabular process has been eroded, as has the tip of the preacetabular process. However, what is preserved of this bone appears to be free from major distortion, apart from some possible slight transverse compression. The left ilium is more complete and forms the basis for much of this description. Its preacetabular process has been crushed transversely in its most distal section and the very tip of the preacetabular process is also missing. The posterodorsal section of the postacetabular process has been lost to post-mortem fracture and erosion, and the distal end of the pubic peduncle is damaged by erosion.

The preacetabular process is transversely compressed along its length, forming a robust and uniformly deep strap-like structure. At the base of the left process, the facet for the transverse process of the first true sacral vertebra is bounded ventrally by a ridge, although its prominence may have been enhanced somewhat by crushing. Proximally the cross-section of the preacetabular process has the outline of a dorsoventrally expanded capsule, which is shallowly concave on its lateral surface (Fig. 19B). This contrasts with *Iguanodon bernissartensis* (Norman 1980) and *Mantellisaurus atherfieldensis* (NHMUK PV R5764), where the proximal process is sub-triangular in cross-section with an almost horizontal ventral shelf. Norman (1986) has also commented on this character difference in two Barremian-aged ilia, which he referred to *Mantellisaurus atherfieldensis*, noting a well-developed shelf in NHMUK PV R5347 from the Wessex Formation of the Isle of Wight, but a weak one in NHMUK PV R6462 from Weald Clay Formation of Surrey. The preacetabular process of *Mantellisaurus atherfieldensis* (NHMUK PV R5764) is also less strap-like in lateral view, being slightly waisted and more gracile in its midsection. In dorsal view, the thickness of the dorsal surface of the process tapers very slightly as it extends distally. The dorsal surface is mediolaterally

rounded but unequally, so that the dorsolateral surface is flatter and forms a bevelled surface. Also, in dorsal view the outline of the left process is gently sinusoidal, being convex laterally in its proximal half and concave laterally in its distal section as it curves slightly outwards. On the right side the process curves gently laterally but the proximal convexity is much less evident. There is no evidence of axial twisting in either of the preacetabular processes. Axial twisting, when present, typically causes the lateral surface to turn dorsolaterally as it extends distally and is seen in *Mantellisaurus atherfieldensis* (NHMUK PV R5764), *Barilium dawsoni* (Norman 2011), *Iguanodon bernissartensis* (Norman 1980), *Ouranosaurus nigeriensis* (Bertoazzo *et al.* 2017) and *Bactrosaurus johnsoni* (Godefroit *et al.* 1998), but is absent in some iguanodontians, for example *Camptosaurus dispar* (McDonald 2011), *Hypselospinus fittoni* (Norman 2015) and *Magnapaulia laticaudus* (Prieto-Márquez *et al.* 2012). In lateral view, the preacetabular process is moderately decurved, the dorsal margin forming a gentle convex arc extending anteroventrally, and the long axis of the process forming an angle of 20° with the dorsal margin of the iliac central plate. This value is typical of many basal iguanodontians such as *Uteodon aphanoeetes* (19°: Carpenter & Wilson 2008), *Osmakasaurus depressus* (19°: McDonald 2011), *Mantellisaurus atherfieldensis* (21°: NHMUK PV R5764) and *Ouranosaurus nigeriensis* (17°: Taquet 1976). Hadrosaurids tend to have greater angles, as in *Edmontosaurus annectens* (48°) and *Magnapaulia laticaudus* (40°: Prieto-Márquez *et al.* 2012); however, variation in this character can differ significantly between individuals of the same taxon, for example in *Gilmoresaurus mongoliensis* (holotype, AMNH 6551, 23° [McDonald *et al.* 2010c], lectotype AMNH FARB 30735, 39°, referred ilium AMNH FARB 30736, 40° [Prieto-Márquez & Norell 2010]) and *Iguanodon bernissartensis* (holotype RBINS R51, 51° [Norman 1980], referred ilium RBINS R352, 2°) (for a full discussion see Verdú *et al.* 2017a). The ventral margin of the preacetabular process is concave in lateral view but forms an obtuse angle at the anterior end, which continues horizontally as the base of a boot-like structure, although this is incomplete anteriorly. A boot-shaped distal preacetabular process is commonly seen in many iguanodontians but is most marked in *Iguanacolossus fortis* (McDonald *et al.* 2010a), *Eolambia caroljonesa* (McDonald *et al.* 2012b), *Ouranosaurus nigeriensis* (Bertoazzo *et al.* 2017), *Proa valdearinnensis* (McDonald *et al.* 2012a) and *Mantellisaurus atherfieldensis* (NHMUK PV R5764). Some have a more tabulate ending such as *Tenontosaurus tilletti* (Forster 1990), *Camptosaurus*

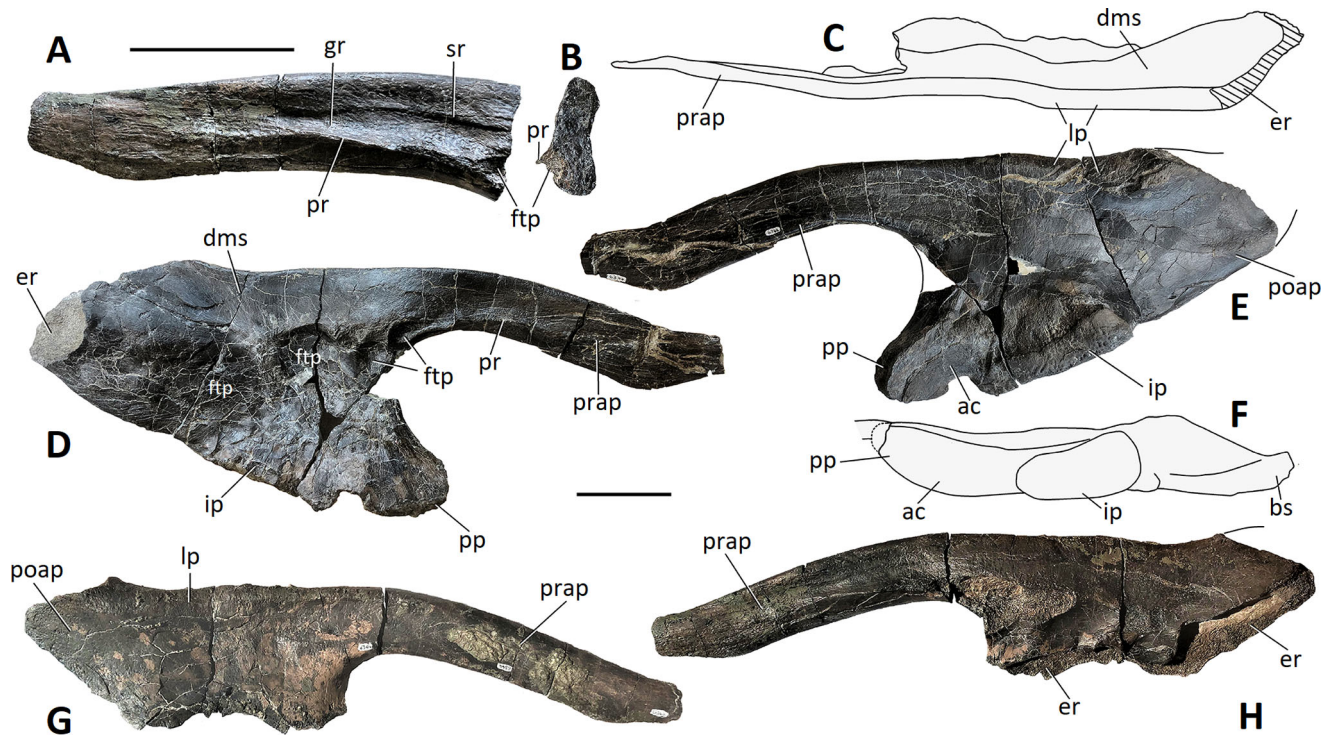


**Figure 19.** *Brighstoneus simmondsi* gen. et sp. nov. (MIWG 6344), ilia. **A**, preacetabular process of right ilium in medial view; **B**, cross-section of base of **A**. **C–F**, left ilium in **C**, dorsal, **D**, medial, **E**, lateral and **F**, ventral views. **G**, **H**, right ilium in **G**, lateral and **H**, medial views. **Abbreviations:** **ac**, acetabulum; **bs**, brevis shelf; **dms**, dorsomedial surface; **er**, eroded area; **ftp**, facet for transverse process; **gr**, groove; **ip**, ischiadic peduncle; **lp**, lateral process; **poap**, postacetabular process; **pp**, pubic peduncle; **pr**, primary ridge; **prap**, preacetabular process; **sr**, secondary ridge. Scale bars = 100 mm.

*dispar* (McDonald 2011), *Bactrosaurus johnsoni* (Godefroit *et al.* 1998) and *Edmontosaurus annectens* (Brett-Surman & Wagner 2007). On the medial surface of the preacetabular process, a prominent ridge (Fig. 19A, B, D) is continuous with the ridge bordering the ventral margin of the first sacral facet. It extends distally along the medial wall of the preacetabular process, dividing it into a larger dorsal section which faces medially and a smaller ventral section that faces medioventrally, forming an angle of approximately 20° with the vertical dorsal section in anterior view. The ventral section corresponds to the horizontal ventral shelf in *Mantellisaurus atherfieldensis* (NHMUK PV R5764). The ridge gradually decreases in prominence so that anteriorly the preacetabular process is represented by a vertical thin structure with flat medial and lateral walls. On the proximal half above the prominent ridge of the better-preserved right preacetabular process the dorsal section is further divided by a fainter secondary ridge (Fig. 19A) that lies parallel to the prominent ridge and is separated from it by a broad but shallow groove, perhaps acting as a vascular channel. The position of the main ridge is variable between taxa, forming the ventral angle to the ventral shelf in *Mantellisaurus*

*atherfieldensis* (NHMUK PV R5764), positioned one-third of the way up in *Brighstoneus simmondsi* (MIWG 6344) and close to the dorsal margin in *Morelladon beltrani* (Gasulla *et al.* 2015).

The body of the ilium in *Brighstoneus simmondsi* is relatively short, with its maximum dimensions forming a vertical rectangular plate with its long axis extending dorsoventrally, with a ratio of depth to length >1.2 (ratio measured following methodology in Prieto-Márquez & Norell [2010], character 234). This is also the case in earlier-diverging ornithomorphs such as *Zalmoxes shqiperorum* (Godefroit *et al.* 2009), *Tenontosaurus tilletti* (Ostrom 1970) and *Hypsilophodon foxii* (Galton 1974), but also in the more derived *Jinzhousaurus yangi* (Wang & Xu 2001; Barrett *et al.* 2009); others have the long axis oriented anteroposteriorly, for example *Iguanodon bernissartensis* (Norman 1980), *Gilmoreosaurus mongoliensis* (Prieto-Márquez & Norell 2010) and *Dryosaurus altus* (Gilmore 1925), while others such as *Barilium dawsoni* (Norman 2011) and *Mantellisaurus atherfieldensis* (Norman 1986) are almost square. The dorsal margin of the ilium is transversely rounded, moderately rugose and expands in thickness as it extends posteriorly. The lateral wall of

the ilium, including the proximal preacetabular process and the postacetabular process, is concave dorsoventrally. In lateral view the anterior margin of the iliac body is deeply concave, producing an embayment extending from the base of the preacetabular process as a thin ridge of bone, which continues as the anteromedial angle of the pubic peduncle.

The pubic peduncle has been eroded distally and its length cannot be reliably estimated. The peduncle is triangular in cross-section with medially, posterolaterally and anteriorly facing surfaces. The anterior surface is smooth and flat, while the medial surface is heavily striated with the striae orientated anteroventrally in line with the long axis of the peduncle. The medial surface is depressed to form a shallow fossa at the base of the peduncle. The posterolateral side of the peduncle forms the smooth surface of the anterior section of the acetabular component, which curves around to meet the ischiadic peduncle. The smooth acetabular surface ends where it meets the ischiadic peduncle. This peduncle is transversely expanded, being broadest posteriorly. The ventral surface is heavily rugose. Laterally the wall is smooth and forms a dorsoventrally deep rim. The ischiadic peduncle is oriented posterolaterally and as it is broadest posteriorly this creates a relatively modest lateral protrusion or step, which then curves medially to continue as the postacetabular process. However, the lateral wall of the ischiadic peduncle is essentially flat and lacks a distinct posterolateral boss. A boss causing a distinct step between the anterior and posterior sections of the lateral wall of the ischiadic peduncle ('posteroventral protuberance' and 'ischial tuberosity' of some authors) is seen in some non-hadrosaurid hadrosauriforms such as *Mantellisaurus atherfieldensis* (NHMUK PV R5764), *Altirhinus kurzanovi* (Norman 1998, fig. 32), *Choyrodon barsboldi* (Gates *et al.* 2018), *Hypselospinus fittoni* (Norman 2015), *Gilmoreosaurus mongoliensis* (Prieto-Márquez & Norell 2010) and all hadrosaurids, although in the latter clade the articular surface is also divided by a groove into anterior and posterior segments (Prieto-Márquez & Norell 2010). A boss is absent in *Morelladon beltrani* (Gasulla *et al.* 2015), *Proa valdearriñoensis* (McDonald *et al.* 2012a), *Iguanodon bernissartensis* (Norman 1980) and *Ouranosaurus nigeriensis* (Taquet 1976).

The ventral margin of the ischiadic peduncle in lateral view is inclined posterodorsally compared to the dorsal margin of the iliac blade and is almost parallel to the angle of the ventral margin of the postacetabular process. This is also seen in *Gilmoreosaurus mongoliensis* (McDonald *et al.* 2010a), *Eolambia caroljonesa* (McDonald *et al.* 2012b), *Bactrosaurus johnsoni* (Godefroit *et al.* 1998) and *Ouranosaurus nigeriensis*

(Taquet 1976), and appears to become increasingly common in more derived hadrosauriform taxa including hadrosaurids (Supplementary material, Fig. S8). In earlier-diverging taxa, the articular surface of the ischiadic peduncle is more horizontal and closer to being parallel with the dorsal margin of the iliac blade, for example in *Hypsilophodon foxii* (Galton 1974), *Zalmoxes robustus* (Weishampel *et al.* 2003), *Rhabdodon* sp. (Chanthasit 2010), *Camptosaurus dispar* (Gilmore 1909), *Mantellisaurus atherfieldensis* (NHMUK PV R5764) and *Iguanodon bernissartensis* (Norman 1980).

In the lateral view *Brighstoneus simmondsi* has virtually no notch or embayment between the posterior ischiadic peduncle and the postacetabular process. The ventral surface of the postacetabular process is incomplete posteriorly, but what remains suggests there was only a modestly developed brevis shelf. The postacetabular process is angled medially to the main body of the ilium (Fig. 19F) and whereas the lateral wall is flat above the acetabulum it is dorsoventrally concave in the postacetabular process. In lateral view, a very gently everted dorsal rim begins at the posterior end of the preacetabular process. This continues posteriorly, eventually expanding dorsoventrally and slightly transversely at the level of the junction between the ischiadic peduncle and the postacetabular process to form a lateral (supraacetabular) process, which slightly overhangs the lateral wall in similar fashion to that seen in many other iguanodontians such as *Iguanodon bernissartensis* (Norman 1980), *Ouranosaurus nigeriensis* (Taquet 1976) and *Mantellisaurus atherfieldensis* (NHMUK PV R5764) but it is not as everted as it is in *Altirhinus kurzanovi* or hadrosaurids (Norman 1998). In lateral view the dorsal margin is almost horizontal anteriorly, but slightly convex over the acetabulum and slightly concave posteriorly.

A broad ridge is seen when the ilium is viewed medially, extending anteroposteriorly across the surface of the iliac blade. Above this ridge the surface of the ilium is slightly concave dorsoventrally and angled so that it faces dorsomedially and overhangs the lateral wall. Its surface is weakly striated with the striations orientated dorsoventrally in the midsection and posterodorsally in the posterior section. There are four crescentic facets ventral to this ridge that are buttressed dorsally by the ridge. These become shallower but much broader posteriorly and would have articulated with the transverse processes of the first four true sacral vertebrae. Posterior to these facets the ridge is heavily rugose. Ventral to the facets the surface of the bone is smooth except for the area just above the ischiadic peduncle, which is striated. The area ventral to the ridge is also heavily striated where it extends across the postacetabular process.

### Ischium

Only the dorsal half of the right ischium is preserved (Fig. 20). As with other parts of this individual there are deep erosions into the articular surfaces, which affect the pubic and iliac peduncles and the obturator process. The shaft of the proximal ischium has a triangular cross-section, with lateral, anteromedial and posteromedial surfaces. In lateral view, the surface of the distal section of the surviving shaft is almost flat. However, as it extends dorsally a wide, shallow central groove develops bounded by two rounded ridges. As the shaft reaches the head the groove on the lateral surface flattens out and expands into a shallowly concave area that forms the ventral margin of the acetabulum. A stout posterodorsally directed iliac peduncle is present posteriorly. This is transversely compressed and probably formed an elliptical articular surface, although an unknown amount of bone has been lost to erosion. There are no deep striae present for ligamentous attachment, indicating that the process was originally much longer. Anteriorly the pubic peduncle is well developed: this is also transversely compressed especially ventrally, and in lateral view it flares out distally. Again, the distal articular surface has been lost and there is little evidence of rugosity. Ventrally the pubic peduncle tapers to a narrow blade, which curves concavely to form an anterior embayment before expanding anteriorly to form the obturator process. This process curves laterally to produce a concavity that probably would have supported the postpubic rod (Norman 1986). The ventral margin continues distally as a keel, which curves diagonally from anterior to posterior before merging with the shaft. The ischium of *Brighstoneus simmondsi* is too incomplete to draw many useful comparisons. The *Mantellisaurus atherfieldensis* holotype includes only fragments of the ischium (Hooley 1925) but that of *Brighstoneus simmondsi* differs from *Iguanodon bernisartensis* (Norman 1980) in having a relatively more robust shaft and a more deeply curved anterior embayment between the pubic peduncle and obturator process. In this respect it more closely resembles the ischium of *Ouranosaurus nigeriensis* (Taquet 1976).

### Pubis

A thin bone fragment might represent the distal end of the prepubic process. It shares similarities in size and shape with the distal end of the prepubic blade of *Altirhinus kurzanovi* (Norman 1998) and a small *Iguanodon bernisartensis* (Norman 1980) but is not compatible with the paddle-shaped processes of *Mantellisaurus atherfieldensis* (Norman 1986) or *Ouranosaurus nigeriensis* (Bertozzo *et al.* 2017). The orientation of the fragment is unknown, but assuming

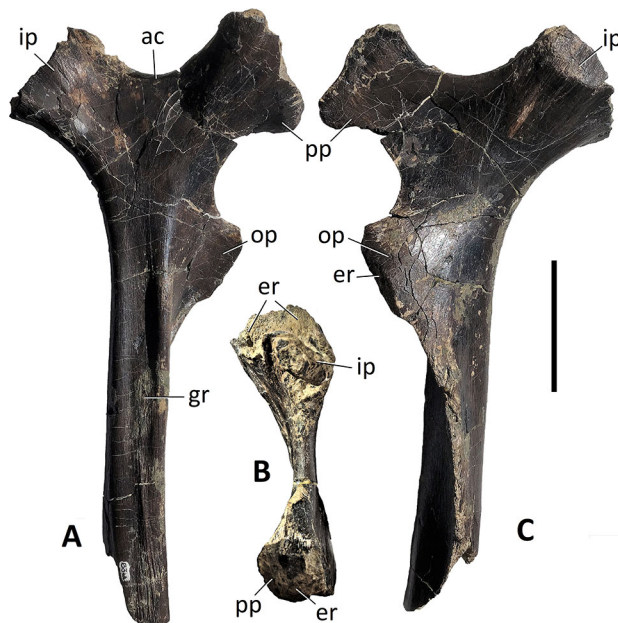


**Figure 20.** *Brighstoneus simmondsi* gen. et sp. nov. (MIWG 6344), ischium in **A**, lateral, **B**, dorsal and **C**, medial views. **Abbreviations:** ac, acetabular component; er, eroded areas; gr, lateral groove; ip, iliac peduncle; op, obturator process; pp, pubic peduncle. Scale bar = 100 mm.

the position in Fig. 21A, the ventral margin is approximately 3 mm thick and cortical bone is visible along its length. The thickness of the specimen in the central region is approximately 9 mm, thinning to 2 mm dorsally. The dorsal margin is obscured by a layer of pyrite but given the thinness of the bone was probably close to the margin. The curved margin (on the left in Fig. 21A) has been eroded, so its shape cannot be defined with certainty but it is compatible with a distal iguanodontian pubic blade. The right margin is curved laterally and has a pathologic appearance perhaps due to hypertrophic callus formation from chronic non-union in a displaced fracture.

### Femur

Only the right femur is preserved (Fig. 22). There are deeply excavated areas proximally that have affected the femoral head, greater trochanter and the dorsal surface of the anterior trochanter, while much of the distal end of the femur, including the condyles, is missing. Other than these eroded areas the bone surface is generally well preserved although is there crushing to the diaphysis posteriorly.

The femur is slender in anterior and posterior views and essentially straight except distally where it curves medially to create a concave medial margin. In medial view the anterior diaphysis describes a gently convex curve.

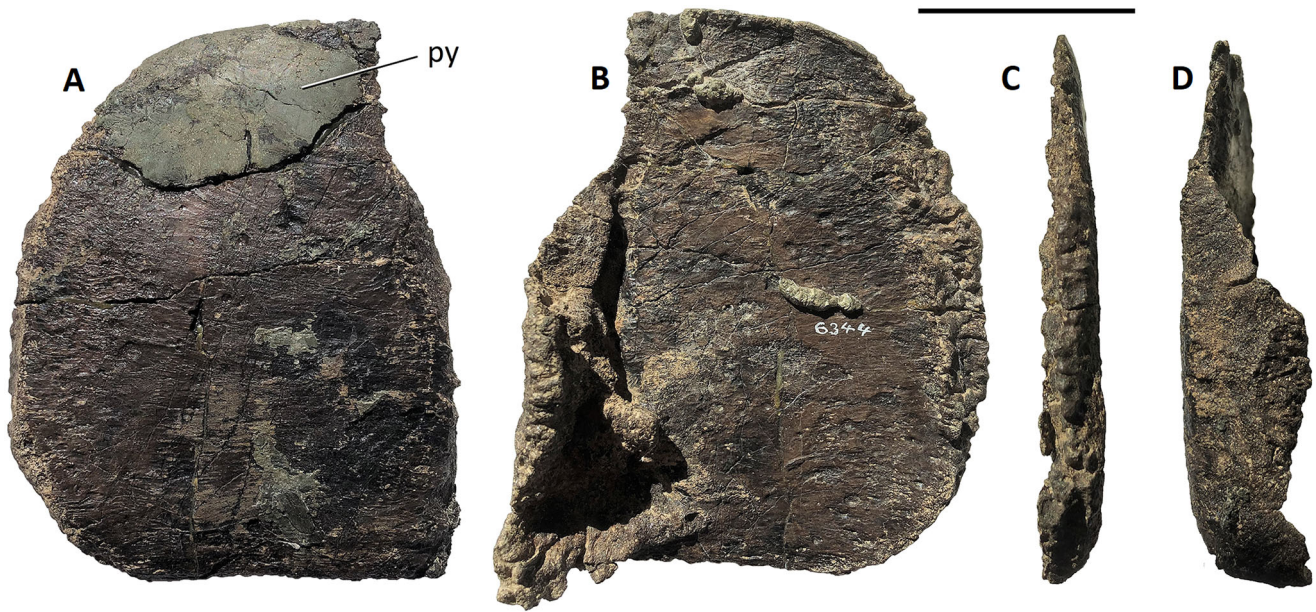


**Figure 21.** *Brighstoneus simmondsi* gen. et sp. nov. (MIWG 6344), possible fragment of anterior pubic process in **A**, lateral, **B**, medial, **C**, anterior and **D**, posterior views. Views assume that the distal end is to the left. **Abbreviation:** py, pyrite. Scale bar = 50 mm.

The head of the femur is directed medially but damage to the dorsal surface means that there is little anatomical information, although the presence of a saddle-shaped surface and an anteroposteriorly elongate greater trochanter seem likely. The anterior trochanter has some erosion dorsally but forms a mediolaterally compressed flange that is separated from the greater trochanter by a definite cleft (although this is filled with matrix). The lateral surface of the anterior trochanter has dorsoventral striations while its anterior margin is also roughened and mediolaterally wider than the posterior margin. The anterior margin continues ventrally as a rounded ridge that extends diagonally down the shaft of the femur towards the medial condyle, gradually becoming smoother and less prominent.

The fourth trochanter is transversely compressed and forms an elongate trapezium (Fig. 22B). Although the femur is incomplete, the fourth trochanter was almost certainly situated predominantly in the dorsal half of the femoral shaft, but it also extended onto the ventral half. The ventral border is angled posterodorsally and is continuous with the concave curve of the posterior surface of the distal femur, while the posterior border for most of its length is parallel with the axis of the mid-diaphysis before curving convexly to join the shaft of the proximal femur. A similarly shaped fourth trochanter is also seen in NHMUK PV R1148, the holotype of '*Iguanodon hollingtoniensis*' (currently regarded as a synonym of *Hypselospinus fittoni*; Norman 2015), NHMUK PV R2503, the femur of '*Iguanodon seelyi*'

(Hulke 1882), in adult (Verdú *et al.* 2017b) and perinate (Verdú *et al.* 2015) *Iguanodon galvensis*, and in RBINS R347 a 'sub-adult' specimen of *Iguanodon bernissartensis* (Verdú *et al.* 2017a). NHMUK PV R2503 has also been referred to *Iguanodon bernissartensis* (McDonald 2012a) and these differences probably represent intra-specific variation from the more usual triangular configuration. The shaft of the femur is shallowly excavated just medial to the base of the fourth trochanter and is heavily scarred.

The ventral articular surface of the femur has been lost but part of its mediolateral expansion is preserved. Anteriorly, the intercondylar extensor groove is narrow and extends distally becoming deeper, 'U'-shaped in mediolateral cross-section and slightly wider transversely. Posteriorly the intercondylar flexor groove is broader and relatively shallower. Both grooves are slightly ventromedially directed.

### Phylogenetic analysis

The systematic position of *Brighstoneus simmondsi* was assessed cladistically using a modified version of the matrix of Xu *et al.* (2018), which is modified from Norman (2015) and McDonald (2012b). The matrix was chosen as it focuses on non-hadrosauriform and hadrosauriform ankylopollexians but is not overly skewed towards hadrosaurids. We rescored *Mantellisaurus athei* using only material from the holotype

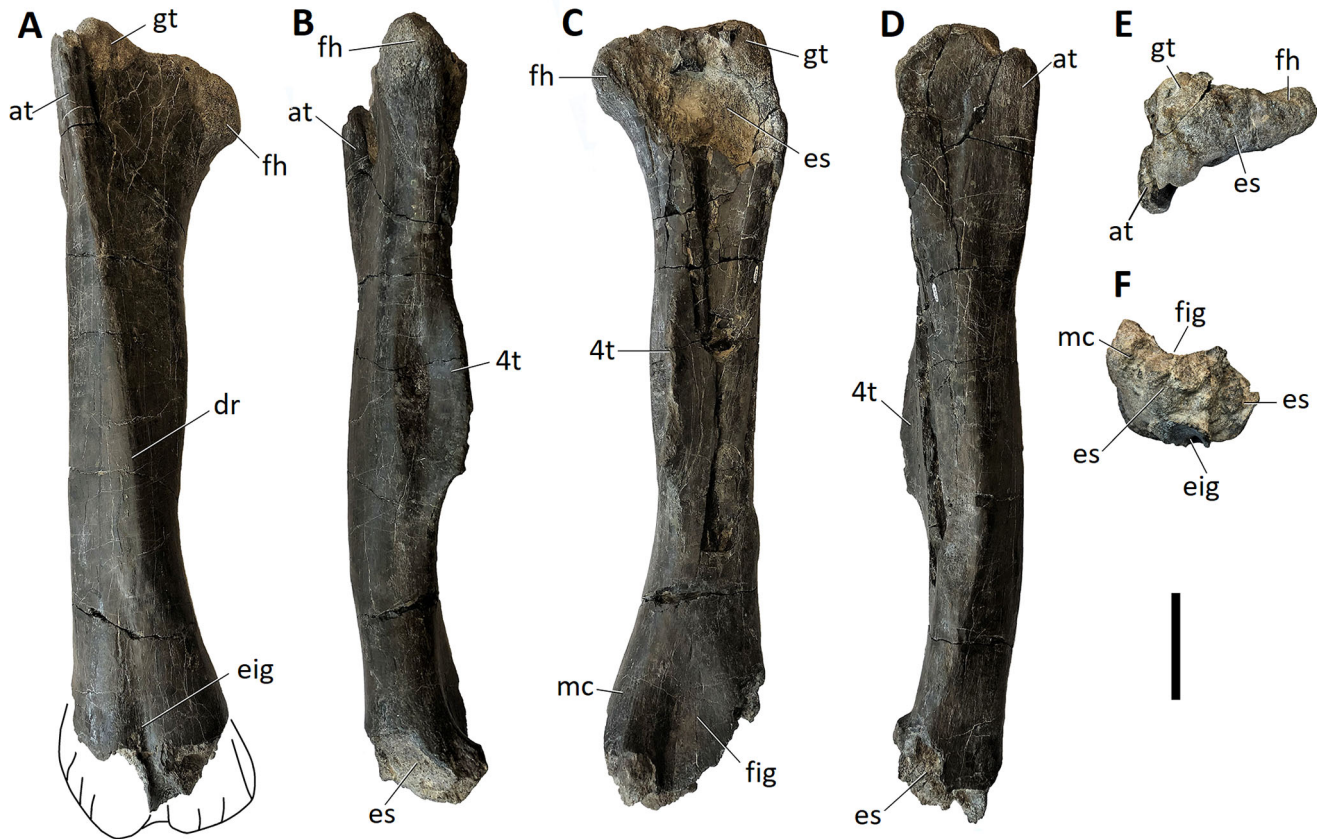


**Figure 22.** *Brighstoneus simmondsi* gen. et sp. nov. (MIWG 6344), right femur in **A**, anterior, **B**, medial, **C**, posterior, **D**, lateral, **E**, dorsal and **F**, ventral views. Reconstruction of distal femur shown in **A** is based on *Mantellisaurus atherfieldensis* (Norman 1986). **Abbreviations:** 4t, fourth trochanter; at, anterior trochanter; dr, diagonal ridge; eig, extensor intercondylar groove; es, eroded surface; fh, femoral head; fig, flexor intercondylar groove; gt, greater trochanter; mc, medial condyle. Scale bar = 100 mm.

specimen (NHMUK PV R5764), given concerns about the taxonomic status of referred material (e.g. Paul 2012). Initially, the analysis was run with the original 123 characters scored in the Xu *et al.* (2018) data matrix with the addition of *Brighstoneus simmondsi* (41 taxa), which produced an unresolved polytomy amongst those hadrosauriforms nested outside of Hadrosauroidea. To further explore the relationships between these earlier diverging hadrosauriforms, two characters (124 and 125) were added based on the observations that: (1) *Brighstoneus simmondsi* and *Ouranosaurus nigeriensis* possess a ventral nasal process, which is not present in *Iguanodon bernissartensis* or *Mantellisaurus atherfieldensis*; and (2) the markedly posterodorsally orientated articular surface to the ischiadic peduncle which is present in *Brighstoneus simmondsi* and *Ouranosaurus nigeriensis* is not present in *Barilium dawsoni*, *Iguanodon bernissartensis*, *Mantellisaurus atherfieldensis* or *Hypselospinus fittoni*.

Character 124: Nasal. Morphology of the nasal contact with the posterodorsal region of the lateral

maxillary process of the premaxilla at the posterior margin of the narial foramen; the nasal forms a sub-rectangular flange, which does not contribute to the ventral border of the narial foramen (0); nasal has anteroventral process, which contributes to the ventral border of the narial foramen. (1) (modified from Prieto-Márquez & Norell 2010, character 78).

Character 125: Ilium. The angle in lateral view between the articular surface of the ischiadic peduncle and the dorsal margin of the iliac central plate is less than 15° (0); is 15° or above (1). (See [Supplementary material, Figs S6–S8 and Table S3](#)).

The matrix was compiled in Mesquite v. 3.61 (Maddison & Maddison 2015) and analysed in TNT v. 1.5 (Goloboff & Catalano 2016), using a traditional search under the tree bisection reconnection (TBR) swapping algorithm, saving 100 trees per replication.

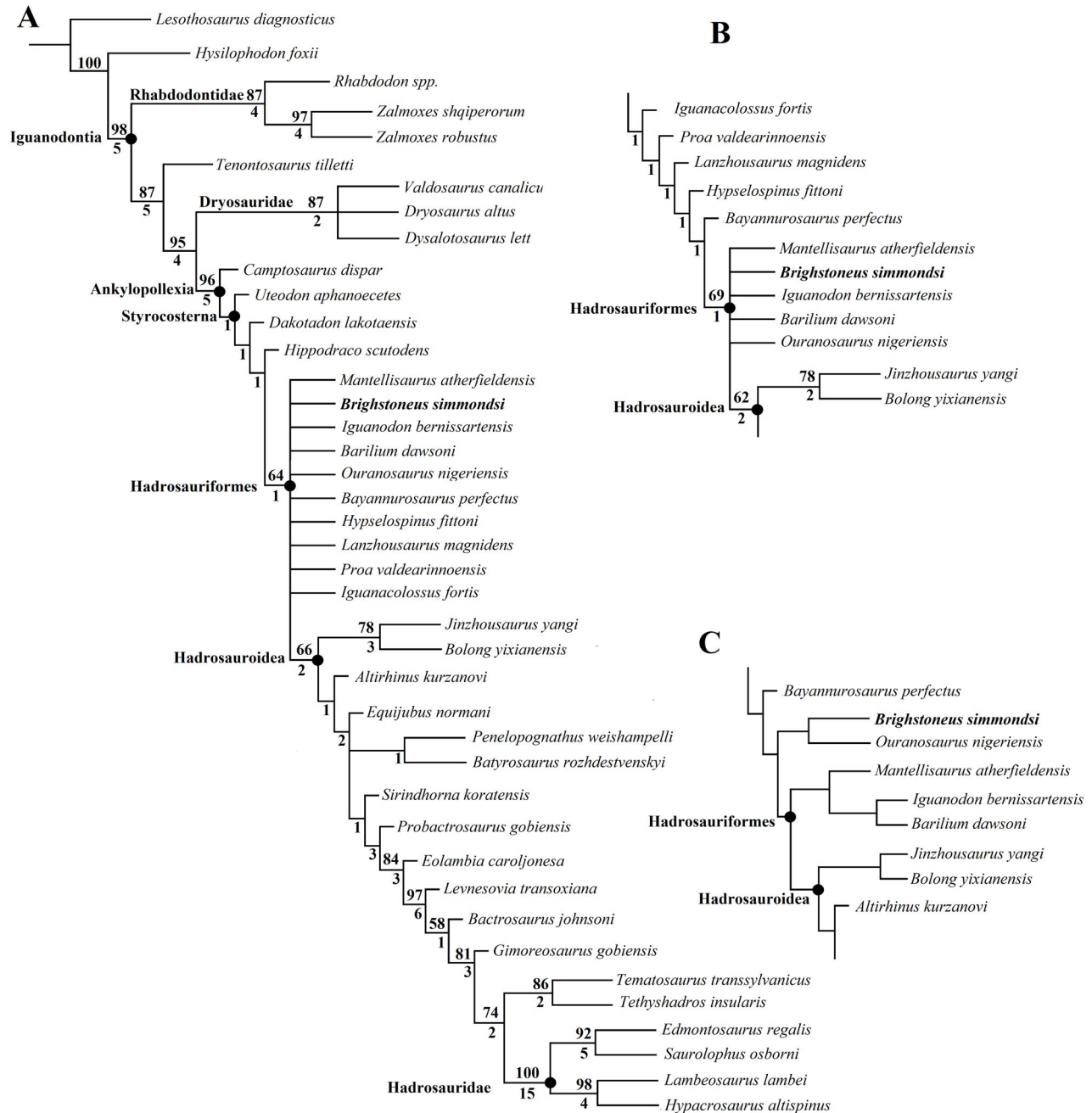


**Figure 23.** Three cladograms depicting the phylogenetic relationships of *Brighstoneus simmondsi*. **A**, strict consensus tree based on the matrix of Xu *et al.* (2018) with two additional characters added. Tree length = 338 steps, consistency index = 0.583, rescaled consistency index = 0.510, retention index = 0.874; **B**, section of strict consensus tree obtained after excluding new nasal character (124) and ilium character (125). Bootstrap values given above line, Bremer support below line; **C**, section of 50% majority rule consensus of 10 MPTs (for full tree see [Supplementary material, Fig. S9](#)).

*Lesothosaurus diagnosticus* was set as the outgroup. Consistency index, rescaled consistency index and retention index were calculated using the TNT script STAT.RUN and clade support using the TNT script BREMER.RUN and TNT bootstrap, set to 1000

replicates, reporting groupings found in >50% of pseudo-replicate datasets. The analysis resulted in 10 most parsimonious trees (MPTs), each with a tree length of 338 steps. The consistency index = 0.583, rescaled consistency index = 0.510 and the retention index = 0.874.

The relationships of the early diverging iguanodontians and hadrosaurids recovered by our analysis did not differ significantly from those of Xu *et al.* (2018) as shown in the strict consensus tree (Fig. 23). However, among hadrosauriforms nested outside of Hadrosauroidea, Xu *et al.* (2018) recovered a monophyletic clade (Iguanodontidae) containing *Mantellisaurus*, *Iguanodon* and *Barilium* with the latter two as sister taxa, while *Ouranosaurus* fell outside of Hadrosauriformes. The addition of *Brighstoneus* and the rescoring of *Mantellisaurus* recovered these five taxa as a polytomy in Hadrosauriformes, which persisted when nasal character 124 was introduced (Fig. 23B). When all 125 characters were used a large polytomy was recovered in Hadrosauriformes, which included five styracosternans, *Proa*, *Bayannurosaurus*, *Lanzhousaurus*, *Hypselospinus* and *Iguanacolossus*, which had previously fallen outside of this clade (Fig. 23A). Due to this poor resolution a 50% majority rule consensus was performed (Fig. 23C; full cladogram in Supplementary material, Fig. S9). This recovered the same topology as originally described in Xu *et al.* (2018) but with *Brighstoneus* as the sister taxon of *Ouranosaurus*, outside of Hadrosauriformes. Apart from characters 124 and 125, *Ouranosaurus* and *Brighstoneus* also differed from other Wealden Group taxa by scoring state '0' in character 100 (absence of axial twist in the preacetabular process). However, when a 50% majority rule consensus analysis was run without characters 124 and 125, *Brighstoneus* fell outside of Iguanodontidae as the most basally branching taxon in Hadrosauroidea. This demonstrates the volatility of these topologies and this study relied on the strict consensus tree to define the position of *Brighstoneus simmondsi* as an early diverging hadrosauriform.

These results neither support nor refute the dissolution of the Iguanodontidae node but confirm the fragile and inconsistent resolution seen among early-diverging styracosternans, especially the non-hadrosauroids at the base of hadrosauriform clade. This includes five genera from the Wealden Group, *Barilium*, *Hypsilospinus*, *Mantellisaurus*, *Iguanodon* and *Brighstoneus*, the latter three represented in the Wessex Formation of the Isle of Wight. The Wealden Group taxa are usually included in Hadrosauriformes (e.g. Prieto-Márquez & Norell 2010; Wu & Godefroit 2012; Norman 2015; Xu *et al.* 2018; Tsogtbaatar *et al.* 2019) although *Barilium* was found outside of this group by McDonald (2011), McDonald *et al.* (2017) and *Mantellisaurus atherfieldensis* in Hadrosauroidea by McDonald (2012b). Further work is clearly required to improve resolution in what is a major section of the iguanodontian clade spanning the Valanginian–early Albian.

## Discussion

### The number of dentary tooth positions in hadrosauriforms

Although the majority of non-hadrosaurid hadrosauriform taxa are represented by single specimens or lack relevant cranial material, there is evidence to support an increase in the number of tooth positions in this clade during ontogeny. Examples where data are available include *Eolambia caroljonesa* (Kirkland 1998; McDonald *et al.* 2012b), *Telmatosaurus transsylvanicus* (Weishampel *et al.* 1993) and *Bolong yixianensis* (Wu *et al.* 2010; Zheng *et al.* 2014), although these largely compare very immature juveniles and perinates with mature specimens. The perinates of *Iguanodon galvensis* were also noted to have relatively low tooth counts compared to a mature *Iguanodon bernissartensis* (Verdú *et al.* 2015).

Dinosaurs may continue to grow as adults, but this represents an asymptotic stage of marked slowing (Erickson *et al.* 2001). There is evidence from hadrosaurids that extra tooth positions are generated during normal growth but do not continue once maturity has been reached. Prieto-Márquez (2001) noted that in *Brachylophosaurus canadensis* the dentary tooth count with one exception was 33 in four adult and four sub-adult dentaries. Fondevilla *et al.* (2018) recorded a non-linear increase in tooth positions describing an asymptote in hadrosaurids. Also, an increase in dentary length during ontogeny can occur without requiring an associated isometric increase in tooth positions, for example by the elongation of the diastema in *Edmontosaurus* spp. (Campione & Evans 2011) and the widening of the tooth positions in *Dysalotosaurus lettowvorbecki*, where an increase in alveolar positions during ontogeny from 10 to 13 was accompanied by a 100% increase in dentary length (Hübner 2010).

Tooth counts, therefore, may have taxonomic utility in mature individuals, and indeed have often been used as a diagnostic character in hadrosauriforms. Norman (1986) cited 21 dentary tooth positions for *Mantellisaurus atherfieldensis* and up to 25 for *I. bernissartensis*. Paul (2008) stated that there were 22 dentary tooth positions in his diagnosis of *Mantellisaurus atherfieldensis* and indicated that 23 were visible in RBINS R57 (the holotype of '*Dollodon bampingi*') although it is unclear how a tooth count was obtained. Paul (2008) also suggested that the high number of dentary tooth positions in MIWG 6344 (*Brighstoneus simmondsi*) might make it referable to '*Dollodon*'.

A partial iguanodontian skeleton, NHMUK PV R11521, from the Wessex Formation that has been referred to *Mantellisaurus atherfieldensis* (Barrett *et al.*

2009; McDonald 2012a; Norman 2013), is an animal whose femoral length is 14% shorter than the holotype of *Mantellisaurus* but whose dentary has 20 teeth (9% less). *Brighstoneus simmondsi* has an estimated femoral length that is 10% greater than the holotype of *Mantellisaurus* but has at least six extra tooth positions (27% more). Ideally, ontogenetic stage should be determined histologically, but it can be observed that dorsal, sacral and caudal vertebral neurocentral sutures are fused in all three of these specimens. Fusion of vertebrae is not a reliable indicator of a fully mature adult (Bailleul *et al.* 2016; Hone *et al.* 2016) and does not preclude further linear growth (Griffin *et al.* 2020) but it is indicative of an animal that is reasonably skeletally mature, and it is unlikely that any of these specimens represents a juvenile (note that Horner [2000] and Evans [2007] define the term ‘juvenile’ as being <50% of adult size). Although the sample size is small, the implication is that *Brighstoneus simmondsi* is not part of an ontogenetic series with NHMUK PV R11521 and NHMUK PV R5764, and its high tooth count is an autapomorphic feature. Similar arguments to those applied to the number of tooth positions could also be raised against ontogenetic explanations for the formation of an elongated rostrum or a nasal bulla.

### Hadrosauriform alpha diversity

In the upper Campanian Dinosaur Park Formation of Alberta, Canada, an alluvial flood plain that experienced increasing transgressive events and had a similar average sediment accumulation rate to the Wessex Formation (40 mm/Ka), Mallon *et al.* (2012) identified two primary assemblage zones each lasting 600 Ka, both of which can be further sub-divided using rarer species into 300 Ka assemblages. Evidence was also seen for phyletic gradualism in hadrosaurids rather than population changes due to migration through those assemblage zones. Dodson (1990) showed that in the better exposures that contained stratigraphically superimposed formations at a specific location (e.g. the Judith River, Horseshoe Canyon and Scollard formations in Alberta, Canada, of late Campanian–Maastrichtian age, and the Djadochta, Barun Goyot and Nemegt formations in the Gobi Desert of Mongolia, of late Santonian–early Campanian to Maastrichtian age), faunal turnover appeared especially rapid. Schopf (1984) has suggested that if the same criteria were applied to fossil groups that are used for modern species, average species longevity might be as little as 200 Ka. This is in stark contrast to the conventional view that from the end of the Hauterivian to the early Aptian, the Wealden Group of England, and the wider ‘Wealden’ of western Europe, were dominated by two unchanging hadrosauriform

taxa: *Iguanodon bernissartensis* and *Mantellisaurus atherfieldensis*.

Historically, new hadrosauriform species and genera were erected on the basis of Isle of Wight Wealden Group material, such as *Iguanodon seelyi* and *Vectisaurus valdensis*, but these have generally entered into synonymy (Norman *et al.* 2004). In recent years other hadrosauriform genera have been proposed as contributing to the Isle of Wight fauna including *Dollodon seelyi* (Hulke, 1882), *Proplanicoxa galtoni* Carpenter & Ishida, 2010 and the Belgian *Dollodon bampingi* Paul, 2008. However, subsequent revisions have relegated these taxa to junior synonyms of either *Mantellisaurus atherfieldensis* or *Iguanodon bernissartensis* (McDonald 2012a; Norman 2012). In the more recent examples, novel taxa had been erected without first-hand examination of the specimens, or were based on a single character or element, leading to problems such as the misinterpretation of taphonomic distortion (McDonald 2012a). However, recent work on material from the Early Cretaceous of Spain is beginning to show a wider range of fauna from the upper Hauterivian–lower Aptian than appreciated even less than a decade ago. *Iguanodon bernissartensis* and *Mantellisaurus atherfieldensis* have been joined by *Iguanodon galvensis* (Verdú *et al.* 2015), *Magnamanus soriaensis* (Vidarte *et al.* 2016), *Morelladon beltrani* (Gasulla *et al.* 2015), *Portellsaurus sosbaynati* (Santos-Cubedo *et al.* 2021) and *Delapparentia turolensis* (Ruiz-Omeñaca 2011), although the latter may be a *nomen dubium* (Norman 2015; Verdú *et al.* 2017a).

The description of *Brighstoneus simmondsi* together with the work in Spain suggests that the Barremian–early Aptian hadrosauriform fauna in western Europe is probably more diverse than usually appreciated and that the evolutionary stability and durability of a two-species-dominated fauna needs to be re-evaluated. It also calls into question some of the referrals that have previously been made to *Mantellisaurus atherfieldensis* and *Iguanodon bernissartensis*, often based principally on size or robusticity rather than autapomorphies.

The question of dinosaur species longevity and expected diversity is complex, and can be subject to biases, which may over-estimate the species duration. These include:

1. More ephemeral taxa are less likely to be preserved in the fossil record than those with a high generic longevity.
2. Waste-basket taxa such as ‘*Iguanodon*’ and ‘*Megalosaurus*’, which existed prior to the 1990s, were to some degree a reflection of the pre-cladistic era, where symplesiomorphies were used to unite

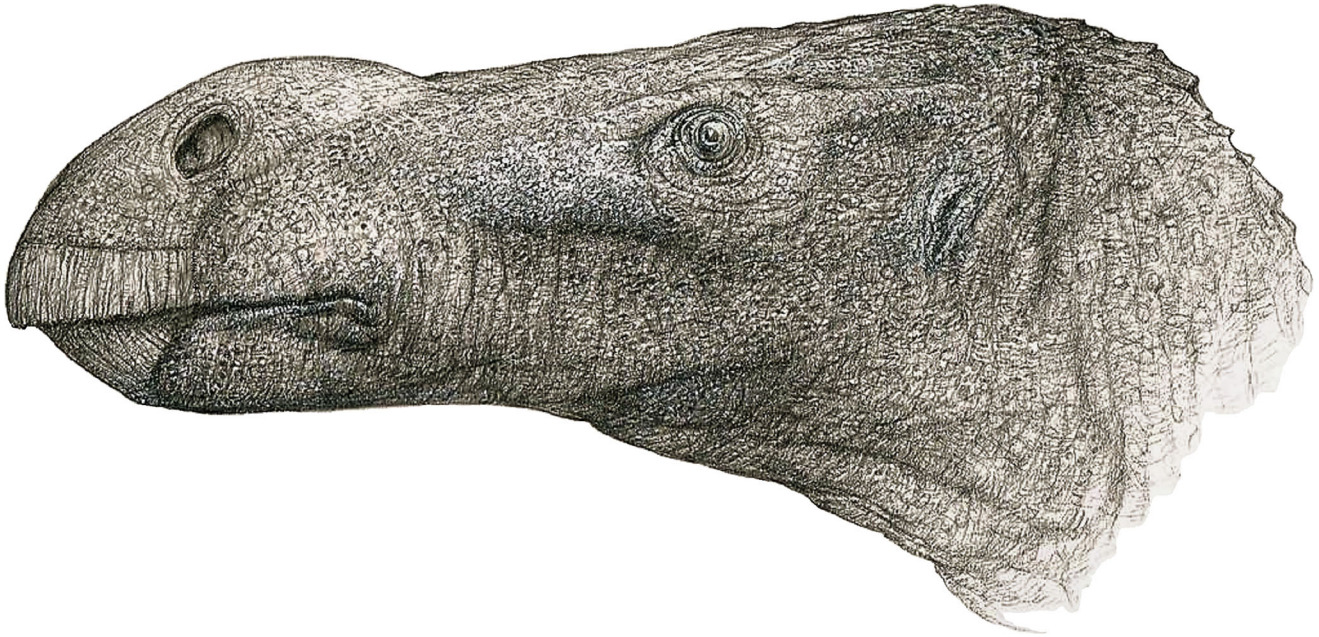


**Figure 24.** *Brighstoneus simmondsi*. gen. et sp. nov. Life restoration by John Sibbick.

groups or species rather than using unique character combinations and autapomorphies to identify individual taxa. Of course, technology and the relative ease of accessing data have also facilitated this change. Work prior to this is perhaps likely to have underestimated diversity and therefore overestimated species longevity.

These factors have probably influenced the taxonomy of Wealden Group hadrosauriforms. *Mantellisaurus atherfieldensis* and *Iguanodon bernissartensis* each have reasonably complete and well-preserved holotypes that have been monographed (Norman 1980, 1986). Their remains are found from the Hauterivian–Barremian boundary on the Isle of Wight (Martill & Naish 2001; McDonald 2012a; Norman 2013) and *Mantellisaurus atherfieldensis* is also recorded from the lower Aptian, Hythe Formation of Kent (McDonald 2012a), and so crosses one and possibly two stage boundaries. Bones, for example dorsal vertebrae, are frequently referred to one taxon or the other based on size, centrum length to height ratio and relative neural spine height. These characters adequately distinguish the *Mantellisaurus* hypodigm (although the holotype has lost nearly all neural spine material) from *Iguanodon* but are not autapomorphic and therefore give no diagnostic information at a specific level. Similar arguments can also be raised against referrals (albeit often tentative) to *Mantellisaurus atherfieldensis* for fragmentary remains in the Barremian–Aptian deposits of Spain (Serrano *et al.* 2013; Ruiz-Omeñaca *et al.* 1998, and references therein), Germany (Huckriede 1982; Norman 1987),

France (Martin & Buffetaut 1992; Knoll 2009) and Romania (Posmosanu 2003).

An important implication of the discovery of *Brighstoneus simmondsi* is that Barremian–early Aptian hadrosauriform finds from the Wealden Group should not be referred to *Mantellisaurus atherfieldensis* or *Iguanodon bernissartensis* unless specific autapomorphies are present. A detailed review of the material from the Isle of Wight is currently being undertaken, but efforts should be made to actively protect and accession Wealden Group iguanodontian specimens, particularly associated and cranial material, which in the past might have been dismissed as being unlikely to provide new data.

## Conclusions

*Brighstoneus simmondsi* (Fig. 24) is recognized as a new genus and species of hadrosauriform ornithomimid from the Wealden Group of the Isle of Wight, on the basis of two autapomorphies and a unique combination of characters. It is likely that the holotype specimen is ~4 Ma older than that of *Mantellisaurus atherfieldensis*, reinforcing the view that the Wealden Group is likely to have supported a higher diversity of iguanodontians than previously realized, both in the Wessex Formation and perhaps in coeval mainland exposures. This study also has systematic implications, questioning the validity of the composite operational taxonomic unit that has

generally been used to score *Mantellisaurus atherfieldensis* in phylogenetic analyses. To provide better resolution of relationships within Iguanodontia and a more complete understanding of iguanodontian alpha diversity in the Wessex Sub-basin, a reassessment of Isle of Wight material is necessary.

## Acknowledgements

We are grateful to Dr Martin Munt and Alex Peaker (Dinosaur Isle Museum, Isle of Wight), Carrie Hampton (Isle of Wight Council) and the Natural History Museum, London, for providing access to specimens under their care. We thank John Sibbick for generously providing the artwork, Tegan Hicks for her assistance with microscopic photography, and collectors Mick Green, Mark Penn, Fiona Wight, Shaun Smith, Andrew Cocks, Martin Simpson and Keith Simmonds for supporting this project. We are also indebted to two anonymous reviewers and the editor Paul Barrett (NHMUK) for their extremely helpful comments. The programme TNT is made freely available courtesy of the Willi Hennig Society.

## Supplementary material

Supplementary material for this article can be accessed here: <https://doi.org/10.1080/14772019.2021.1978005>.

## ORCID

Jeremy A. F. Lockwood  <http://orcid.org/0000-0002-3233-0819>

David M. Martill  <http://orcid.org/0000-0002-3208-5702>

Susannah C. R. Maidment  <http://orcid.org/0000-0002-7741-2500>

## References

- Allen, P. 1998. Purbeck–Wealden (Early Cretaceous) climates. *Proceedings of the Geologists' Association*, **109**, 1972–1936.
- Allen, P. & Wimbledon, W. A. 1991. Correlation of NW European Purbeck–Wealden (non-marine Lower Cretaceous) as seen from the English type-areas. *Cretaceous Research*, **12**, 511–526.
- Bailleul, A. M., Scannella, J. B., Horner, J. R. & Evans, D. C. 2016. Fusion patterns in the skulls of modern archosaurs reveal that sutures are ambiguous maturity indicators for the Dinosauria. *PLoS ONE*, **11**, e0147687. doi:10.1371/journal.pone.0147687
- Barrett, P. M. 2016. A new specimen of *Valdosaurus canaliculatus* (Ornithopoda: Dryosauridae) from the Lower Cretaceous of the Isle of Wight, England. *Memoirs of Museum Victoria*, **74**, 29–48.
- Barrett, P. M., Butler, R. J., Wang, X.-L. & Xu, X. 2009. Cranial anatomy of the iguanodontoid ornithopod *Jinzhouosaurus yangi* from the Lower Cretaceous Yixian Formation of China. *Acta Palaeontologica Polonica*, **54**, 35–48.
- Barrett, P. M., Butler, R. J., Twitchett, R. J. & Hutt, S. 2011. New material of *Valdosaurus canaliculatus* (Ornithischia: Ornithopoda) from the Lower Cretaceous of southern England. *Special Papers in Palaeontology*, **86**, 131–163.
- Barrett, P. M. & Bonsor, J. A. 2021. A revision of the non-avian dinosaurs *Eucercosaurus tanypondylus* and *Syngonosaurus macrocerus* from the Cambridge Greensand, UK. *Cretaceous Research*, **118**, 1–13.
- Bartholomai, A. & Molnar, R. E. 1981. *Muttaborrasaurus*, a new iguanodontid (Ornithischia: Ornithopoda) dinosaur from the Lower Cretaceous of Queensland. *Memoirs of the Queensland Museum*, **20**, 319–49.
- Behrensmeyer, A. K. 1978. Taphonomic and ecologic information from bone weathering. *Paleobiology*, **4**, 150–162.
- Bertozzo, F., Della Vecchia, F. M. & Fabbri, M. 2017. The Venice specimen of *Ouranosaurus nigeriensis* (Dinosauria, Ornithopoda). *PeerJ*, **5**, e3403. doi:10.7717/peerj.3403
- Bodin, S., Godet, A., Föllmi, K. B., Vermeulen, J., Arnaud, H. & Strasser, A. 2006. The late Hauterivian Faraoni oceanic anoxic event in the western Tethys: evidence from phosphorus burial rates. *Palaeogeography, Palaeoclimatology, Palaeoecology*, **235**, 245–264.
- Brett-Surman, M. K. & Wagner, J. R. 2007. Discussion of character analysis of the appendicular anatomy in Campanian and Maastrichtian North American hadrosaurids – variation and ontogeny. Pp. 135–169 in K. Carpenter (ed.) *Horns and beaks: ceratopsian and ornithopod dinosaurs*. Indiana University Press, Bloomington and Indianapolis.
- Britt, B. B., Scheetz, R. D. & Dangerfield, A. 2008. A suite of dermestid beetle traces on dinosaur bone from the Upper Jurassic Morrison Formation, Wyoming, USA. *Ichnos*, **15**, 59–71.
- Brown, B. 1910. The Cretaceous Ojo Alamo Beds of New Mexico with description of the new dinosaur genus *Kritosaurus*. *Bulletin of the American Museum of Natural History*, **28**, 267–274.
- Brusatte, S. L., Benson, R. B. J. & Hutt, S. 2008. The osteology of *Neovenator salerii* (Dinosauria: Theropoda) from the Wealden Group (Barremian) of the Isle of Wight. *Palaeontographical Society Monographs*, **162**, 1–75 + 45 pls.
- Buckland, W. 1835. On the discovery of fossil bones of the *Iguanodon*, in the Iron Sand of the Wealden Formation in the Isle of Wight, and in the Isle of Purbeck. *Transactions of the Geological Society of London*, **2**, 425–432.
- Campione, N. E. & Evans, D. C. 2011. Cranial growth and variation in *Edmontosaurus* (Dinosauria: Hadrosauridae): implications for latest Cretaceous megaherbivore diversity in North America. *PLoS ONE*, **6**, e25186. doi:10.1371/journal.pone.0025186

- Carpenter, K. & Wilson, Y.** 2008. A new species of *Camptosaurus* (Ornithopoda: Dinosauria) from the Morrison Formation (Upper Jurassic) of Dinosaur National Monument, Utah, and a biomechanical analysis of its forelimb. *Annals of Carnegie Museum*, **76**, 227–263.
- Carpenter, K. & Ishida, Y.** 2010. Early and "Middle" Cretaceous iguanodonts in time and space. *Journal of Iberian Geology*, **36**, 145–164.
- Chanthasit, P.** 2010. *The ornithopod dinosaur Rhabdodon from the Late Cretaceous of France: anatomy, systematics and paleobiology*. Unpublished PhD thesis, Université Claude Bernard – Lyon, 196 pp. [https://tel.archives-ouvertes.fr/tel-00841228/file/TH2010\\_Chanthasit\\_Phorphen.pdf](https://tel.archives-ouvertes.fr/tel-00841228/file/TH2010_Chanthasit_Phorphen.pdf)
- Dalla Vecchia, F. M.** 2009. *Tethyshadros insularis*, a new hadrosauroid dinosaur (Ornithischia) from the Upper Cretaceous of Italy. *Journal of Vertebrate Paleontology*, **29**, 1100–1116.
- Dodson, P.** 1990. Counting dinosaurs; how many kinds were there? *Proceedings of the National Academy of Science of the United States of America*, **87**, 7608–7612.
- Dollo, L.** 1888. Iguanodontidae et Camptonotidae. *Comptes Rendus de l'Académie des Sciences*, **106**, 775–777.
- Edmund, A. G.** 1957. On the special foramina in the jaws of many ornithischian dinosaurs. *Contributions of the Royal Ontario Museum*, **48**, 3–14.
- Erickson, G. M., Curry, P. J., Rogers, K. & Yerby, S.** 2001. Dinosaur growth patterns and rapid avian growth rates. *Nature*, **412**, 429–33.
- Evans, D. C.** 2007. *Ontogeny and evolution of lambeosaurine dinosaurs (Ornithischia: Hadrosauridae)*. Unpublished PhD thesis, University of Toronto, 529 pp.
- Falcon, N. L. & Kent, P. E.** 1960. Geological results of petroleum exploration in Britain. 1945–1957. *Memoir of the Geological Society of London*, **2**, 1–56.
- Fondevilla, V., Dalla Vecchia, F. M., Gaete, R., Galobart, A., Moncunill-Sole, B. & Kohler, M.** 2018. Ontogeny and taxonomy of the hadrosaur (Dinosauria, Ornithopoda) remains from Basturs Poble bonebed (late early Maastrichtian, Tremp Syncline, Spain). *PLoS ONE*, **13**, e0206287. doi:10.1371/journal.pone.0206287
- Forster, C. A.** 1990. The postcranial skeleton of the ornithopod dinosaur *Tenontosaurus tilletti*. *Journal of Vertebrate Paleontology*, **10**, 273–294.
- Francis, J. E.** 1987. The palaeoclimatic significance of growth rings in the Late Jurassic/Early Cretaceous fossil wood from southern England. Pp. 21–36 in R. G. W. Ward (ed.) *Applications of tree ring studies. Current research in dendrochronology and related subjects*. BAR International Series, **333**. University of Virginia, Charlottesville.
- Gale, A. S., Mutterlose, J., Batenburg, S., Gradstein, F. M., Agterberg, F. P., Ogg, J. G. & Petrizzo, M. R.** 2020. The Cretaceous Period. Pp. 1–63 in F. M. Gradstein, J. G. Ogg, M. D. Schmitz & G. M. Ogg (eds) *Geologic time scale 2020. Volume 2*. Elsevier, Amsterdam.
- Galton, P. M.** 1974. The ornithischian dinosaur *Hypsilophodon* from the Wealden of the Isle of Wight. *Bulletin of the British Museum (Natural History), Geology*, **25**, 1–152.
- Galton, P. M.** 1975. English hypsilophodontid dinosaurs (Reptilia: Ornithischia). *Palaeontology*, **18**, 741–752.
- Galton, P. M.** 1983. The cranial anatomy of *Dryosaurus*, a hypsilophodontid dinosaur from the Upper Jurassic of North America and East Africa, with a review of hypsilophodontids from the Upper Jurassic of North America. *Geologica et Palaeontologica*, **17**, 207–243.
- Galton, P. M.** 2009. Notes on Neocomian (Lower Cretaceous) ornithopod dinosaurs from England – *Hypsilophodon*, *Valdosaurus*, “*Camptosaurus*”, “*Iguanodon*” – and referred specimens from Romania and elsewhere. *Revue de Paléobiologie*, **28**, 211–273.
- Gasulla, J. M., Escaso, F., Narvaez, I., Otega, F. & Sanz, J. L.** 2015. A new sail-backed stirocosterian (Dinosauria: Ornithopoda) from the Early Cretaceous of Morella, Spain. *PLoS ONE*, **10**, e0144167. doi:10.1371/journal.pone.0144167
- Gates, T. A., Tsogtbaatar, K., Zanno, L. E., Chinzorig, T. & Watabe, M.** 2018. A new iguanodontian (Dinosauria: Ornithopoda) from the Early Cretaceous of Mongolia. *PeerJ*, **6**, e5300. doi:10.7717/peerj.5300
- Gilmore, C. W.** 1909. Osteology of the Jurassic reptile *Camptosaurus*, with a revision of the species of the genus, and descriptions of two new species. *Proceedings of the United States National Museum*, **36**, 197–332.
- Gilmore, C. W.** 1913. A new dinosaur from the Lance Formation of Wyoming. *Smithsonian Miscellaneous Collections*, **61**, 1–5.
- Gilmore, C. W.** 1925. Osteology of ornithopodous dinosaurs from the Dinosaur National Monument, Utah, *Camptosaurus medius*, *Dryosaurus altus*, *Laosaurus gracilis*. *Memoirs of the Carnegie Museum*, **10**, 385–409.
- Gilmore, C. W.** 1933. On the dinosaurian fauna of the Iren Dabasu Formation. *Bulletin of the American Museum of Natural History*, **67**, 23–78.
- Gilpin, D., DiCroce, T. & Carpenter, K.** 2007. A possible new basal hadrosaur from the Lower Cretaceous Cedar Mountain Formation of eastern Utah. Pp. 79–89 in K. Carpenter (ed.) *Horns and beaks: ceratopsian and ornithopod dinosaurs*. Indiana University Press, Bloomington and Indianapolis.
- Godefroit, P., Dong, Z.-M., Bultynck, P., Li, H. & Feng, L.** 1998. Sino-Belgian Cooperative Program. Cretaceous dinosaurs and mammals from Inner Mongolia: 1) New *Bactrosaurus* (Dinosauria: Hadrosauroida) material from Iren Dabasu (Inner Mongolia, P.R. China). *Bulletin de l'Institut Royal des Sciences Naturelles du Belgique*, **68**, 1–70.
- Godefroit, P., Codrea, V. & Weishampel, D. B.** 2009. Osteology of *Zalmoxes shqiperorum* (Dinosauria, Ornithopoda), based on new specimens from the Upper Cretaceous of Nalat-Vad (Romania). *Geodiversitas*, **31**, 525–553.
- Godefroit, P., Escuille, F., Bolotsky, Y. L. & Lauters, P.** 2012. A new basal hadrosauroid dinosaur from the Upper Cretaceous of Kazakhstan. Pp. 335–362 in P. Godefroit (ed.) *Bernissart dinosaurs and Early Cretaceous terrestrial ecosystems*. Indiana University Press, Bloomington and Indianapolis.
- Goloboff, P. A. & Catalano, S. A.** 2016. TNT version 1.5, including a full implementation of phylogenetic morphometrics. *Cladistics*, **32**, 221–238.
- Griffin, C. T., Stocker, M. R., Colleary, C., Stefanic, C. M., Lessner, E. J., Riegler, M., Formosal, K., Koeller, K. & Nesbitt, S. J.** 2020. Assessing ontogenetic maturity in extinct saurian reptiles. *Biological Reviews*, **96**, 470–525.

- Head, J. J.** 1998. A new species of basal hadrosaurid (Dinosauria, Ornithopoda) from the Cenomanian of Texas. *Journal of Vertebrate Paleontology*, **18**, 718–738.
- Hone, D. W. E., Farke, A. A. & Wedel, M. J.** 2016. Ontogeny and the fossil record: what, if anything, is an adult dinosaur? *Biology Letters*, **12**, 20150947. doi:10.1098/rsbl.2015.0947
- Hooley, R. W.** 1917. On the integument of *Iguanodon bernissartensis* (Boulenger) and of *Morosaurus becklesii* (Mantell). *Geological Magazine*, **64**, 140–150.
- Hooley, R. W.** 1925. On the skeleton of *Iguanodon atherfieldensis* sp. nov., from the Wealden Shales of Atherfield (Isle of Wight). *Quarterly Journal of the Geological Society of London*, **81**, 1–61.
- Horner, J. R.** 2000. Dinosaur reproduction and parenting. *Annual Review of Earth and Planetary Sciences*, **28**, 19–45.
- Horner, J. R., Weishampel, D. B. & Forster, C. A.** 2004. Hadrosauridae. Pp. 436–463 in D. B. Weishampel, P. Dodson & H. Osmólska (eds) *The Dinosauria*. Second edition. University of California Press, Berkeley.
- Hübner, T. R.** 2010. *Ontogeny in Dyalosotaurus lettowvorbecki*. Unpublished PhD thesis, Ludwig Maximilians Universität, 318 pp. [https://edoc.ub.uni-muenchen.de/12598/1/Huebner\\_Tom.pdf](https://edoc.ub.uni-muenchen.de/12598/1/Huebner_Tom.pdf)
- Huchet, J. B., Deverley, D., Gutierrez, B. & Chauchat, C.** 2011. Taphonomic evidence of a human skeleton gnawed by termites in a Moche-civilisation grave at Huaca de la Luna, Peru. *International Journal of Osteoarchaeology*, **21**, 92–102.
- Huckriede, R.** 1982. Die unterkretazische Karsthöhlen-Füllung von Nehden im Sauerland. 1. Geologische, paläozoologische und paläobotanische befunde und datierung. *Geologica et Palaeontologica*, **16**, 183–242.
- Hughes, N. F. & McDougall, A. D.** 1990. New Wealden correlation for the Wessex Basin. *Proceedings of the Geologists' Association*, **101**, 85–90.
- Hulke, J. W.** 1879. *Vectisaurus valdensis*, a new Wealden Dinosaur. *Quarterly Journal of the Geological Society of London*, **35**, 421–424.
- Hulke, J. W.** 1882. Description of some *Iguanodon* remains indicating a new species *I. seelyi*. *Quarterly Journal of the Geological Society of London*, **150**, 135–144.
- Hutt, S., Martill, D. M. & Barker, M. J.** 1996. The first European allosauroid dinosaur (Lower Cretaceous, Wealden Group, England). *Neues Jahrbuch für Geologie und Paläontologie, Monatshefte*, **10**, 635–644.
- Huxley, T. H.** 1869. On *Hypsilophodon*, a new genus of Dinosauria. *Abstracts of the Proceedings of the Geological Society of London*, **204**, 3–4.
- Jarzewowski, E.** 1981. An Early Cretaceous termite from southern England (Isoptera: Hodotermitidae). *Systematic Entomology*, **6**, 91–96.
- Jin, L.-Y., Chen, J., Zan, S.-Q., Butler, R. J. & Godefroit, P.** 2010. Cranial anatomy of the small ornithischian dinosaur *Changchunsaurus parvus* from the Qiantou Formation (Cretaceous: Aptian–Cenomanian) of Jilin Province, northeastern China. *Journal of Vertebrate Paleontology*, **30**, 196–214.
- Kerth, M. & Hailwood, E. A.** 1988. Magnetostratigraphy of the Lower Cretaceous Vectis Formation (Wealden Group) on the Isle of Wight, southern England. *Journal of the Geological Society of London*, **145**, 351–360.
- Kirkland, J. I.** 1998. A new hadrosaurid from the upper Cedar Mountain Formation (Albian–Cenomanian: Cretaceous) of eastern Utah – the oldest known hadrosaurid (lambeosaurine?). *New Mexico Museum of Natural History and Science, Bulletin*, **14**, 283–295.
- Knoll, F.** 2009. A large iguanodont from the upper Barremian of the Paris Basin. *Geobios*, **42**, 755–764.
- Kobayashi, Y. & Azuma, Y.** 2003. A new iguanodontian (Dinosauria: Ornithopoda) from the Lower Cretaceous Kitadani Formation of Fukui Prefecture, Japan. *Journal of Vertebrate Paleontology*, **23**, 392–396.
- Lambe, L. M.** 1914. On *Gryposaurus notabilis*, a new genus and species of trachodont dinosaur from the Belly River Formation of Alberta, with a description of the skull of *Chasmosaurus belli*. *The Ottawa Naturalist*, **27**, 145–155.
- Maddison, W. P. & Maddison, D. R.** 2015. Mesquite: a modular system for evolutionary analysis. Version 3.61. [www.mesquiteproject.org/](http://www.mesquiteproject.org/)
- Mallon, J. C., Evans, D. C., Ryan, M. J. & Anderson, J. S.** 2012. Megaherbivorous dinosaur turnover in the Dinosaur Park Formation (upper Campanian) of Alberta, Canada. *Palaeogeography, Palaeoclimatology, Palaeoecology*, **350–352**, 124–138.
- Mantell, G. A.** 1825. Notice on the *Iguanodon*, a newly discovered fossil reptile, from the sandstone of Tilgate Forest, in Sussex. *Philosophical Transactions of the Royal Society*, **115**, 179–186.
- Mantell, G. A.** 1847. *Geological excursions round the Isle of Wight and along the adjacent coast of Dorsetshire*. R. Clay, London, 430 pp.
- Marsh, O. C.** 1881. Principal characters of American Jurassic dinosaurs. Part IV. Spinal cord, pelvis, and limbs of *Stegosaurus*. *American Journal of Science, Series 3*, **21**, 167–170.
- Martill, D. M. & Naish, D.** 2001. *Dinosaurs of the Isle of Wight*. Field Guide to Fossils, 10. The Palaeontological Association and Wiley-Blackwell, London, 433 pp.
- Martin, V. & Buffetaut, E.** 1992. Les iguanodons (Ornithischia – Ornithopoda) du Crétacé inférieur de la région de Saint-Dizier (Haute-Marne). *Revue de Paléobiologie*, **11**, 67–96.
- Maryńska, T. & Osmólska, H.** 1979. Aspects of hadrosaurian cranial anatomy. *Lethaia*, **12**, 265–273.
- McDonald, A. T.** 2011. The taxonomy of species assigned to *Camptosaurus* (Dinosauria: Ornithopoda). *Zootaxa*, **2783**, 52–68.
- McDonald, A. T.** 2012a. The status of *Dollodon* and other basal iguanodonts (Dinosauria: Ornithischia) from the upper Wealden beds (Lower Cretaceous) of Europe. *Cretaceous Research*, **33**, 1–6.
- McDonald, A. T.** 2012b. Phylogeny of basal iguanodonts (Dinosauria: Ornithischia): an update. *PLoS ONE*, **7**, e36745. doi:10.1371/journal.pone.0036745
- McDonald, A. T., Kirkland, J. I., DeBlieux, D. D., Madsen, S. K., Cavin, J., Milner, A. R. C. & Panzarin, I.** 2010a. New basal iguanodonts from the Cedar Mountain Formation of Utah and the evolution of thumb-spiked dinosaurs. *PLoS ONE*, **5**, e14075. doi:10.1371/journal.pone.0014075
- McDonald, A. T., Barrett, P. M. & Chapman, S. D.** 2010b. A new basal iguanodont (Dinosauria: Ornithischia) from the Wealden (Lower Cretaceous) of England. *Zootaxa*, **2569**, 1–43.

- McDonald, A. T., Wolfe, D. G. & Kirkland, J. I.** 2010c. A new basal hadrosauroid (Dinosauria: Ornithopoda) from the Turonian of New Mexico. *Journal of Vertebrate Paleontology*, **30**, 799–812.
- McDonald, A. T., Espilez, E., Mampel, L., Kirkland, J. I. & Alcalá, L.** 2012a. An unusual new basal iguanodont (Dinosauria: Ornithopoda) from the Lower Cretaceous of Teruel, Spain. *Zootaxa*, **3595**, 61–76.
- McDonald, A. T., Bird, J., Kirkland, J. I. & Dodson, P.** 2012b. Osteology of the basal hadrosauroid *Eolambia caroljonesa* (Dinosauria: Ornithopoda) from the Cedar Mountain Formation of Utah. *PLoS ONE*, **7**, e45712. doi: [10.1371/journal.pone.0045712](https://doi.org/10.1371/journal.pone.0045712)
- McDonald, A. T., Maidment, S. C. R., Barrett, P. M., You, H.-L. & Dodson, P.** 2014. Osteology of the basal Hadrosauroid *Equijubus normani* (Dinosauria, Ornithopoda) from the Early Cretaceous of China. Pp. 44–72 in D. A. Eberth & D. C. Evans (eds) *Hadrosaurs*. Indiana University Press, Bloomington and Indianapolis.
- McDonald, A. T., Gates, T. A., Zanno, L. E. & Makovicky, P. J.** 2017. Anatomy, taphonomy, and phylogenetic implications of a new specimen of *Eolambia caroljonesa* (Dinosauria: Ornithopoda) from the Cedar Mountain Formation, Utah, USA. *PLoS ONE*, **12**, 176896. doi: [10.1371/journal.pone.0176896](https://doi.org/10.1371/journal.pone.0176896)
- Naish, D. & Martill, D. M.** 2008. Dinosaurs of Great Britain and the role of the Geological Society of London in their discovery: Ornithischia. *Journal of the Geological Society*, **165**, 613–623.
- Norman, D. B.** 1980. On the ornithischian dinosaur *Iguanodon bernissartensis* of Bernissart (Belgium). *Mémoires de l'Institut Royal des Sciences Naturelles de Belgique*, **178**, 1–105.
- Norman, D. B.** 1986. On the anatomy of *Iguanodon atherfieldensis* (Ornithischia: Ornithopoda). *Bulletin de l'Institut Royal des Sciences Naturelles de Belgique, Sciences de la Terre*, **56**, 281–372.
- Norman, D. B.** 1987. A mass-accumulation of vertebrates from the Lower Cretaceous of Nehden (Sauerland), West Germany. *Proceedings of the Royal Society of London, Series B, Biological Sciences*, **230**, 215–255.
- Norman, D. B.** 1990. A review of *Vectisaurus valdensis*, with comments on the family Iguanodontidae. Pp. 147–162 in K. Carpenter & P. J. Currie (eds) *Dinosaur systematics: approaches and perspectives*. Cambridge University Press, Cambridge.
- Norman, D. B.** 1998. On Asian ornithopods (Dinosauria, Ornithischia). 3. A new species of iguanodontid dinosaur. *Zoological Journal of the Linnean Society*, **122**, 291–348.
- Norman, D. B.** 2002. On Asian ornithopods (Dinosauria: Ornithischia). 4. *Probactrosaurus* Rozhddestvensky, 1966. *Zoological Journal of the Linnean Society*, **136**, 113–144.
- Norman, D. B.** 2010. A taxonomy of iguanodontians (Dinosauria: Ornithopoda) from the lower Wealden Group (Cretaceous: Valanginian) of southern England. *Zootaxa*, **2489**, 47–66.
- Norman, D. B.** 2011. On the osteology of the lower Wealden (Valanginian) ornithopod *Barilium dawsoni* (Iguanodontia: Styracosterna). *Special Papers in Palaeontology*, **86**, 165–194.
- Norman, D. B.** 2012. Iguanodontian taxa (Dinosauria: Ornithischia) from the Lower Cretaceous of England and Belgium. Pp. 175–212 in P. Godefroit (ed.) *Bernissart dinosaurs and Early Cretaceous terrestrial ecosystems*. Indiana University Press, Bloomington and Indianapolis.
- Norman, D. B.** 2013. On the taxonomy and diversity of Wealden iguanodontian dinosaurs (Ornithischia: Ornithopoda). *Revue de Paleobiologie*, **32**, 385–404.
- Norman, D. B.** 2015. On the history, osteology, and systematic position of the Wealden (Hastings Group) dinosaur *Hypselospinus fittoni* (Iguanodontia: Styracosterna). *Zoological Journal of the Linnean Society*, **173**, 92–189.
- Norman, D. B., Sues, H.-D., Witmer, L. M. & Coria, R. A.** 2004. Basal Ornithopoda. Pp. 393–412 in D. B. Weishampel, P. Dodson & H. Osmólska (eds) *The Dinosauria*. Second edition. University of California Press, Berkeley.
- Oldham, T. C. B.** 1976. The plant debris beds of the English Wealden. *Palaeontology*, **19**, 437–502.
- Ösi, A., Prondvai, E., Butler, R. J. & Weishampel, D. B.** 2012. Phylogeny, histology and inferred body size evolution in a new rhabdodontid dinosaur from the Late Cretaceous of Hungary. *PLoS ONE*, **7**, e44318. doi: [10.1371/journal.pone.0044318](https://doi.org/10.1371/journal.pone.0044318)
- Ostrom, J. H.** 1970. Stratigraphy and paleontology of the Cloverly Formation (Lower Cretaceous) of the Bighorn Basin area, Wyoming and Montana. *Bulletin of the Peabody Museum of Natural History*, **35**, 1–234.
- Owen, R.** 1842. Report on British fossil reptiles. Part II. *Reports of the British Association for the Advancement of Science*, **11**(for 1841), 60–204.
- Parks, W. A.** 1922. *Parasaurolophus walkeri*, a new genus and species of trachodont dinosaur. *University of Toronto Studies: Geological Series*, **13**, 5–32.
- Paul, G. S.** 2008. A revised taxonomy of the iguanodont dinosaur genera and species. *Cretaceous Research*, **29**, 192–216.
- Paul, G. S.** 2012. Notes on the rising diversity of iguanodont taxa, and iguanodonts named after Darwin, Huxley, and evolutionary science. Pp. 123–133 in P. Heurta, F. T. Fernández-Baldor & J. I. Canudo (eds) *Actas de V jornadas internacionales sobre Paleontología de dinosaurios y su entorno*. Colectivo Arqueológico y Paleontológico de Salas, C.A.S., Salas de Los Infantes, Burgos.
- Possoanu, E.** 2003. Iguanodontian dinosaurs from the Lower Cretaceous bauxite site from Romania. *Acta Palaeontologica Romaniae*, **4**, 431–439.
- Prieto-Márquez, A.** 2001. *Osteology and variation of Brachylophosaurus canadensis (Dinosauria, Hadrosauridae) from the Upper Cretaceous Judith River Formation of Montana*. Unpublished Master's thesis, Montana State University, Bozeman, 390 pp.
- Prieto-Márquez, A.** 2012. The skull and appendicular skeleton of *Gryposaurus latidens*, a saurolophine hadrosaurid (Dinosauria: Ornithopoda) from the early Campanian (Cretaceous) of Montana, USA. *Canadian Journal of Earth Sciences*, **49**, 510–532.
- Prieto-Márquez, A. & Norell, M. A.** 2010. Anatomy and relationships of *Gilmoresaurus mongoliensis* (Dinosauria: Hadrosauroidea) from the Late Cretaceous of Central Asia. *American Museum Novitates*, **3694**, 1–52.
- Prieto-Márquez, A., Chiappe, L. M. & Joshi, S. H.** 2012. The lambeosaurine dinosaur *Magnapaulia laticaudus* from the Late Cretaceous of Baja, California, northwestern

- Mexico. *PLoS ONE*, **7**, e38207. doi:10.1371/journal.pone.0038207
- Prieto-Márquez, A., Erickson, G. M. & Ebersole, J. A.** 2016. Anatomy and osteohistology of the basal hadrosaurid dinosaur *Eotrachodon* from the uppermost Santonian (Cretaceous) of southern Appalachia. *PeerJ*, **4**, e1872. doi:10.7717/peerj.1872
- Radley, J. D. & Barker, M. J.** 1998. Stratigraphy, palaeontology and correlation of the Vectis Formation (Wealden Group, Lower Cretaceous) at Compton Bay, Isle of Wight, southern England. *Proceedings of the Geologists' Association*, **109**, 187–195.
- Radley, J. D., Barker, M. J. & Harding, I.** 1998. Palaeoenvironment and taphonomy of dinosaur tracks in the Vectis Formation (Lower Cretaceous) of the Wessex Sub-basin, southern England. *Cretaceous Research*, **19**, 471–487.
- Radley, D. J. & Barker, M. J.** 2000. Palaeoenvironmental significance of storm coquinas in a Lower Cretaceous coastal lagoonal succession (Vectis Formation, Isle of Wight, southern England). *Geological Magazine*, **137**, 193–205.
- Robinson, S. A. & Hesselbo, S. P.** 2004. Fossil-wood carbon-isotope stratigraphy of the non-marine Wealden Group (Lower Cretaceous, southern England). *Journal of the Geological Society of London*, **161**, 133–145.
- Romer, A. S.** 1956. *Osteology of the reptiles*. University of Chicago Press, Chicago, 772 pp.
- Ruiz-Omeñaca, J. I.** 2011. *Delapparentia turolensis* nov. gen et sp., un nuevo dinosaurio iguanodontoideo (Ornithischia: Ornithopoda) en el Cretácico Inferior de Galve. *Estudios Geológicos*, **67**, 83–110.
- Ruiz-Omeñaca, J. I., Canudo, J. I. & Cuenca-Bescós, G.** 1998. Sobre las especies de *Iguanodon* (Dinosauria, Ornithischia) encontradas en el Cretácico inferior de España. *Geogaceta*, **24**, 275–278.
- Ruiz-Omeñaca, J. I., Pereda Suberbiola, X. & Galton, P. M.** 2007. *Callososaurus leedsi*, the earliest dryosaurid dinosaur (Ornithischia: Euornithopoda) from the Middle Jurassic of England. Pp. 3–16 in K. Carpenter (ed.) *Horns and beaks: ceratopsian and ornithopod dinosaurs*. Indiana University Press, Bloomington and Indianapolis.
- Santos-Cubedo, A., de Santisteban, C., Poza, B. & Meseguer, S.** 2021. A new styracosternan hadrosaurid (Dinosauria: Ornithischia) from the Early Cretaceous of Portell, Spain. *PLoS ONE*, **16**, e0253599. doi:10.1371/journal.pone.0253599
- Schopf, T. J. M.** 1984. Rates of evolution and the notion of “living fossils”. *Annual Review of Earth and Planetary Sciences*, **12**, 245–292.
- Seeley, H. G.** 1887. On the classification of the fossil animals commonly named Dinosauria. *Proceedings of the Royal Society of London*, **43**, 165–171.
- Sereno, P. C.** 1986. Phylogeny of the bird-hipped dinosaurs (Order Ornithischia). *National Geographic Research*, **2**, 234–256.
- Sereno, P. C.** 1997. The origin and evolution of dinosaurs. *Annual Review of Earth and Planetary Sciences*, **25**, 435–489.
- Sereno, P.** 2005. Iguanodontia, Taxon Search. [http://taxonsearch.uchicago.edu/?tax\\_id=178&exe=display&ke=key](http://taxonsearch.uchicago.edu/?tax_id=178&exe=display&ke=key). Data retrieved 25 January 2021.
- Serrano, M. L., Vullo, R., Marugan-Lobon, J., Ortega, F. & Buscalioni, A.** 2013. An articulated hindlimb of a basal iguanodont (Dinosauria, Ornithopoda) from the Early Cretaceous, Las Hoyas Lagerstätte (Spain). *Geological Magazine*, **150**, 572–576.
- Shibata, M. & Azuma, Y.** 2015. New basal hadrosaurid (Dinosauria: Ornithopoda) from the Lower Cretaceous Kitadani Formation, Fukui, central Japan. *Zootaxa*, **3914**, 421–440.
- Shibata, M., Jintasakul, P., Azuma, Y. & You, H.-L.** 2015. A new basal hadrosaurid dinosaur from the Lower Cretaceous Khok Kruat Formation in Nakhon Ratchasima province, north eastern Thailand. *PLoS ONE*, **10**, e0145904. doi:10.1371/journal.pone.0145904
- Stewart, D. J.** 1978. *The sedimentology and palaeoenvironment of the Wealden Group of the Isle of Wight, southern England*. Unpublished PhD thesis, University of Portsmouth, 346 pp.
- Sues, H.-D. & Averianov, A.** 2009. A new basal hadrosaurid dinosaur from the Late Cretaceous of Uzbekistan and the early radiation of duck-billed dinosaurs. *Proceedings of the Royal Society B*, **276**, 2549–2555.
- Sweetman, S. C.** 2007. *Aspects of the microvertebrate fauna of the Early Cretaceous (Barremian) Wessex Formation of the Isle of Wight, southern England*. Unpublished PhD thesis, University of Portsmouth, 316 pp. [https://pure.port.ac.uk/ws/portalfiles/portal/6060512/SCS\\_2007\\_PhD\\_Thesis.pdf](https://pure.port.ac.uk/ws/portalfiles/portal/6060512/SCS_2007_PhD_Thesis.pdf)
- Sweetman, S. C.** 2011. The Wealden of the Isle of Wight. Pp. 69–71 in D. J. Batten (ed.) *English Wealden fossils*. Palaeontological Association, London.
- Sweetman, S. C. & Insole, A. N.** 2010. The plant debris beds of the Early Cretaceous (Barremian) Wessex Formation of the Isle of Wight, southern England: their genesis and palaeontological significance. *Palaeogeography, Palaeoclimatology, Palaeoecology*, **292**, 409–424.
- Taquet, P.** 1976. *Géologie et paléontologie du gisement de Gadoufaoua (Aptien du Niger)*. Cahiers de paléontologie. Éditions du Centre National de la Recherche Scientifique, Paris, 191 pp.
- Thomas, D. A.** 2015. The cranial anatomy of *Tenontosaurus tilletti* Ostrom, 1970 (Dinosauria, Ornithopoda). *Palaeontologia Electronica*, **18**(2), 37A. doi:10.26879/450
- Torrens, H.** 2014. The English Isle of Wight and its crucial role in the invention of dinosaurs. *Biological Journal of the Linnean Society*, **113**, 664–676.
- Tsogtbaatar, K., Weishampel, D. B., Evans, D. C. & Watabe, M.** 2014. A new hadrosaurid (*Plesiohadros djadokhtaensis*) from the Late Cretaceous Djadokhtan fauna of southern Mongolia. Pp. 108–135 in D. A. Eberth & D. C. Evans (eds) *Hadrosaurs*. Indiana University Press, Bloomington and Indianapolis.
- Tsogtbaatar, K., Weishampel, D. B., Evans, D. C. & Watabe, M.** 2019. A new hadrosaurid (Dinosauria: Ornithopoda) from the Late Cretaceous Baynshire Formation of the Gobi Desert (Mongolia). *PLoS ONE*, **14**, e0208480. doi:10.1371/journal.pone.0208480
- Van Beneden, P. J.** 1881. Sur l'arc pelvien chez les dinosauriens de Bernissart. *Bulletins de l'Académie royale des sciences, des lettres et des beaux-arts de Belgique*, **3**, 600–608.
- Verdú, F. J., Royo-Torres, R., Cobos, A. & Alcalá, L.** 2015. Perinates of a new species of *Iguanodon* (Ornithischia: Ornithopoda) from the lower Barremian of Galve (Teruel, Spain). *Cretaceous Research*, **56**, 250–264.

- Verdú, F. J., Godefroit, P., Royo-Torres, R., Cobos, A. & Alcalá, L.** 2017a. Individual variation in the postcranial skeleton of the Early Cretaceous *Iguanodon bernissartensis* (Dinosauria: Ornithopoda). *Cretaceous Research*, **74**, 65–86.
- Verdú, F. J., Royo-Torres, R., Cobos, A. & Alcalá, L.** 2017b. New systematic and phylogenetic data about the early Barremian *Iguanodon galvensis* (Ornithopoda: Iguanodontioidea) from Spain. *Historical Biology*, **30**, 437–474.
- Vidarte, C. F., Calvo, M. M., Fuentes, F. M. & Fuentes, M. M.** 2016. Un nuevo dinosaurio estiracosterno (Ornithopoda: Ankylopollexia) del Cretácico Inferior de España. *Spanish Journal of Palaeontology*, **31**, 407–446.
- Wagner, J. R. & Lehman, T. M.** 2009. An enigmatic new lambeosaurine hadrosaur (Reptilia: Dinosauria) from the Upper Shale member of the Campanian Aguja Formation of Trans-Pecos Texas. *Journal of Vertebrate Paleontology*, **29**, 605–611.
- Wang, X. & Xu, X.** 2001. A new iguanodontid (*Jinzhouosaurus yangi* gen. et sp. nov.) from the Yixian Formation of western Liaoning, China. *Chinese Science Bulletin*, **46**, 1669–1672.
- Weishampel, D. B.** 1984. Evolution of jaw mechanisms in ornithopod dinosaurs. *Advances in Anatomy, Embryology and Cell Biology*, **87**, 1–59.
- Weishampel, D. B. & Bjork, P. R.** 1989. The first indisputable remains of *Iguanodon* (Ornithischia: Ornithopoda) from North America: *Iguanodon lakotaensis*, sp. nov. *Journal of Vertebrate Paleontology*, **9**, 56–66.
- Weishampel, D. B., Norman, D. B. & Grigorescu, D.** 1993. *Telmatosaurus transsylvanicus* from the Late Cretaceous of Romania: the most basal hadrosaurid dinosaur. *Palaeontology*, **36**, 361–385.
- Weishampel, D. B., Jianu, C.-M., Csiki, Z. & Norman, D. B.** 2003. Osteology and phylogeny of *Zalmoxes* (n. g.), an unusual euornithopod dinosaur from the latest Cretaceous of Romania. *Journal of Systematic Palaeontology*, **1**, 65–123.
- Winkler, D. A., Murry, P. A. & Jacobs, L. L.** 1997. A new species of *Tenontosaurus* (Dinosauria: Ornithopoda) from the Early Cretaceous of Texas. *Journal of Vertebrate Paleontology*, **17**, 330–348.
- Wu, W.-H., Godefroit, P. & Hu, D.-Y.** 2010. *Bolong yixianensis* gen. et sp. nov.: a new iguanodontoid dinosaur from the Yixian Formation of Western Liaoning, China. *Geology and Resources*, **19**, 127–133.
- Wu, W. & Godefroit, P.** 2012. Anatomy and relationships of *Bolong yixianensis*, an Early Cretaceous iguanodontoid dinosaur from Western Liaoning, China. Pp. 292–333 in P. Godefroit (ed.) *Bernissart dinosaurs and Early Cretaceous terrestrial ecosystems*, Indiana University Press, Bloomington and Indianapolis.
- Xing, H., Wang, D., Han, F., Sullivan, C., Ma, Q., He, Y., Hone, D. W. E., Yan, R., Du, F. & Xu, X.** 2014. A new basal hadrosauroid dinosaur (Dinosauria: Ornithopoda) with transitional features from the Late Cretaceous of Henan Province, China. *PLoS ONE*, **9**, e98821. doi:10.1371/journal.pone.0098821
- Xu, X., Tan, Q., Gao, Y., Bao, Z., Yin, Z., Guo, B., Wang, J., Tan, L., Zhang, Y. & Xing, H.** 2018. A large-sized basal ankylopollexian from East Asia, shedding light on early biogeographic history of Iguanodontia. *Science Bulletin*, **63**, 556–563.
- You, H., Ji, Q., Li, J. & Li, Y.** 2003. A new hadrosauroid dinosaur from the mid-Cretaceous of Liaoning, China. *Acta Geologica Sinica*, **77**, 148–154.
- You, H., Ji, Q. & Li, D.** 2005. *Lanzhouosaurus magnidens* gen. et sp. nov. from Gansu Province, China: the largest-toothed herbivorous dinosaur in the world. *Geological Bulletin of China*, **24**, 785–794.
- You, H., Li, D. & Lui, W.** 2011. A new hadrosauriform Dinosaur from the Early Cretaceous of Gansu Province, China. *Acta Geologica Sinica*, **85**, 51–57.
- Zhang, Y., Ogg, J. G., Minguetz, D. A., Hounslow, M., Olausson, S., Gradstein, F. M. & Esmeray Senlet, S.** 2019. Magnetostratigraphy of U/Pb-dated boreholes in Svalbard, Norway, implies that the Barremian–Aptian boundary (beginning of Chron M0r) is 121.2604 Ma. *AGU Annual Meeting* (San Francisco, 9–13 December 2019). #GP44A-06. <https://agu.confex.com/agu/fm19/meetingapp.cgi/Paper/577991>.
- Zheng, W., Jin, X., Shibata, M. & Azuma, Y.** 2014. An early juvenile specimen of *Bolong yixianensis* (Ornithopoda: Iguanodontia) from the Lower Cretaceous of Ningcheng County, Nei Mongol, China. *Historical Biology*, **26**, 236–251.

Associate Editor: Paul Barrett